AD-A071 542 BOEING COMMERCIAL AIRPLANE CO SEATTLE WASH F/G 11/6
STANDARDIZATION OF TI-6AL-4V PROCESSING CONDITIONS.(U)
SEP 78 R R BOYER, R BAJORAITIS F33615-74-C-5176
UNCLASSIFIED D6-48016 AFML-TR-78-131 NL

1 OF 2
AD
A071542

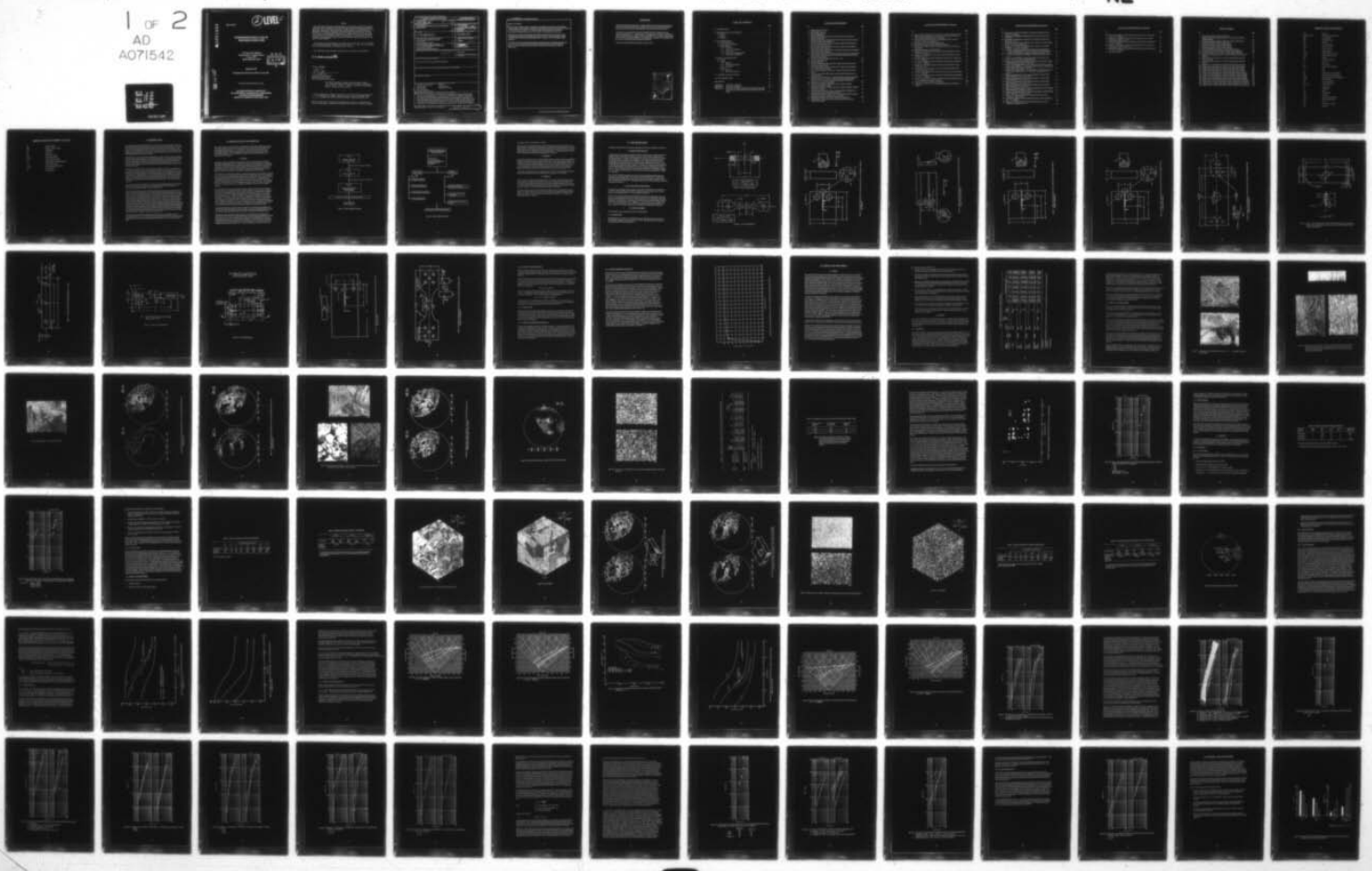

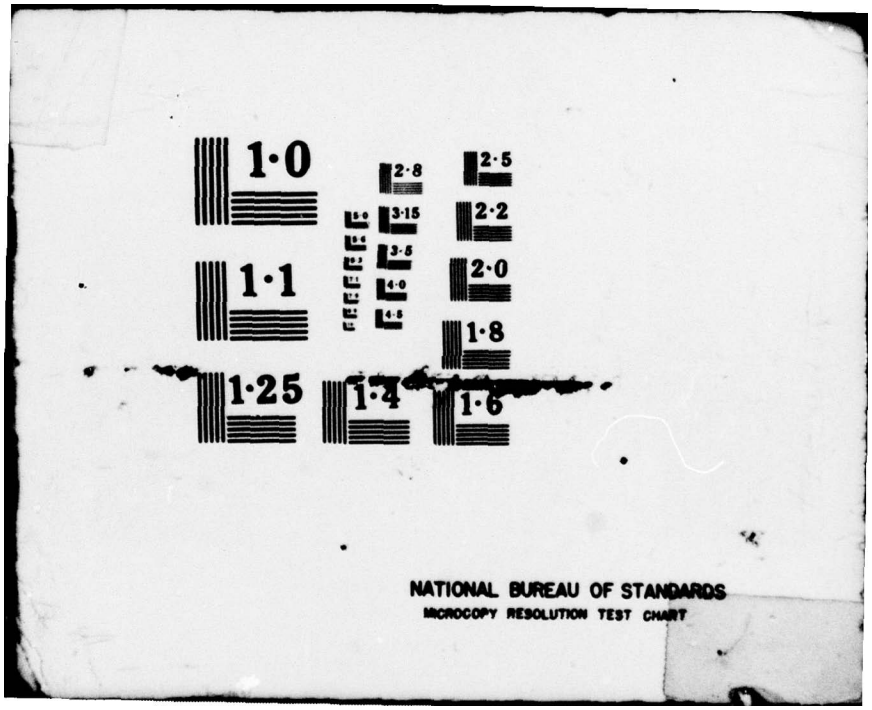
1·0
1·1
1·25
2·8
3·15
3·5
4·0
1·4
2·5
2·2
2·0
1·8
1·6
NATIONAL BUREAU OF STANDARDS
MICROCOPY RESOLUTION TEST CHART

AFML-TR-78-131

(2) LEVEL II

STANDARDIZATION OF Ti-6Al-4V PROCESSING CONDITIONS

R.R. Boyer and R. Bajoraitis
Boeing Commercial Airplane Company
P. O. Box 3707
Seattle, Washington 98124

September 1978

Final Report for Period 15 June 1975 to 31 July 1978

AIR FORCE MATERIALS LABORATORY
AIR FORCE WRIGHT AERONAUTICAL LABORATORIES
AIR FORCE SYSTEMS COMMAND
WRIGHT-PATTERSON AIR FORCE BASE, OHIO

NOTICE

When Government drawings, specifications, or other data are used for any purpose other than in connection with a definitely related Government procurement operation, the United States Government thereby incurs no responsibility nor any obligation whatsoever; and the fact that the government may have formulated, furnished, or in any way supplied the said drawings, specifications, or other data, is not to be regarded by implication or otherwise as in any manner licensing the holder or any other person or corporation, or conveying any rights or permission to manufacture, use, or sell any patented invention that may in any way be related thereto.

This report has been reviewed by the Information Office (OI) and is releasable to the National Technical Information Service (NTIS). At NTIS, it will be available to the general public, including foreign nations.

This technical report has been reviewed and is approved for publication.

C L Harmsworth

FOR THE COMMANDER

R D Cooper

T. D. COOPER, Chief
Materials Integrity Branch
Systems Support Division
Air Force Materials Laboratory

This report has been reviewed by the Information Office (OI) and is releasable to the National Technical Information Service (NTIS). At NTIS, it will be available to the general public, including foreign nations.

"If your address has changed, if you wish to be removed from our mailing list, or if the addressee is no longer employed by your organization please notify _____,W-PAFB, OH 45433 to help us maintain a current mailing list".

Copies of this report should not be returned unless return is required by security considerations, contractual obligations, or notice on a specific document.

SECURITY CLASSIFICATION OF THIS PAGE (When Data Entered)

(19) REPORT DOCUMENTATION PAGE

READ INSTRUCTIONS BEFORE COMPLETING FORM

(18) 1. REPORT NUMBER: AFML-TR-78-131

2. GOVT ACCESSION NO.

3. RECIPIENT'S CATALOG NUMBER

(6) 4. TITLE (and Subtitle): STANDARDIZATION OF Ti-6Al-4V PROCESSING CONDITIONS

(9) Final

5. TYPE OF REPORT & PERIOD COVERED: Technical Report, 15 June 1975 to 31 July 1978

(14) 6. PERFORMING ORG. REPORT NUMBER: D6-48016

(10) 7. AUTHOR(s): R. R. Boyer and R. Bajoraitis

(15) 8. CONTRACT OR GRANT NUMBER(s): F33615-74-C-5176

9. PERFORMING ORGANIZATION NAME AND ADDRESS
Boeing Commercial Airplane Company
P.O. Box 3707
Seattle, Washington 98124

(16) 10. PROGRAM ELEMENT, PROJECT, TASK AREA & WORK UNIT NUMBERS: 73810688 (17) 06

(11) 11. CONTROLLING OFFICE NAME AND ADDRESS
Air Force Materials Laboratory, AFML/MXE
Systems Support Division
Wright-Patterson AFB, Ohio 45433

12. REPORT DATE: Sept 1978

13. NUMBER OF PAGES

14. MONITORING AGENCY NAME & ADDRESS (if different from Controlling Office)

(12) 166p.

15. SECURITY CLASS. (of this report): Unclassified

15a. DECLASSIFICATION/DOWNGRADING SCHEDULE

16. DISTRIBUTION STATEMENT (of this Report)

Approved for public release; distribution unlimited

17. DISTRIBUTION STATEMENT (of the abstract entered in Block 20, if different from Report)

18. SUPPLEMENTARY NOTES

19. KEY WORDS (Continue on reverse side if necessary and identify by block number)

Fatigue crack propagation
Mill processing
Microstructure
Fracture toughness
Stress-Corrosion resistance
Fatigue
Heat treatment
Titanium (Ti-6Al-4V)

20. ABSTRACT (Continue on reverse side if necessary and identify by block number)

The effects of microstructure, composition, and crystallographic texture on the mechanical, fracture, and fatigue properties of Ti-6Al-4V sheet and plate were evaluated. This program was directed toward defining the processing approach for both product forms that provides the best damage-tolerance characteristics for fracture-critical applications. Specifications were written for premium-grade damage-tolerant Ti-6Al-4V sheet and plate defining processing, and mechanical, and fracture property requirements. The sheet and plate material was produced in accordance with the proposed specifications and characterized. Tensile, fracture toughness,

DD FORM 1 JAN 73 1473 EDITION OF 1 NOV 65 IS OBSOLETE

390 145

SECURITY CLASSIFICATION OF THIS PAGE (When Data Entered)

Abstract (Continued)

stress-corrosion resistance, fatigue, and fatigue crack propagation (air and salt water) properties were generated. Testing variables incorporated in the fatigue tests included R ratio (0.05, 0.5, and -1), and test orientation (L-T and T-L). Variables in fatigue crack propagation tests included environment (air and salt water), R ratio (0.05 and 0.5), and frequency (6 and 60 cpm).

Material and heat treatment (microstructural) variables included variations in oxygen content, crystallographic texture, mill annealing (covering the extremes in time and temperature ranges allowed per MIL-H-81200), duplex-annealing (with air cooling and furnace cooling), and beta-annealing.

The results of the tests are presented in tabular and graphical form, for individual specimens and specimen groups. Comparisons to mill-annealed and recrystallization-annealed material are made. The effects of the various material and test variables on the pertinent properties are discussed.

FOREWORD

This report describes a development of damage-tolerance Ti-6A1-4V alloy plate and sheet performed by the Boeing Commercial Airplane Company (BCAC), Seattle, Washington from 15 June 1975 to 31 July 1978 under Air Force contract F33615-74-C-5176.

This work was sponsored by the Air Force Materials Laboratory (AFML) under the technical direction of Mr. C. L. Harmsworth. The program was conducted by the Boeing Material Technology group of BCAC under the supervision of D. D. Goehler, program manager, R. R. Boyer, principal investigator, and R. Bajoraitis, test design and coordination and W. F. Spurr, technical consultant (formerly with BCAC).

This report was submitted by the authors on July 28, 1978.

TABLE OF CONTENTS

LIST OF ILLUSTRATIONS

LIST OF ILLUSTRATIONS (Continued)

LIST OF ILLUSTRATIONS (Continued)

LIST OF ILLUSTRATIONS (Concluded)

LIST OF TABLES

ABBREVIATIONS AND SYMBOLS

AC	air cool
ASTM E-8, E-24	ASTM testing specifications
BA	beta annealed
CHF	center hole fatigue
℄	centerline
CNP	center notch panel
cpm	cycles per minute
CT	compact tension
DA	duplex annealed
da/dN	crack growth rate, in./cycle
DCB	double cantilever beam
dia	diameter
ELI	extra low interstitial
f	frequency
FC	furnace cool
FCP	fatigue crack propagation
hr	hour
in.	inch
K_C	plane-stress fracture toughness
K_{IC}	plane-strain fracture toughness
K_{ISCC}	salt water stress corrosion threshold
K_Q	conditional K_{IC}
ksi	kips per square inch
ksi $\sqrt{\text{in.}}$	stress intensity unit
K_t	notch factor
L	longitudinal
lb	pound
MA	mill annealed
max	maximum
min	minimum, minute (time)
NaCl	sodium chloride, salt
R	ratio
RA	recrystallize annealed
ref.	reference

ABBREVIATIONS AND SYMBOLS (Continued)

ST	solution treated
STA	solution treated and aged
sym	symmetrical
T	transverse
TD	tranverse direction
YTS	yield tensile strength
TUS	tensile ultimate strength
α	low temperature titanium allotrope
ΔK	stress intensity range
ΔK_{avg}	average stress intensity range
σ_g	gross area stress
σ	net area stress

1.0 INTRODUCTION

The mechanical properties of titanium alloy Ti-6A1-4V can vary dramatically, yet meet current industry specification requirements for mill processing and tensile properties. The variations of mechanical properties present a problem in using titanium alloys effectively, since designs are usually based on the lower range of mechanical properties. Consequently, most aerospace companies have had to write more stringent titanium specifications for Ti-6A1-4V alloy applied to the more critical components.

Documentation to date of properties showing greatest variations includes fracture toughness, stress-corrosion resistance (K_{ISCC}), and environmental fatigue crack propagation (FCP) rates. The wide variations in properties have been directly related to three primary metallurgical variables: microstructure, composition, and basal plane crystallographic texture (refs. 1, 2). Of these, microstructure and texture are directly controlled by the thermal and mechanical processing of the alloy.

Some data in the literature have shown fatigue crack initiation to also be controlled by texture and microstructure. Until now, no systematic study had been conducted to collect and generate sufficient statistical data so that valid relationships can be established between processing and mechanical properties. Once these relationships were determined, they could be used to develop a materials specification covering a premium-grade Ti-6A1-4V material possessing consistently superior fatigue and damage-tolerant properties. The primary purpose of this Air Force program was to ultimately produce specifications of this nature for sheet and plate.

The overall objective of this program was to determine valid relationships between alloy composition, mill processing, microstructure, and properties leading to the development of specifications for premium-quality Ti-6A1-4V mill products.

Major testing emphasis was placed on notched fatigue testing and environmental FCP characteristics, since previous programs have reasonably established relationships between fracture characteristics and metallurgical variables. The program was divided into three phases. Phase I was conducted to determine the effects of heat treatment variations and mill processing on notched fatigue, environmental FCP, plane strain fracture toughness, and tensile strength. Phase II extended the testing of Phase I to include effects of variations in alloy composition allowed by MIL-T-9046 and MIL-T-9047, using the optimum thermal and mechanical processing established in Phase I. Phase II also included drafting preliminary sheet and plate specifications from which to obtain industry comments. Damage-tolerant and fatigue design data suitable for inclusion into MIL-H-5 for the optimum alloy composition and processing determined in Phases I and II were generated in Phase III. Finally, specifications were developed for a damage-tolerant grade Ti-6A1-4V alloy providing consistently high fracture and fatigue properties suitable for building a superior airframe structure.

This final report describes the overall program, briefly reports the highlights of Phase I (already reported in ref. 3), summarizes the results of Phases II and III, and contains suggested procurement specifications for premium-grade damage-tolerant Ti-6A1-4V alloy plate and sheet.

2.0 PROGRAM GOALS AND APPROACH

The overall objective of this program was to optimize the thermal and mechanical processing and define an optimum Ti-6A1-4V composition that will consistently produce high fatigue and damage-tolerant properties. As an end result, a specification was prepared for this damage-tolerant grade material to adequately control thermal and mechanical processing and resulting properties. The overall program divided into three phases, is shown in the master flow chart of figure 1.

2.1 PHASE I

A systematic study to establish the relationships of Ti-6A1-4V microstructural variations, including crystallographic texture, to fatigue crack initiation and propagation was conducted. The objective of this program was to determine the effects of various thermal and mechanical processing on Ti-6A1-4V notched fatigue properties and environmental FCP. A total of 24 material conditions were tested. The microstructural appearance and basal plane crystallographic texture were characterized and related to resultant mechanical properties.

The fatigue life of each material condition was determined using five notched fatigue specimens (K_t = 2.53) tested at a single stress level (σ_g) of 50 ksi and stress ratio of 0.05. This number of fatigue specimens provided statistically valid data for log average life. The stress level of 50 ksi is considered sufficiently low to be comparable to service stresses, yet sufficiently high to minimize the high data scatter associated with stress near the endurance limit. Typical fatigue failures at this stress level occur in the neighborhood of 10^5 cycles. The stress concentration factor of 2.53 was selected since it is considered comparable to fastener holes of airframe structure.

The heat treatment and material variables studied are outlined in the flow chart for Phase I shown in figure 2. The full range of times and temperatures for low-temperature annealing in accordance with MIL-H-81200A were investigated. Solution anneals (with both air and furnace cools) from 1675°F to beta transus minus 30°F and beta annealing were also studied. Beta annealing was done at 1900°F and 2200°F and included air cooling (AC) and furnace cooling (FC). All solution and beta anneals were followed by a 1350°F for 2 hours stabilization treatment. Air cooling and furnace cooling from the solution annealing temperature result in different microstructures. It is common practice to refer to two-stage anneals (regardless of cooling rate) as duplex anneals (DA). To distinguish the two different structures, the former will be referred to as duplex anneal and the latter as recrystallization anneal.

Strengthening treatments involving solution treating and water quenching plus aging (STA) were not included in this program since they usually cause manufacturing problems associated with distortion and residual stress, and they produce low toughness and high FCP rates.

The majority of the thermal processing variations were evaluated using as-rolled plate to eliminate the effects of previous thermal processing. The alpha-beta cross-rolled plate supplied by the Air Force was used to evaluate effects of variations in crystallographic texture and thermomechanical processing. Heat treatments applied to the sheet material were limited to those below the beta-transus temperature. Beta processing of Ti-6A1-4V sheet was found to be highly detrimental to formability (ref. 4). Some heat treatment conditions, to be used

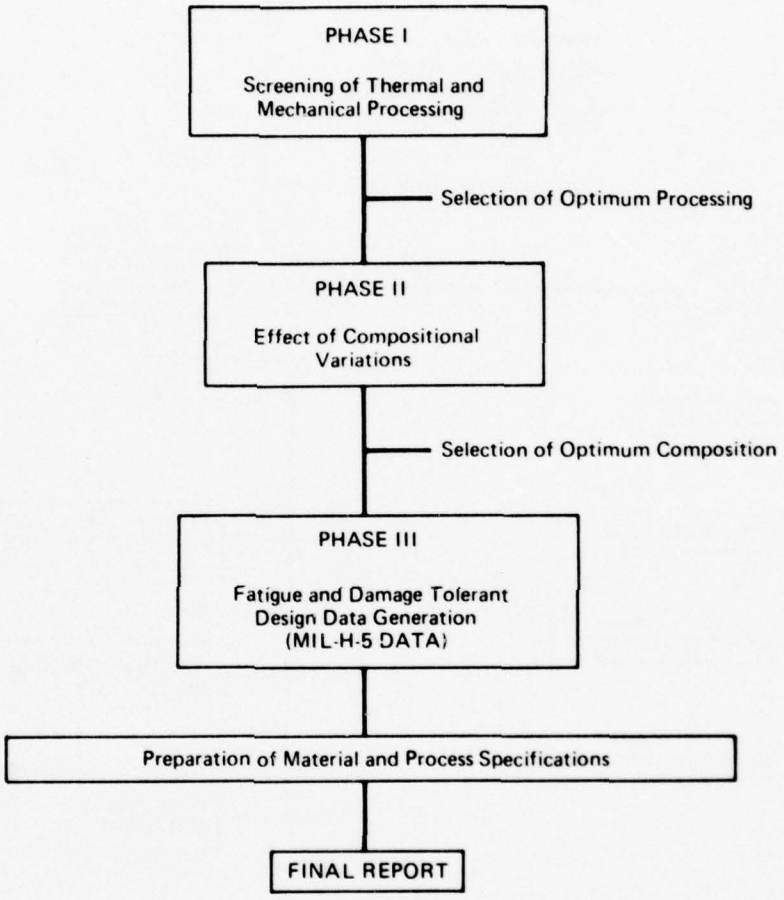

Figure 1.—Program Master Flow Chart

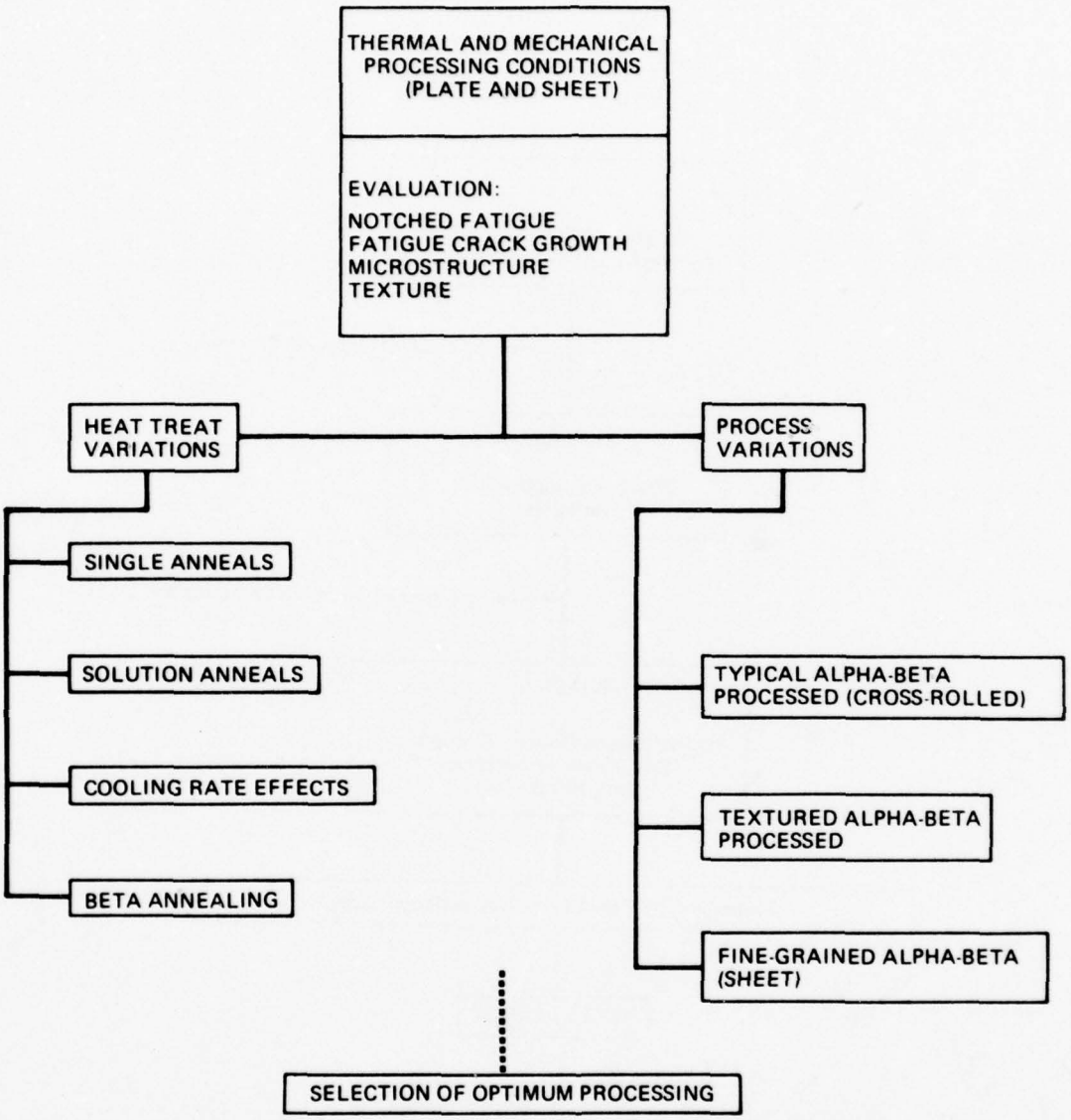

Figure 2.—Phase I Master Flow Chart

as a reference base, were applied to both plates.

The test results were evaluated with the aim of selecting optimum heat treatments for both plate and sheet. Although the testing emphasis was placed on notched fatigue and, to a lesser degree, fatigue crack propagation, heat treatment selection was also based on previously generated data for fracture toughness and stress-corrosion resistance. Overall performance potential for damage-tolerant and fatigue design governed the selection.

2.2 PHASE II

The objective of Phase II was to extend the Phase I effort to include variations in composition. Oxygen content was the primary variable in this analysis. Three oxygen levels of plate were evaluated, all within the limits specified for Ti-6Al-4V in MIL-T-9046 and MIL-T-9047. Due to cost constraints and material availability, only one sheet composition was tested in this phase of the program. The materials were heat treated in accordance with the treatment found in Phase I to provide the most damage-tolerant structure for each product form.

A first draft of specifications for the damage-tolerant Ti-6Al-4V sheet and plate were assembled and coordinated with industry (potential users and suppliers) for comments.

2.3 PHASE III

The objectives of this phase of the program were to (1) generate data on material procured with the optimum composition and heat treatment for each product form to demonstrate the damage-tolerant nature of the material, and (2) write suitable specifications for procurement of premium-grade damage-tolerant Ti-6Al-4V sheet and plate incorporating appropriate industrial comments or technical modifications obtained from Phase II.

The data generated included notched and smooth fatigue, fracture toughness (K_{IC} and K_C), fatigue crack growth rate in air and 3.5% NaCl, and the stress-corrosion cracking threshold (K_{ISCC} and K_{SCC}). The data are presented in accordance with MIL-H-5, "Guidelines for Presentation of Data," Chapter 9.

3.0 TEST PROCEDURES

Procedures used for specimen preparation, handling, and testing are described in this section.

3.1 SPECIMEN PREPARATION

Tensile properties were determined using two smooth tensile specimen configurations shown in figures 3 and 4. Static fracture toughness tests were conducted using compact tension (CT) specimens (fig. 5). Fatigue crack propagation tests of plate were conducted using DCB and compact tension specimens shown in figures 6-8. FCP testing of sheet material was accomplished using the center-notch panel (CNP) specimens illustrated in figures 9 and 10. Fatigue tests were conducted using flat center-hole fatigue (CHF) specimens shown in figure 11, smooth fatigue specimens shown in figure 12, and lap splice specimens shown in figure 13. Stress-corrosion testing of the plate (Phase III) was done using the DCB specimen shown in figure 14. Stress-corrosion testing of sheet utilized the CNP specimen configuration of figure 10. Four surface flaw specimens (fig. 15) were fabricated at Boeing and submitted to AFML for FCP testing.

All specimens were fabricated using conventional sawing and milling processes outlined in Boeing process specification BAC 5492, "Machining and Cutting Titanium." CHF and lap splice specimens were finish ground using the low-stress grinding process specified in attachment 2 to RFQ F33615-75-R-5176. This grinding process for the CHF and lap splice specimens is discussed in reference 3.

3.2 HEAT TREATMENT PROCEDURES

All material was heat treated in an air furnace. Each piece of material (heat treat blank) was individually thermocoupled and monitored throughout the heat treatment cycle. The temperature was maintained within ± 5°F of the reported temperature.

The beta transus was determined by heating individual specimens at temperatures above and below the anticipated beta transus with a 20-minute hold time, water quenching, and metallographically examining them to determine at what temperature the material passed through the beta transus. The temperatures in the range from 1775 to 1835°F at 10°F increments were used. A low-temperature age (1150 or 1200°F) was employed following the solution treatment to enhance the etching characteristics of the material to facilitate the examination.

3.3 TESTING METHODS

The procedures for the various types of tests are outlined below.

3.3.1 TENSILE TEST

Tensile specimens were tested in a 20-kip Baldwin model 20B-1040 universal test machine per ASTM E8. Elongation was measured over 1 inch on round specimens (fig. 3) and over a 2-inch gage length on flat specimens (fig. 4).

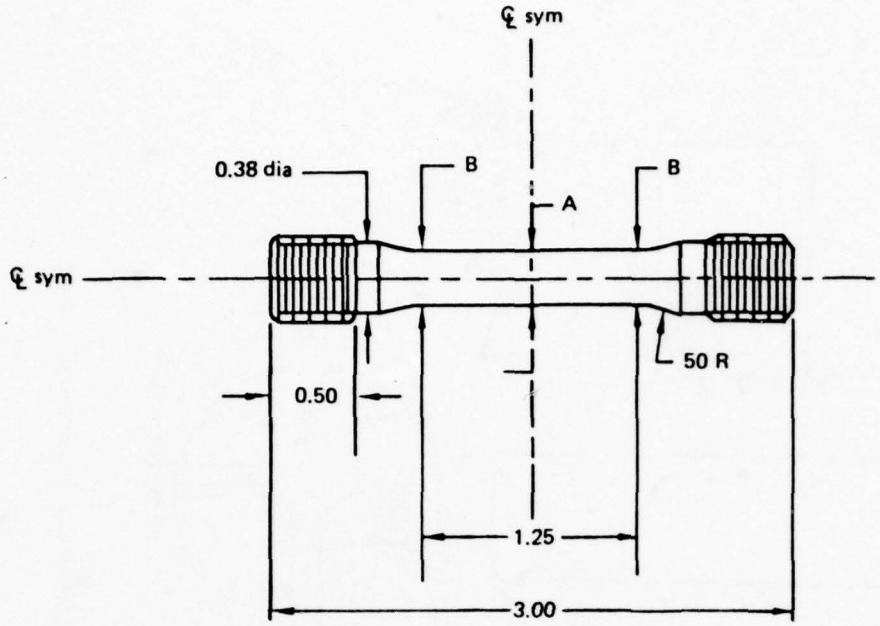

A	0.250 max; 0.247 min
B	A + 0.003 to A + 0.005

Figure 3.—Round Tensile Specimen

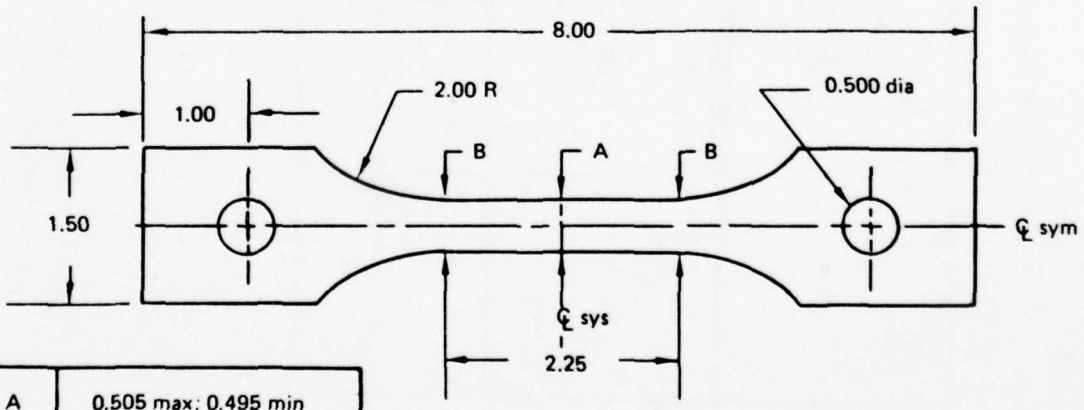

A	0.505 max; 0.495 min
B	A + 0.003 to A + 0.005

Figure 4.—Flat Tensile Specimen

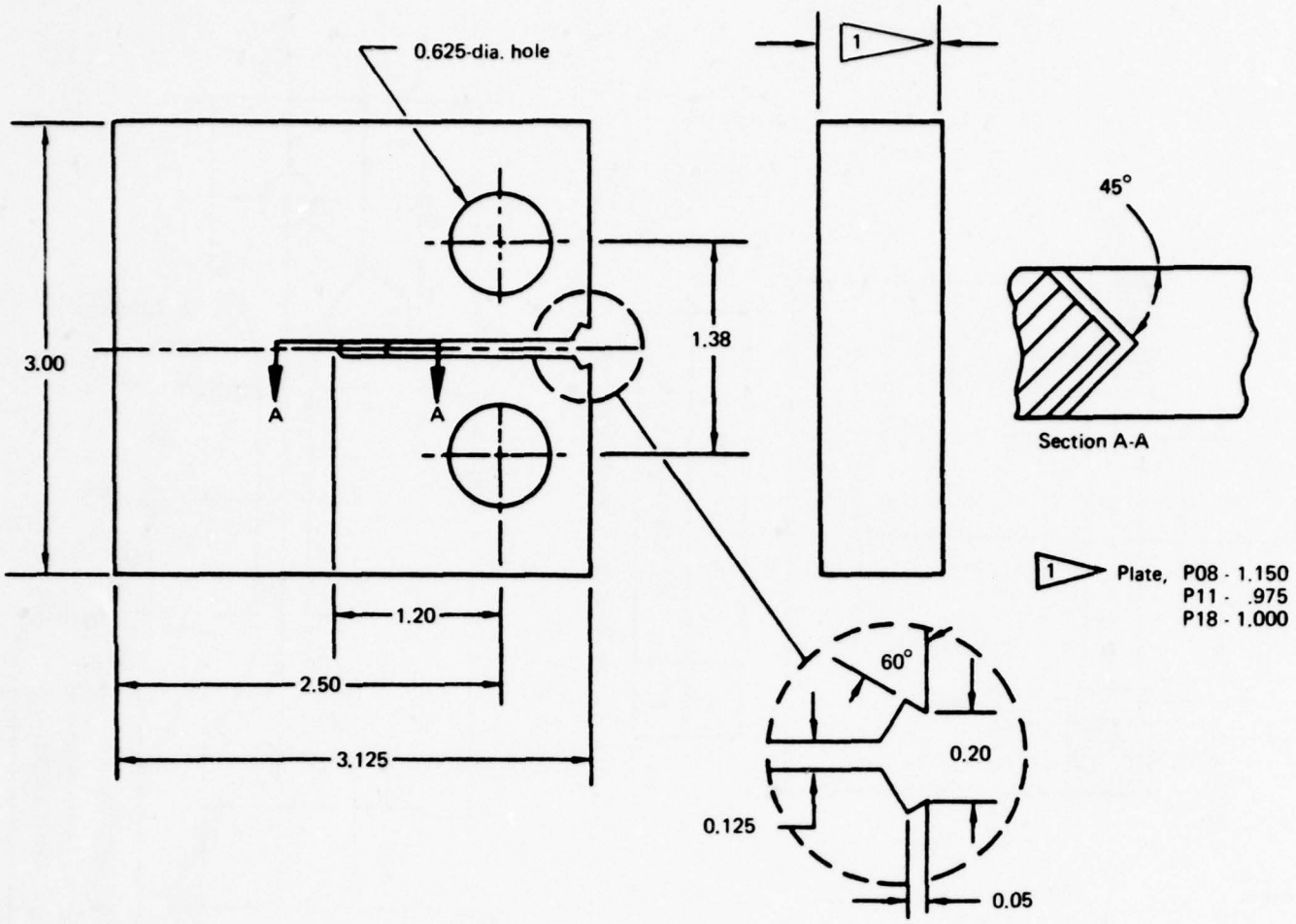

Figure 5.—Compact Tension Specimen Used to Determine Fracture Toughness of Phase III Plate Material.

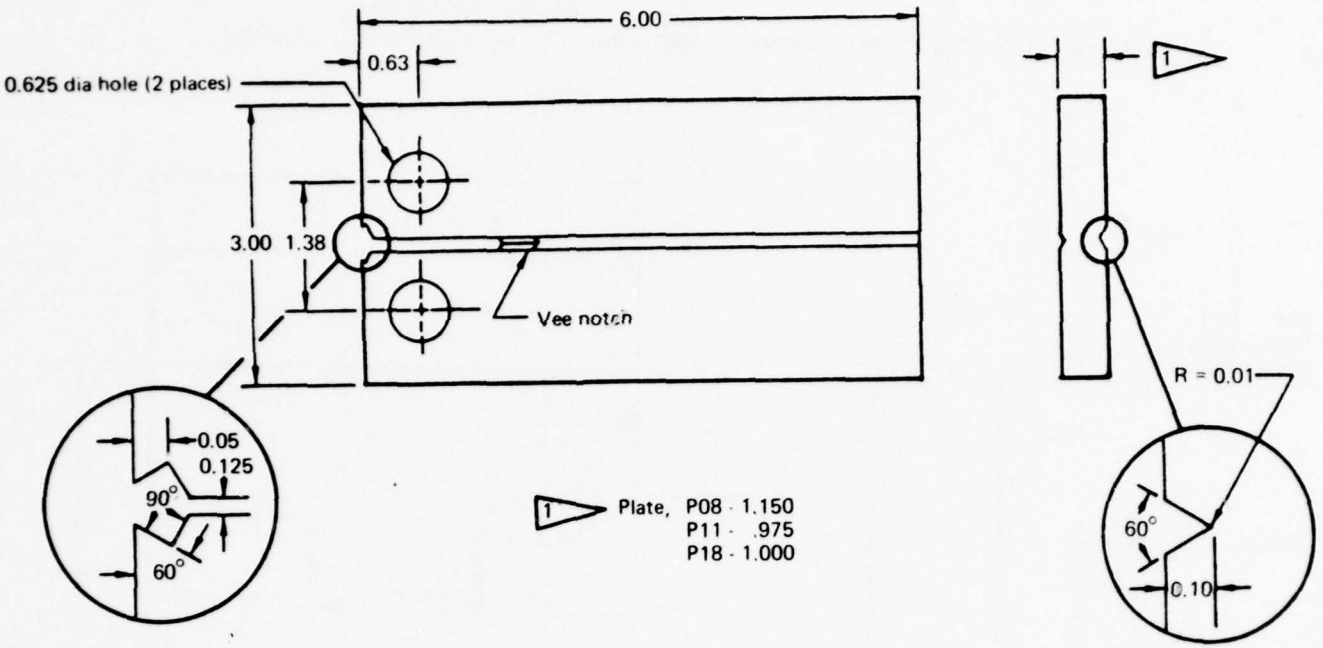

Figure 6.—Double Cantilever Beam Specimen Used to Determine Fatigue Crack Propagation Rates of Phase II Plate Material

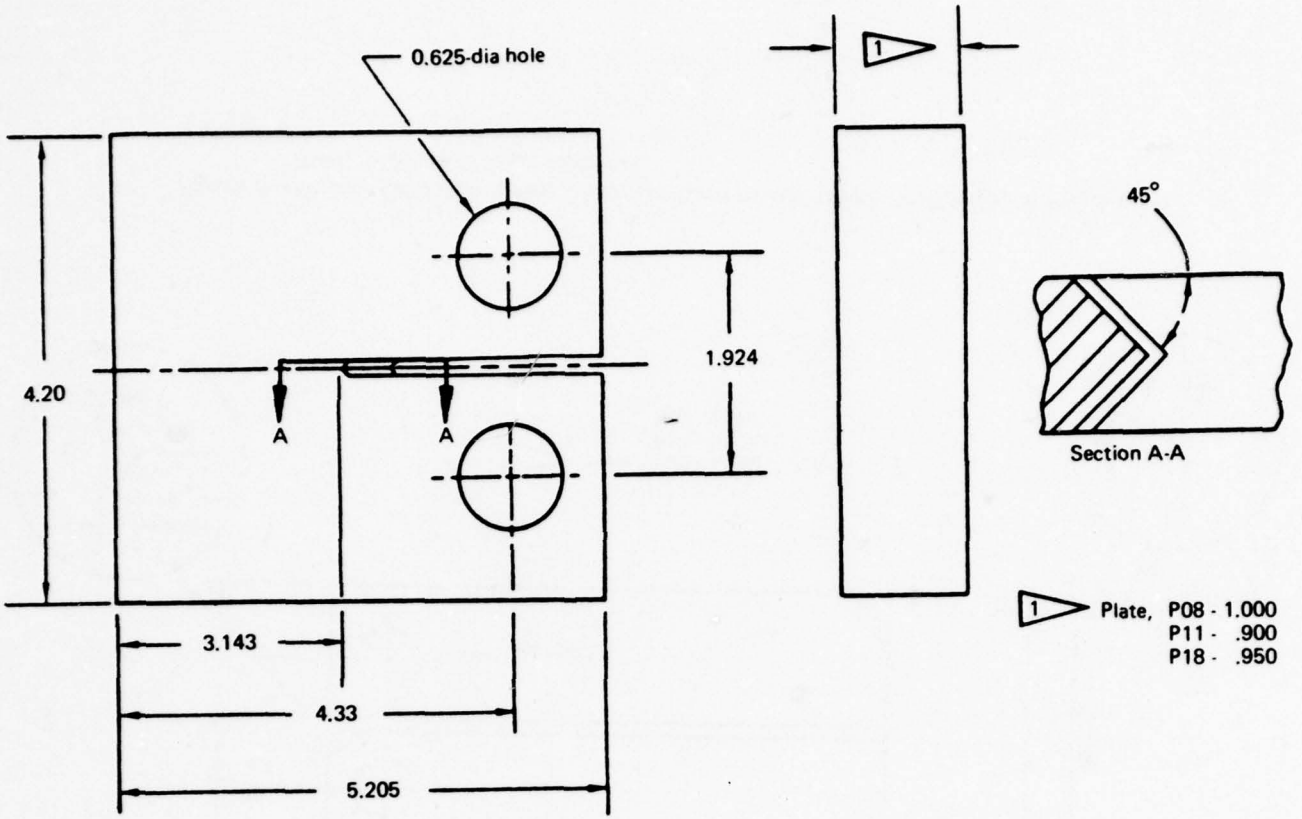

Figure 7.—Compact Tension Specimen Used to Determine Crack Propagation Rates of Phase II Plate Material.

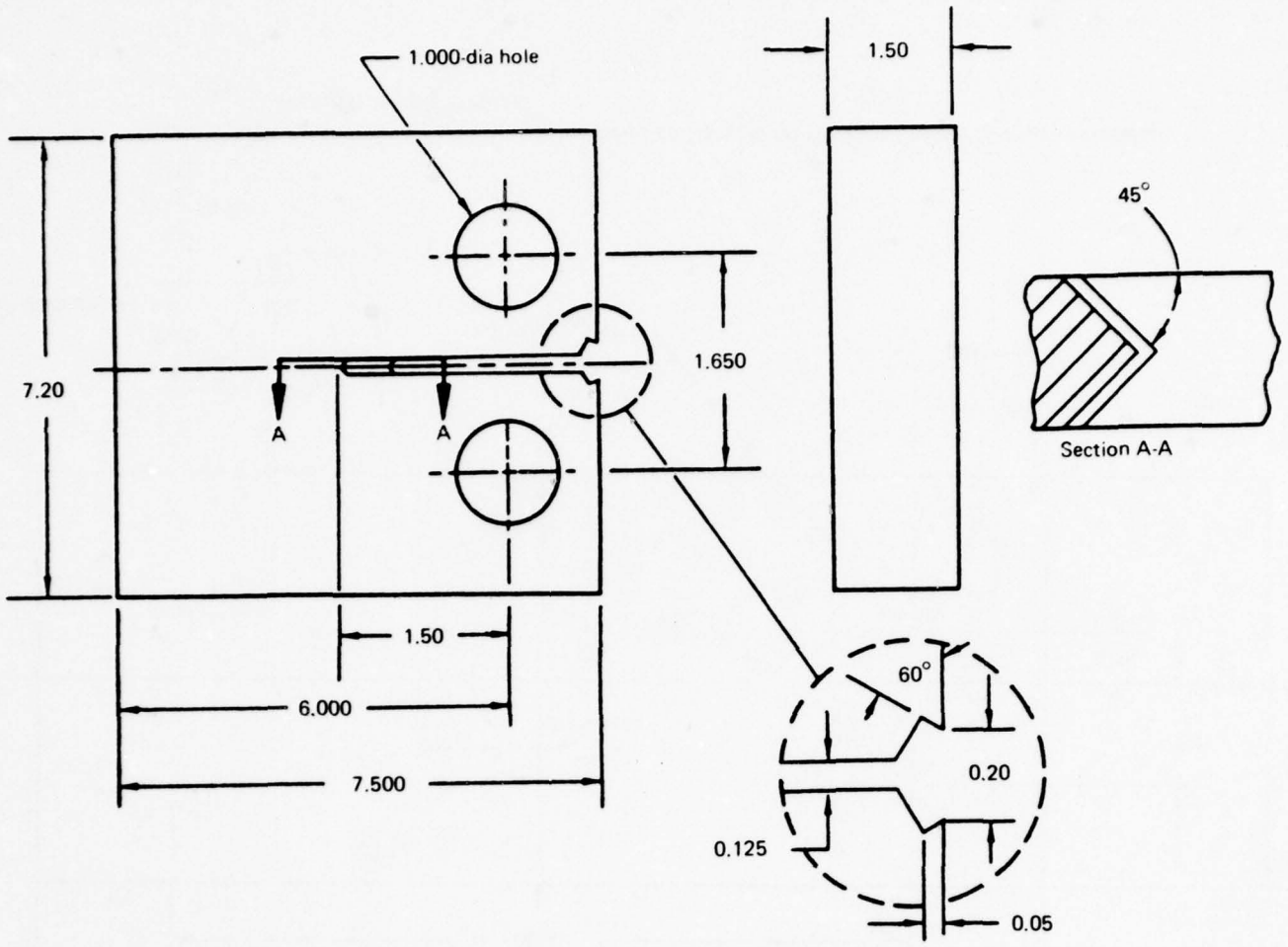

Figure 8.—Compact Tension Specimen Used to Determine Fatigue Crack Propagation Rates of Phase III Plate Material.

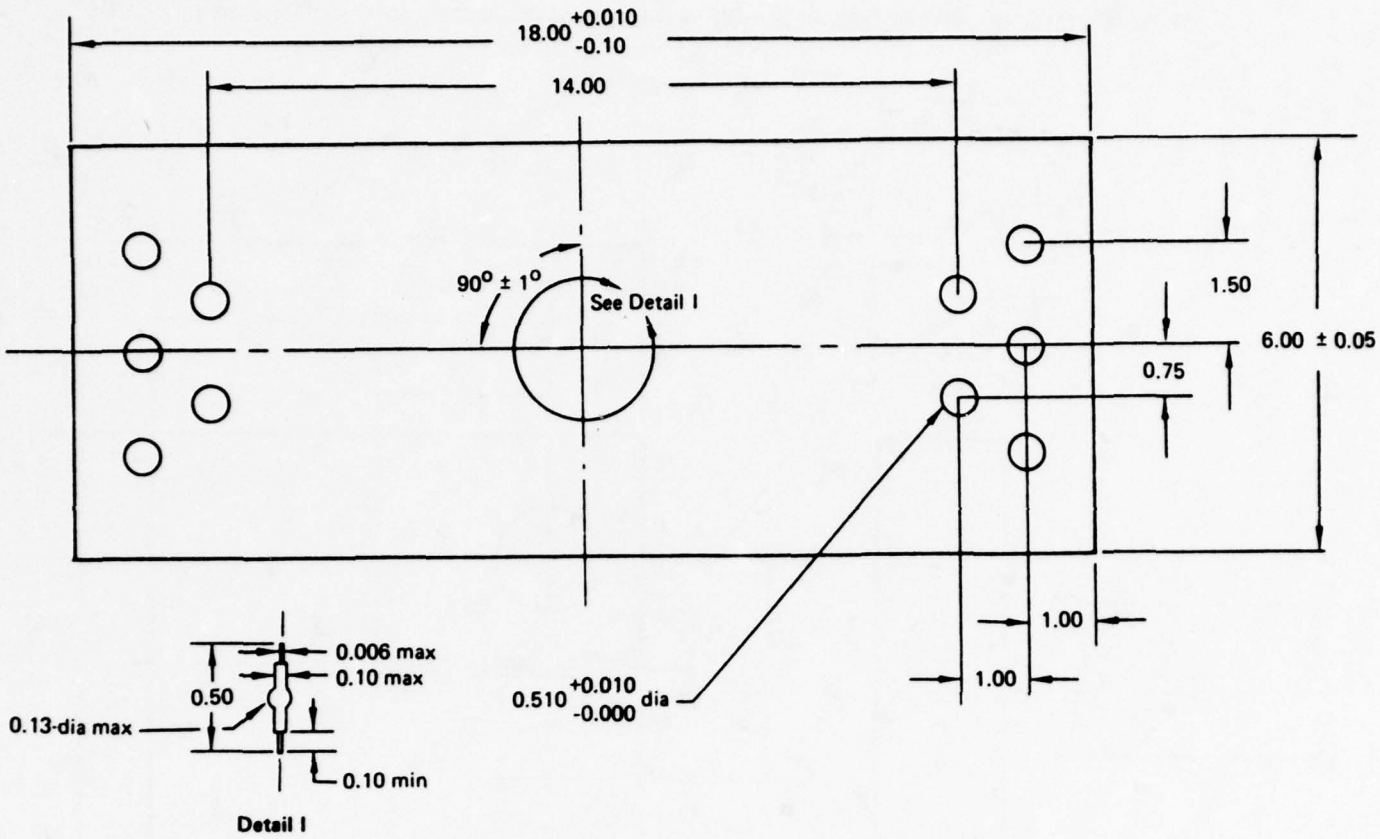

Figure 9.—Center-notched Panel Specimen Used to Determine Fatigue Crack Propagation Rates of Phase II Sheet Material.

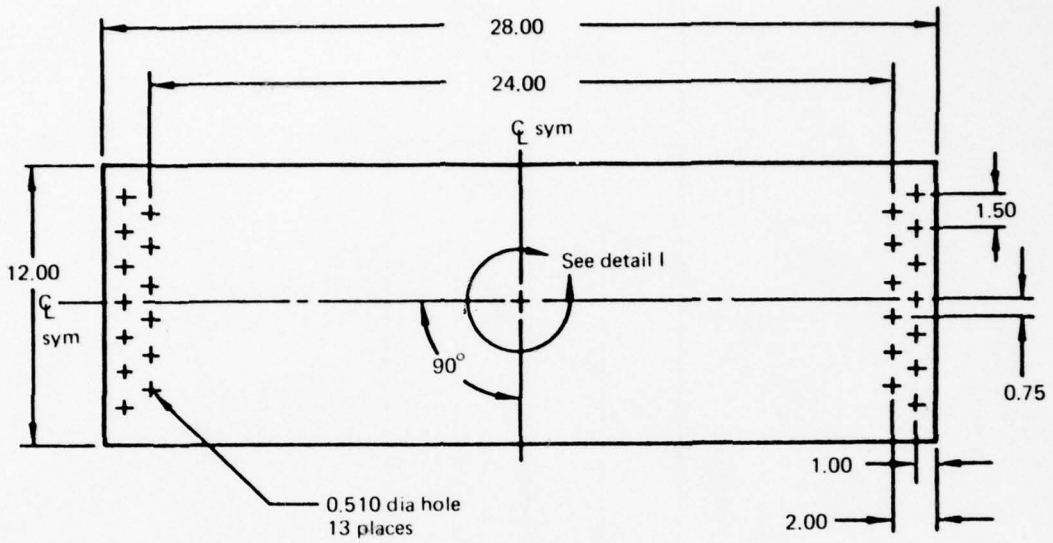

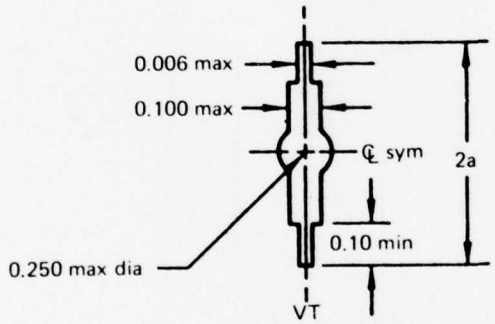

Detail I

$$K = \sigma_g \sqrt{\left[\frac{W}{\pi a} \text{ TAN } \frac{\pi a}{W}\right]}^{1/2}$$

Figure 10.—Center-notched Panel Specimen Used to Determine Fatigue Crack Propagation Rates, Fracture Toughness, and Stress-corrosion Cracking Threshold Values of Phase III Sheet Material.

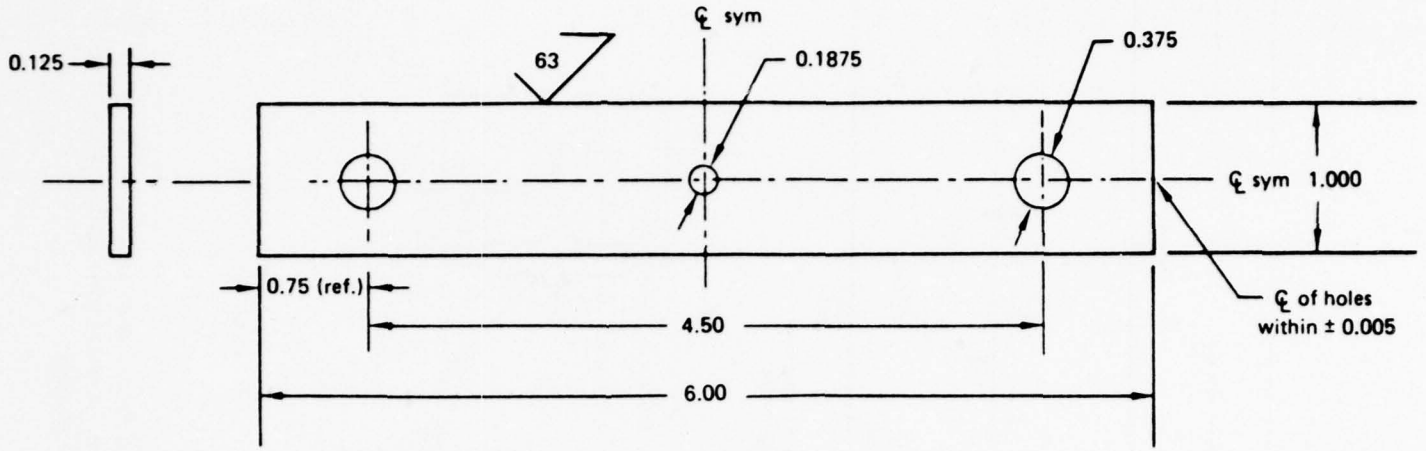

Figure 11.—Center Hole Notched Fatigue Specimen (K_t = 2.53)

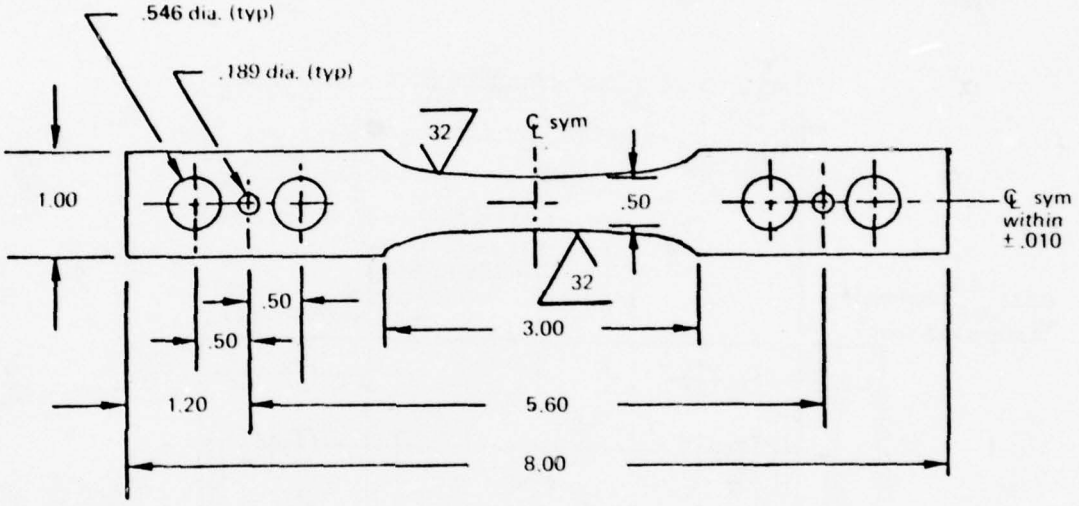

Note: Ellipse test section; minor dia. .50 in., major dia. 3.00 in. to be machined symmetrical to transverse centerline within ± .010 in.

Figure 12.–Smooth Fatigue Specimen.

▷ Size bolts prior to drilling holes. Holes to be drilled so as to have 0.0004 interference with bolt. Hole tolerance will be , -0.0000

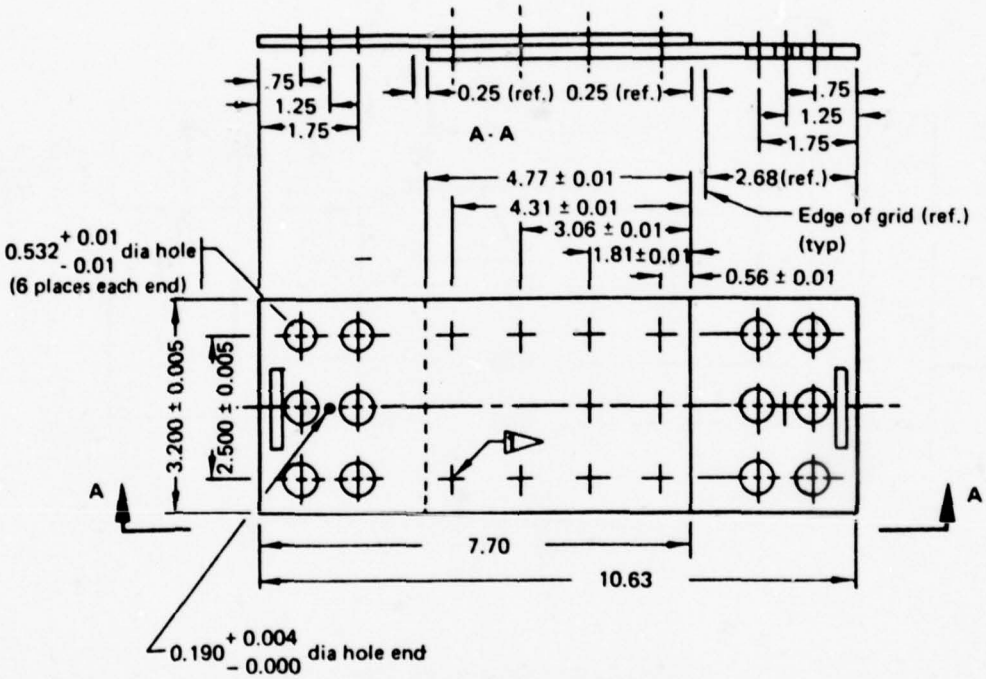

Figure 13.—Lap Splice Specimen.

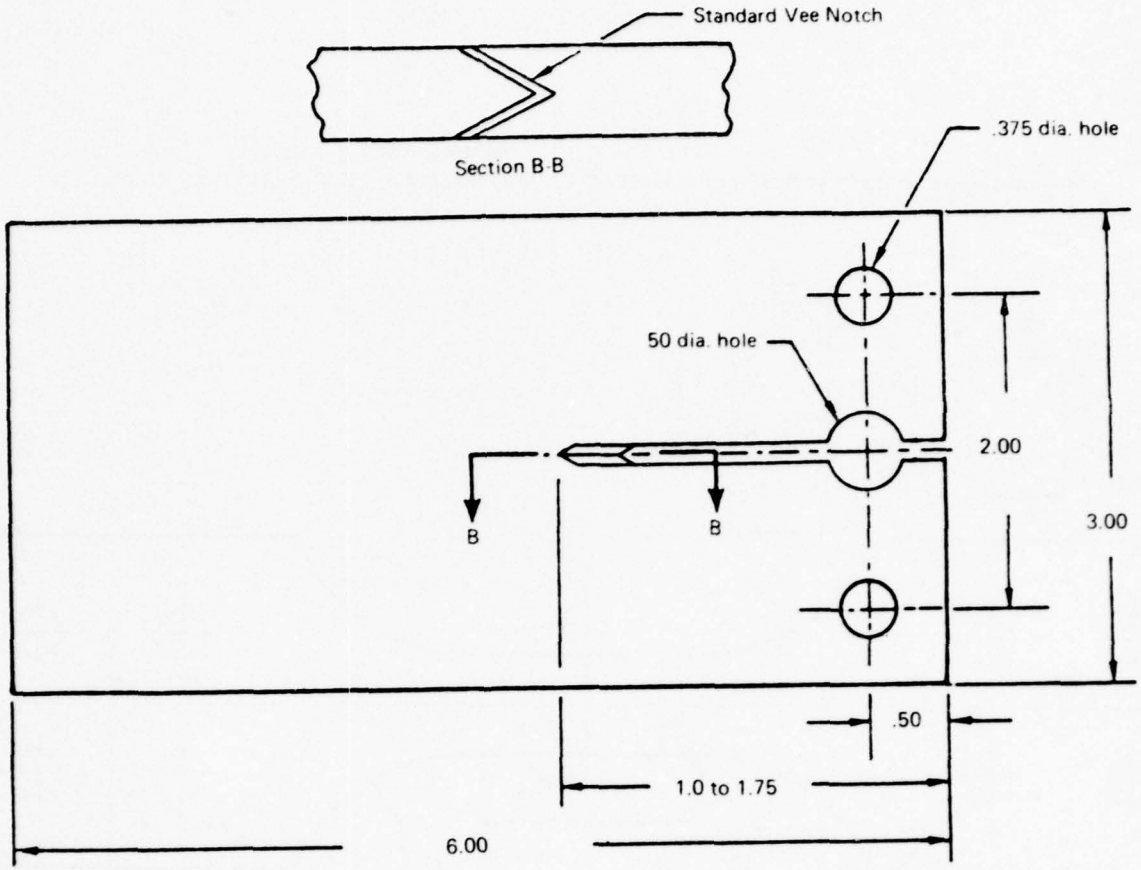

Figure 14.—Double Cantilever Beam Specimen Used to Measure the Stress-corrosion Cracking Threshold of Plate.

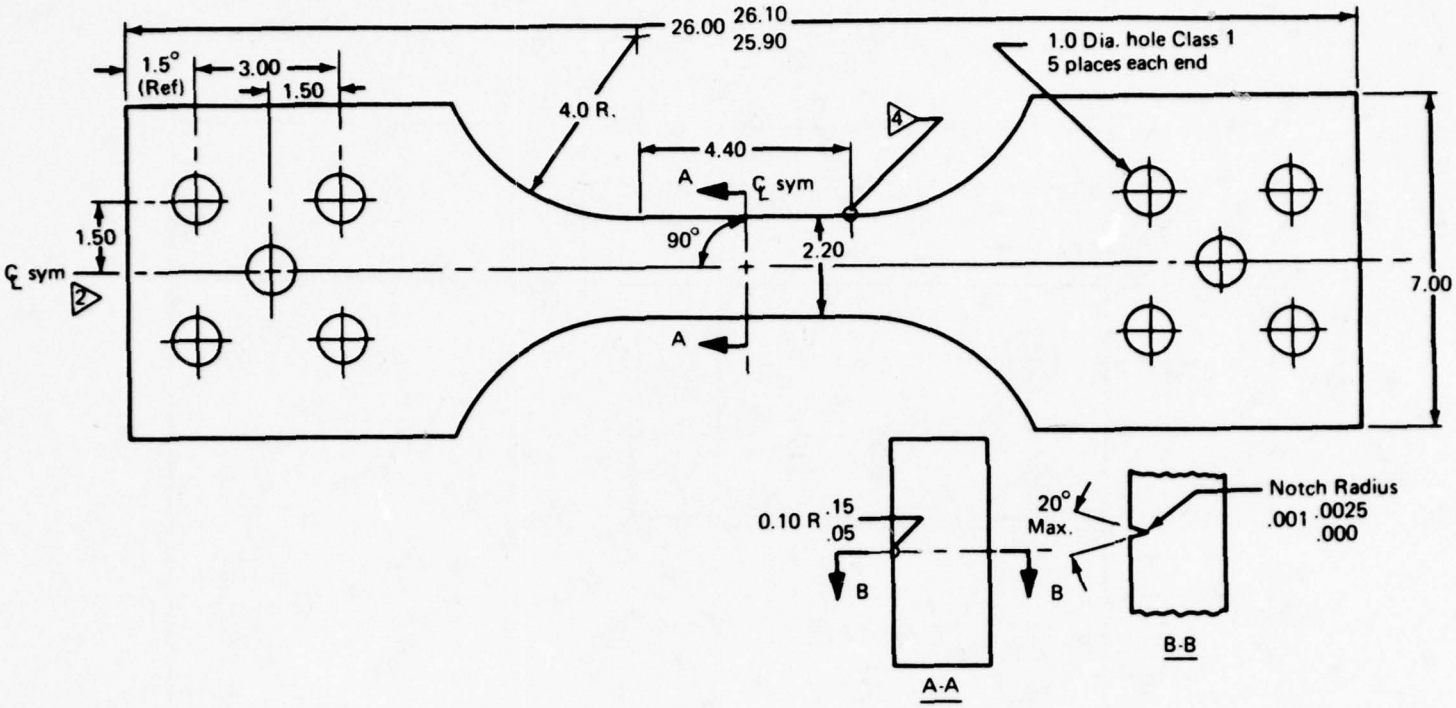

Figure 15.—Surface Flaw Specimen Used to Determine the Fatigue Crack Propagation Rate of Phase III Plate Material.

3.3.2 FRACTURE TOUGHNESS TEST

Fracture toughness of plate was determined with compact tension specimens that were precracked in a 30-kip vibraphore fatigue test machine at 4500 cpm and tested for fracture toughness per the ASTM method of test for plane strain fracture toughness of metallic materials (E399-72).

Fracture toughness of sheet was determined using center-notched panels (CNP) shown in figure 10. The size of the panel was dictated by the amount of material available, as well as the requirement that the ratio of net area stress to yield strength be less than 0.8. The total crack length (2a) was kept at one-third the panel width. For these conditions, the panel width W must obey the following:

$$W \geq 5.91\,(K_C/TYS)^2$$

The center-notched panels are tension-tension fatigue cycled to grow the fatigue crack from 0.5 inch. After fatigue cycling, the panels were fracture tested in room-temperature air at a stress rate of 1000 psi/sec. K_C is calculated from the following equation:

$$K_C = \sigma_g \sqrt{\pi a} \left[\frac{W}{\pi a} \tan \frac{\pi a}{W}\right]^{1/2}$$

The last term here is the finite panel size correction factor and is 1.06 for a 12-inch-wide panel with $2a/W = 0.35$. The calculation of K_C was based on maximum failure load and the initial fatigue crack length (a) prior to dynamic loading at 1000 psi/sec.

3.3.3 FATIGUE TEST

In Phases I and II, center-hole-notch fatigue specimens (fig. 11) were tested at 50-ksi stress (gross area), 0.05 stress ratio, and 1800 cpm on a Sontag model SF-10-U test machine; lap splice specimens (fig. 13) were tested at 30-ksi stress (gross area), 0.05 stress ratio, and 1800 cpm on the same test machine. In Phase III, center-hole and smooth fatigue specimens were tested at a cyclic frequency of 1800 cpm and stress ratios of 0.05, 0.5, and -1.0 to develop data for constant-life diagrams.

3.3.4 FATIGUE CRACK PROPAGATION TEST

Fatigue crack propagation rate tests were made in air and 3.5% aqueous NaCl solution. Precracking was accomplished in a fatigue machine at 1800 cpm. The first increment of crack propagation was induced using a constant peak cyclic load slightly greater than the load used to precrack the specimen. The stress ratios used were 0.5 and 0.05; the cyclic rates were 60 and 6 cpm for the plate (only 60 cpm was used for the sheet). After sufficient data at a given load were obtained, the peak cyclic load was increased by approximately 5 ksi, and the next increment of crack growth was induced. This procedure was repeated for three to six ΔK levels in air and NaCl solution.

3.3.5 STRESS-CORROSION RESISTANCE

Stress-corrosion tests were made using DCB specimens for plate (fig. 14) and CNP specimens for sheet (fig. 10), and a sustained loading technique in an environment of 3.5% aqueous NaCl solution. The specimens were fatigue precracked and sustained loaded for 60 minutes minimum at a lower level than the anticipated threshold K. When the specimen did not fail, it was re-fatigue-cracked and reloaded at a higher K level. This process was repeated until failure occurred.

The specimen was re-fatigue-cracked between sustained loadings to eliminate any chemical or electrochemical passivation effects at the crack tip, as well as to eliminate plastic yield zone effects on the stress-corrosion cracking mechanism. Here, the K level during fatigue cracking was kept at a lower level than the next sustained load. This prevented a large plastic yield zone from inhibiting stress-corrosion cracking. Past experience has shown that when the fatigue K level is higher than the level used in the subsequent sustained load test, the "threshold" can be erroneously tested to be much higher than its actual value. To ensure no plastic zone effect, the length of the fatigue crack was usually kept at a minimum of $(1/\pi)\,(K_{fatigue}/TYS)^2$, which is twice the amount generally accepted as the radius of the plastic yield zone. The number of re-fatigue-cracking steps and hence the number of subsequent sustained loadings were restricted to keep the ratio of crack length to specimen width at generally 0.5 or less. The minimum sustained loading time of 60 minutes was justified on the basis of 484 specimens tested during the SST program (ref. 4). Figure 16 is a plot of time to failure versus cumulative percent of failure from that reference, which shows that 96% of the specimens that failed did so before 60 minutes.

The threshold values were determined using the highest no-failure and lowest failure loads. Using the one specimen and re-cracking approach, there would be only one failure level. For example, if a specimen did not fail at a K of 40 but failed at a K of 50, an approach would be to simply call the threshold value 45, keeping in mind that the accuracy would be ± 5 ksi$\sqrt{\text{in}}$. A refinement of this approach was used that considered the time the specimen took to fail at the failure level. If, for example, a specimen did not fail at 40 but failed at 50 in 59 minutes, the actual threshold would be closer to 50 than 40. By analyzing the shape of many failure curves, a series of factors was developed to permit this refinement. The details of this procedure are given in appendix A of reference 1.

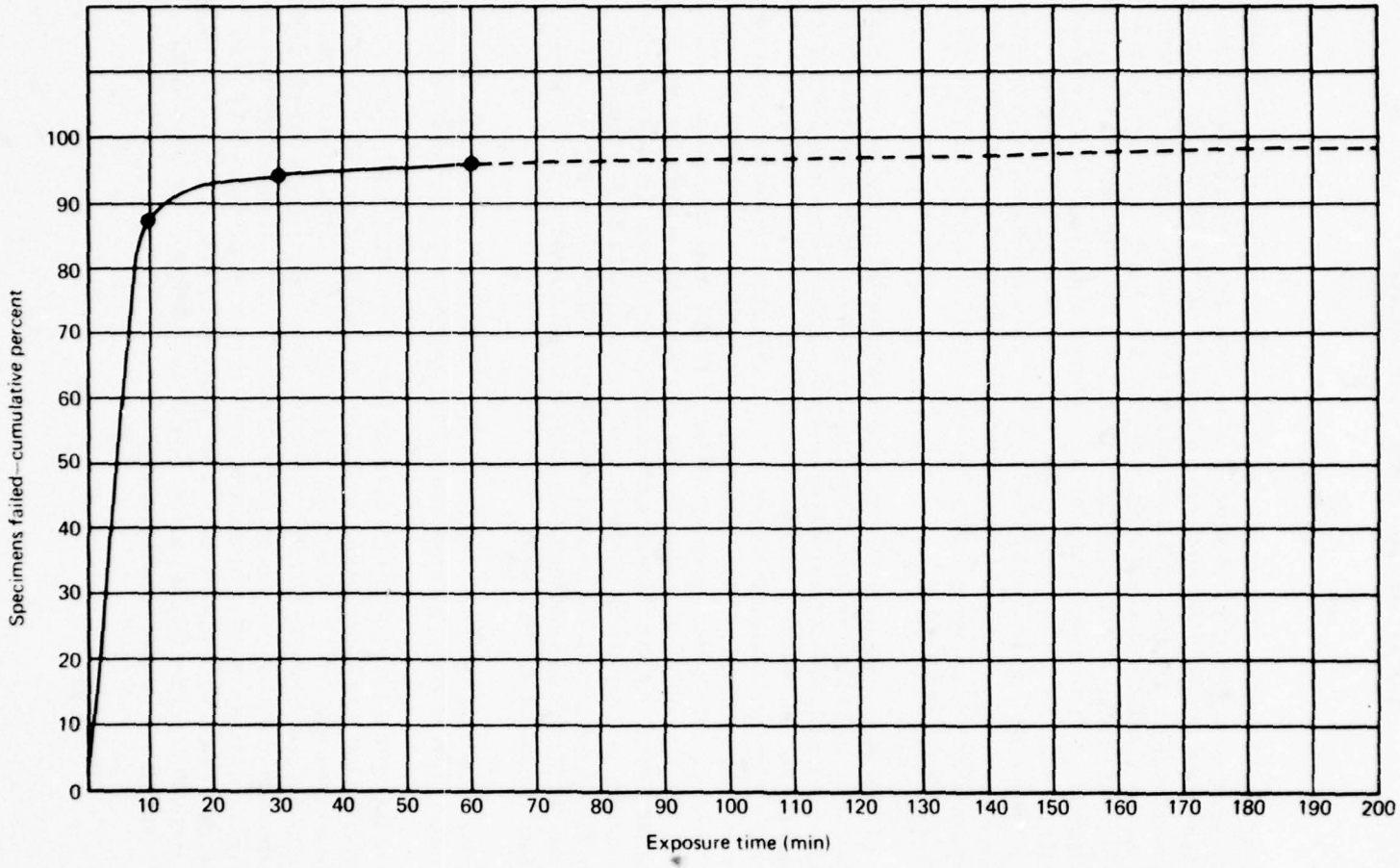

Figure 16.—Percent Failed Specimens Vs. Test Time—Sustained-Load Stress Corrosion (Ref. 4).

4.0 RESULTS AND DISCUSSION

4.1 PHASE I

The results of Phase I have been presented in detail in an interim report (ref. 3). Heat treatment study variations ranged from mill annealed (MA) covering the ranges of time and temperatures allowed per MIL-H-81200, duplex and recrystallize anneals (DA and RA, respectively), and beta annealing (BA). The DA and RA heat treatments are differentiated by the cooling rate from the first annealing temperature, air cool for the former and furnace cool for the latter. Briefly summarizing the Phase I effort, beta annealing was selected as the best damage-tolerant thermal treatment for plate and a sub-transus duplex anneal was selected for sheet. Beta annealing was not considered viable for sheet because (1) formability is a consideration for sheet and beta annealing significantly reduces it, (2) there is concern with thin sheet gages that a single prior beta grain could span the thickness of the sheet, and (3) the increased chem-milling required after beta annealing (as opposed to sub-transus annealing) for sheet gages represents a significant material loss.

A number of compromises and tradeoffs were considered in the selection of beta annealing for the plate. The fatigue life is reduced substantially, at least for simple tension-tension tests, and there is considerable concern of premature crack nucleation associated with a large alpha colony size (ref. 5). However, with the philosophy of AFFDL (ref. 6) being that 95% of the fatigue life in aircraft structure is spent in crack propagation, beta annealing was the logical choice. This treatment provides the slowest crack growth rate and maximum toughness. (Beta-quenched material has been shown to have slower fatigue crack propagation characteristics (ref. 7), but water-quenched treatments were not considered due to the inherent distortion and residual stress problems. The same reference indicates BA and RA material to have equivalent toughness. That was not the case in this investigation; the BA was significantly superior to the RA condition.) The beta-annealed material will require a strength decrease of about 10 ksi, but the FCP and toughness properties are much superior to those presently attained when purchasing to MIL-T-9046.

An additional advantage to beta annealing plate is that this treatment reduces the crystallographic texture. Less anisotropy of properties is thus associated with beta-annealed material.

Selection of the optimum thermal processing for the sheet was more difficult, as only minor differences in the test data for the various processing conditions were observed. Ultimately, a DA of beta transus minus 50°F, 30 minutes, air cool plus 1350°F, 2 hours, air cool was selected. The decision to use this heat treatment was based on three primary considerations: (1) microstructure-properties relationships established for plate, i.e., as annealing temperature increased (increasing the amount of transformed beta), fracture toughness and FCP characteristics improved. Hence, the annealing temperature is close to the beta transus but low enough to ensure that it does not go over the transus. (2) Previously generated fracture data for sheet. (3) Practical mill processing considerations.

The conclusions drawn in Phase I were:

1. Strength is reduced by increasing the primary alpha or prior beta grain sizes and by increasing the amount of transformed beta (acicular alpha-beta).

2. Resistance to fatigue crack initiation is enhanced by reducing primary alpha grain size, by increasing the ratio of primary alpha to transformed beta, and by reducing the degree of basal plane texture.

3. High fracture toughness and good fatigue crack propagation characteristics are associated with low ratios of primary alpha phase to transformed beta, large primary alpha grain size, and large prior beta grain size. Fully acicular microstructures provided maximum damage-tolerant characteristics.

4. Fracture toughness, fatigue crack propagation characteristics, and resistance to fatigue crack initiation can be reduced by texture effects; i.e., when the stress direction is normal to the greater number of basal planes.

5. High-temperature processing of Ti-6A1-4V results in high fracture toughness and low fatigue crack propagation rates. Annealing above the beta transus produces the best damage-tolerant characteristics, but moderate strength and notched fatigue properties.

6. Low-temperature processing results in high strength and good notched fatigue characteristics, but low fracture toughness and high rates of fatigue crack propagation.

7. Beta annealing is the optimum thermal processing for Ti-6A1-4V plate used in the fabrication of airframe damage-tolerant structure. Duplex annealing is the optimum processing for sheet material.

4.2 PHASE II

The objective of Phase II was to determine the effects of chemistry variation (primarily oxygen), utilizing the heat treatments generated in Phase I, to provide a basis for the composition limits for the specification to be written. In addition, the first draft of specification for sheet and plate products was written and coordinated with the aerospace industry (suppliers and potential users).

4.2.1 MATERIALS

Three Ti-6A1-4V plates of varying composition and one sheet were tested in Phase II. The material was coded according to product form (P for plate and S for sheet) and oxygen content. Thus, P08 designated plate with nominally 0.08% oxygen and S15 designated sheet with 0.15% oxygen. The chemical composition of these materials is listed in table 1. The discrepancy between the Boeing and Timet oxygen contents on P08 cannot be explained. The Boeing analyses are extremely low, but they are consistent. The Boeing and vendor data correlate reasonably well for the other material heats. Beta transus for the plate was not determined. It was all annealed at 1900°F. At that temperature, we could be assured that we were over the beta transus, yet it was not high enough to cause excessive grain growth.

Table 1.–Chemical Compositions of Phase II Materials

Material description	Heat no.	Chemistry source	Beta transus temp., °F	Sample location	Alloying elements, wt percent						
					O_2	Al	V	Fe	N_2	C	H_2
1.125-inch	G8080	Timet		*	0.07	5.80	4.1	0.04	0.01	0.023	0.0038
ue P08		Boeing		P08-1**	0.0448	5.90	4.05	0.08	0.015	0.045	0.0063
				-3	0.0456	5.95	4.10	0.08	0.017	0.065	0.0059
				-5	0.0466	6.10	4.10	0.08	0.018	0.07	0.0061
1-inch plate	295452	RMI		*	0.126	6.1	4.0	0.19	0.011	0.02	0.0043
code P11		Boeing		P11-1	0.1272	6.00	3.85	0.18	0.016	0.070	0.0065
				-3	0.1148	5.95	3.85	0.21	0.020	0.020	0.0063
				-5	0.1221	6.03	3.93	0.24	0.020	0.025	0.0057
1-inch plate	294231	RMI		***	0.181	6.5	4.3	0.15	0.008	0.02	--
code P18		Boeing		-1	0.1935	6.60	4.05	0.16	0.017	0.045	0.0051
				-3	0.1855	6.70	4.15	0.19	0.017	0.045	0.0048
				-5	0.1339	6.60	4.02	0.16	0.014	0.050	0.0044
0.075-inch sheet	N0507	Timet		*	0.155	6.45	4.15	0.12	0.015	0.022	--
code S15		Boeing	1835	S15-1	0.1487	6.58	4.10	0.13	0.012	0.050	0.0073
				-4	0.1463	6.40	3.92	0.11	0.011	0.025	0.0066

*Ingot chemistry.

**Numbers denote fatigue specimens from which chemistries were taken. For plate, these specimens came from both surfaces and the center of one location.

***Plate chemistry.

The P08 and P18 materials were conventionally alpha-beta cross-rolled and annealed in accordance with MIL-T-9046F. These plates were subsequently beta annealed at 1900°F/20 minutes/AC + 1350°F/2 hours/AC. The microstructures of the as-received condition and following the beta anneal are presented in figures 17-19. It can be seen that P18 is heavily banded (fig. 18). Some areas have a BA structure, while other areas are indicative of an MA microstructure. The banding was eliminated with the BA. Basal plane pole figures for P08 and P18 prior and subsequent to the beta anneal are illustrated in figures 20 and 21.

The P11 plate was alpha-beta rolled and beta annealed. The microstructure and texture of this material are illustrated in figures 22 and 23. This plate was re-beta-annealed to assure that all three plates had the same beta anneal. The initial annealing temperature is not known.

The texture-controlled sheet material was produced under a previous Air Force contract (ref. 8). This sheet was supplied to Boeing by the Air Force to evaluate the effect of texture. It has a strong basal plane texture, as illustrated in figure 24. Microstructures of the MA (as received) and DA conditions can be seen in figure 25.

4.2.2 RESULTS AND DISCUSSION

Properties evaluated in this phase of the program included tensile, fatigue (center-notched and lap splice), fracture toughness, and FCP rates in air and 3.5% NaCl. The tensile, fatigue, and toughness data are summarized in table 2.

Only one clear trend is evident in table 2: the strength increases with increased oxygen content, already a well-established fact. (The tensile and fatigue specimens in this phase of the program were all stressed in the transverse direction.)

Neither the notched fatigue nor the lap splice data exhibited trends as a function of the oxygen level when the Phase I data are included. (The lives of each specimen are contained in appendix A.) The data may be related to microstructure, but the relationship is not obvious. Prior beta grain size and alpha colony packet size were measured and are displayed in table 3. There is an inverse prior beta grain size-notched fatigue life relationship that can be seen when comparing tables 2 and 3. There is not, however, nearly enough data nor a large enough spread in grain size to discern if this apparent trend is real.

The absence of an oxygen-fatigue life correlation led to testing of the lap splice specimens. It was decided to use a specimen more closely simulating aircraft structure, a 10-fastener lap splice specimen. No trend as a function of oxygen was observed in fatigue life from this test either, except that the fatigue lives observed in this test fluctuated in the same fashion as in the center-notched fatigue test. In this case, no trend with regard to prior beta grain size was observed.

Fracture toughness did not vary significantly with oxygen content. The value for P11 was significantly higher than the others, although it was an invalid value. A decrease in K_{IC} with increasing oxygen was anticipated. The high toughness anticipated for the P08 material, compared to the P11 material, may have been masked by the invalidity of the K_{IC} test.

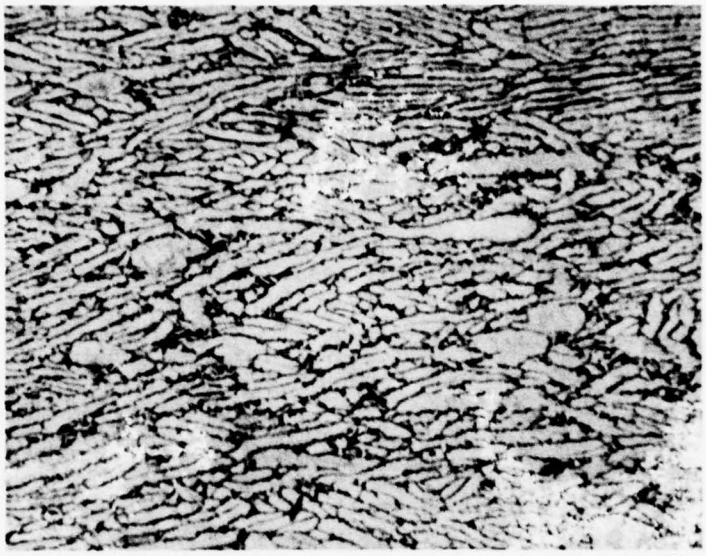

a) 500x

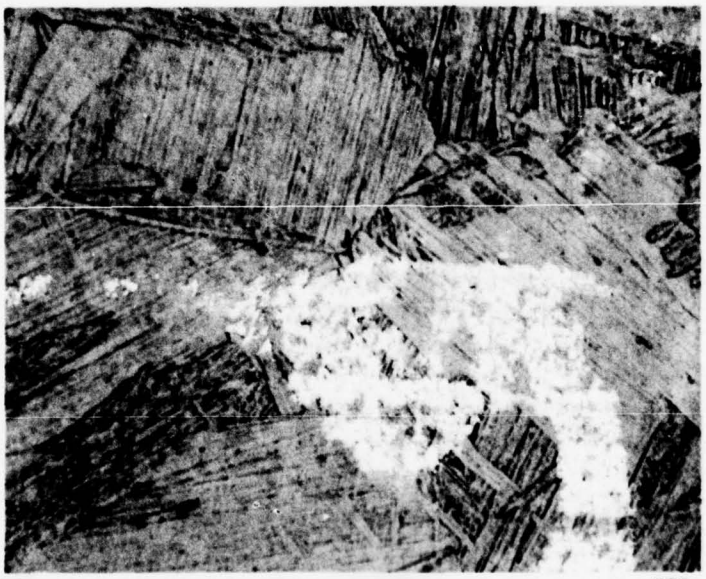

b) 500x

Figure 17.—Microstructures of Plate P08 in the (a) As-received (AA) Condition, and (b) BA Condition.

a) 4.2x

b) 500x

c) 500x

Figure 18.—Microstructures of Plate P18 in the As-received (MA) Condition Illustrating the Banded Nature of the Plate. (a) Macrophotograph Indicating Banding, (b) A Portion of the Plate Indicating a BA Structure, and (c) A Portion of the Plate Exhibiting an MA Structure.

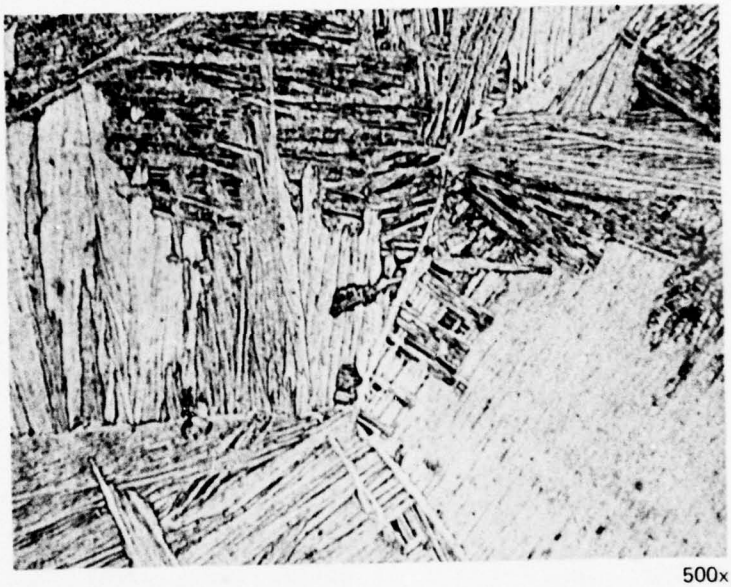

500x

Figure 19.—Microstructure of Plate P18 After BA.

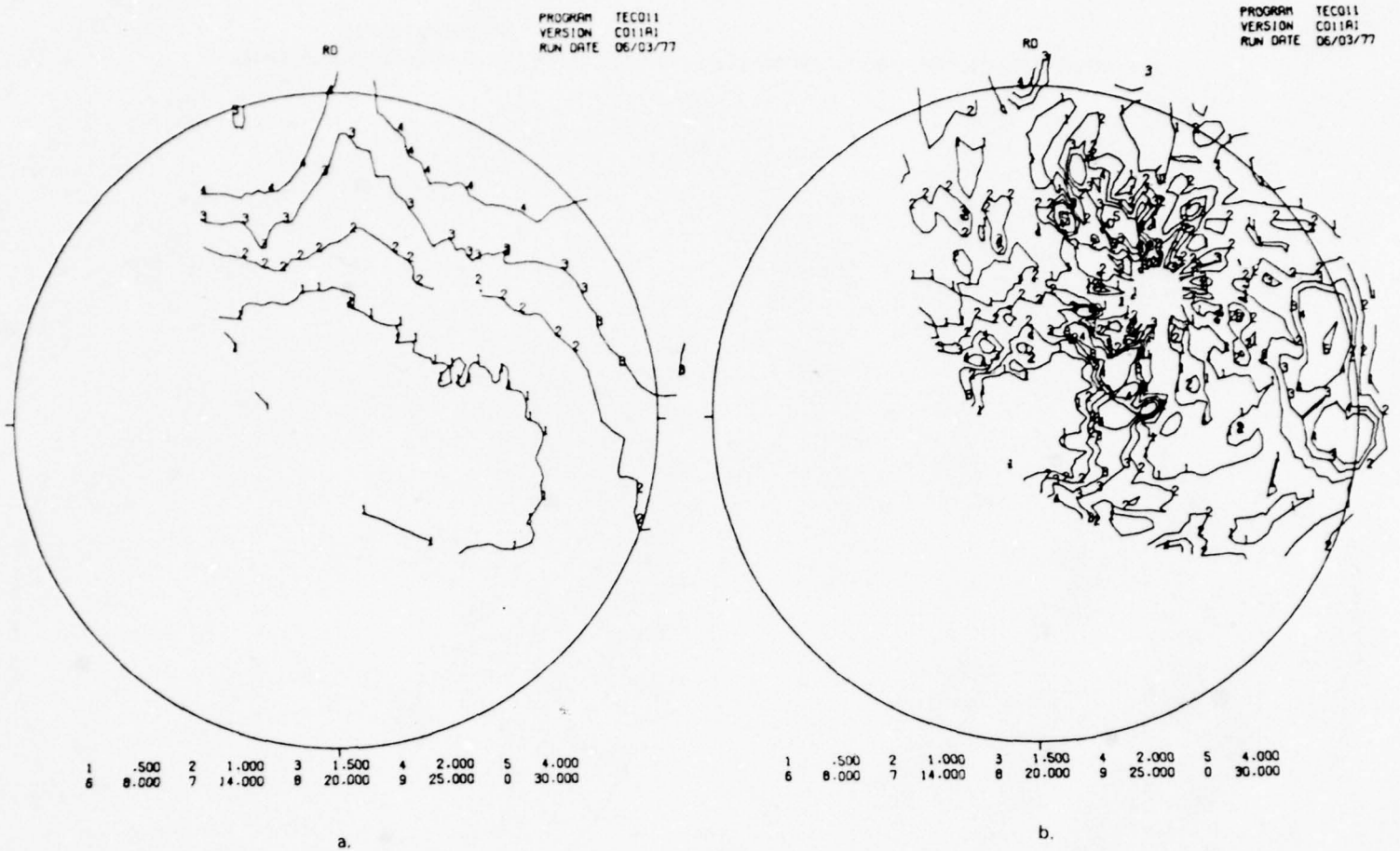

Figure 20.—Basal Plane Pole Figures of Plate P08 in the (a) As-received (MA) Condition, and (b) BA Condition.

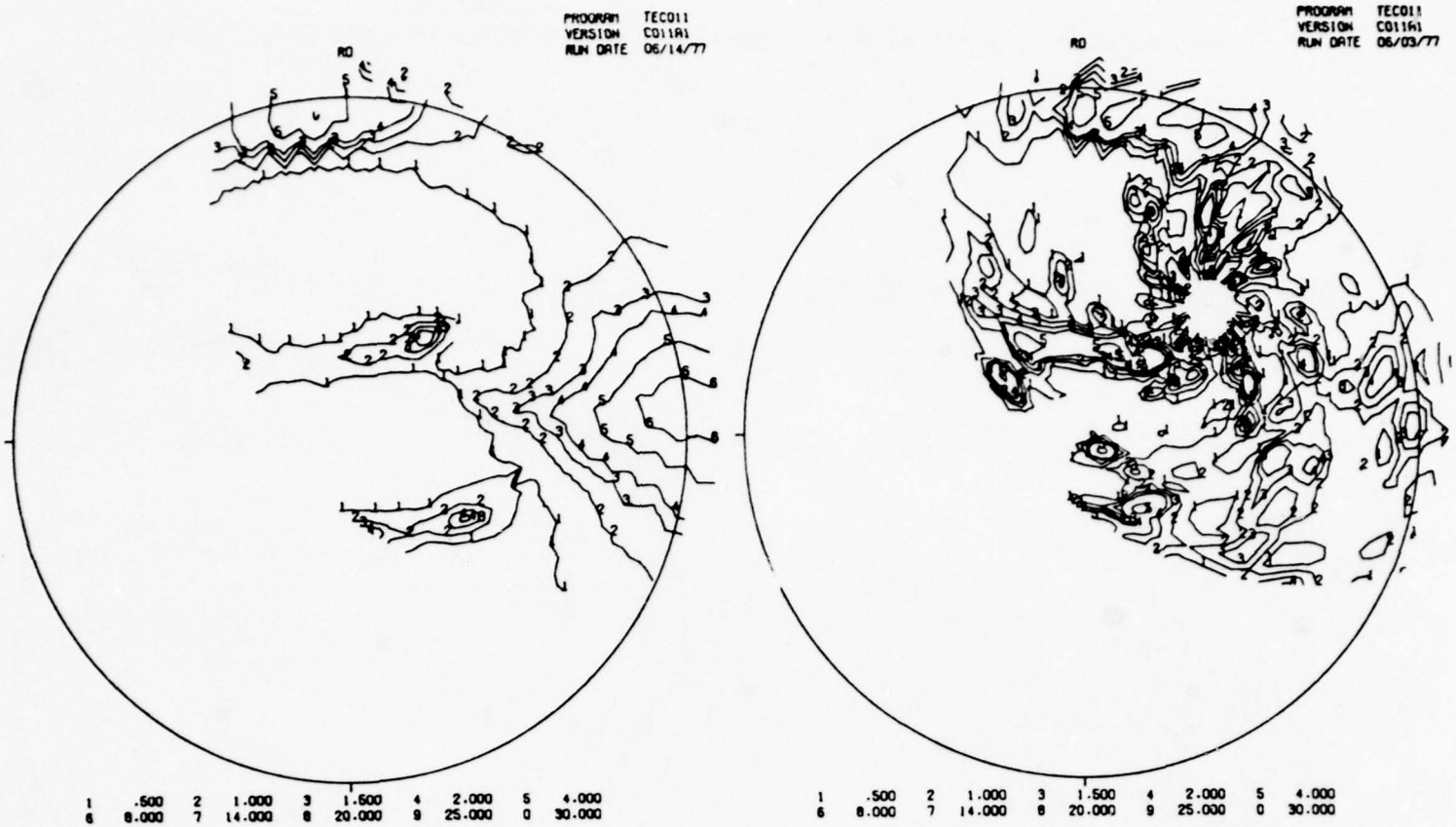

Figure 21.—Basal Plane Pole Figures of Plate P18 in the (a) As-received (MA) Condition, and (b) BA Condition.

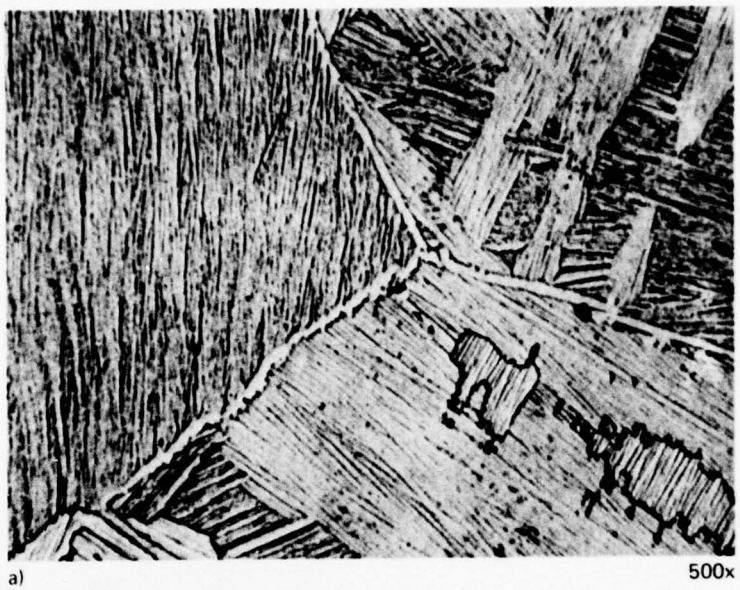

a) 500x

b) 40x

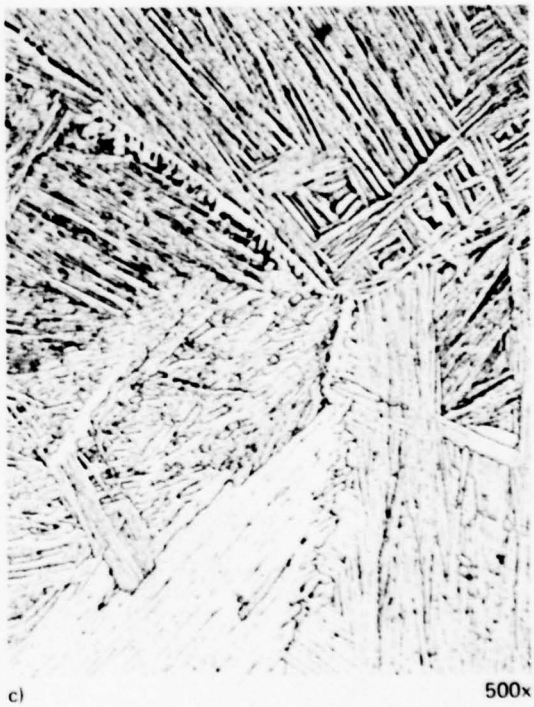

c) 500x

Figure 22.—Microstructures of Plate P11 in the (a) As-received (BA) Condition, and (b) and (c) BA Condition After Phase II Heat Treatment.

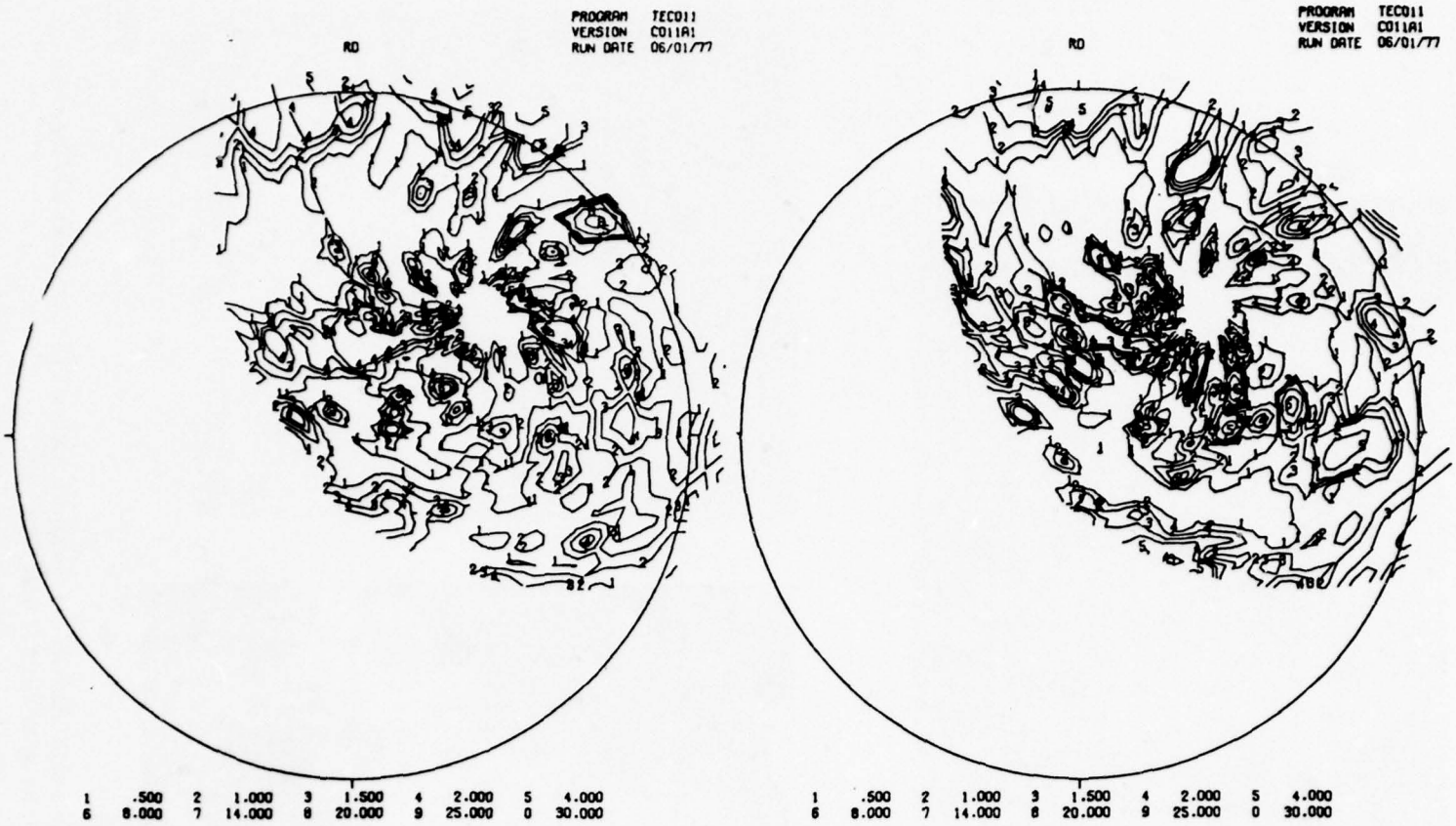

Figure 23.—Basal Plane Pole Figures of Plate P11 in the (a) As-received (BA) Condition, and (b) BA Condition After Phase II Heat Treatment.

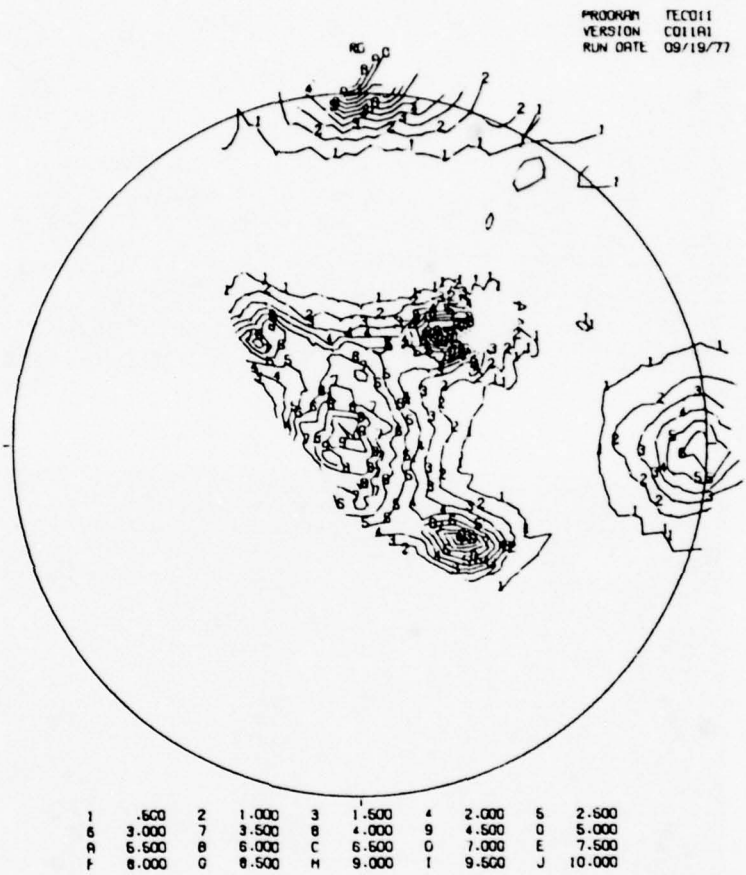

Figure 24.—Basal Plane Pole Figure of Sheet S15 After the DA Treatment.

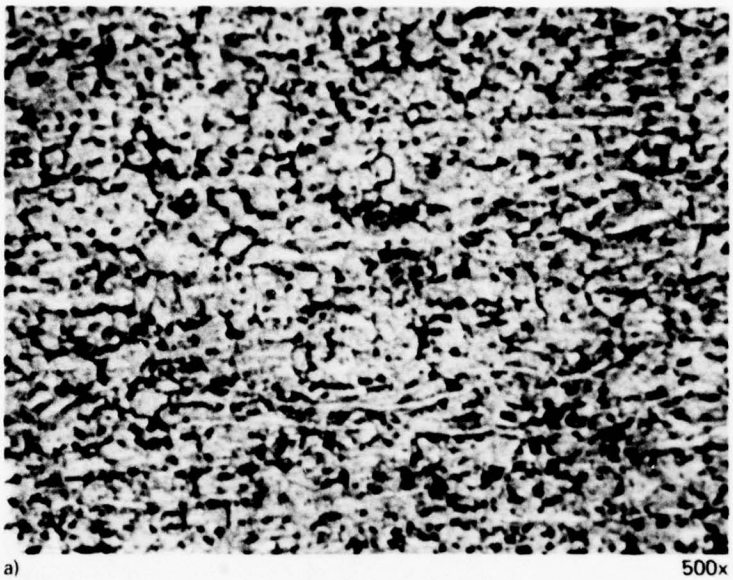

a) 500x

b) 500x

Figure 25.—Microstructures of Sheet S15 in the (a) As-received (MA) Condition, and (b) DA Condition.

Table 2.—Tensile, Fracture, and Fatigue Properties of Ti-6Al-4V Sheet and Plate (Phase II Material)

Form	Heat treatment	Nominal oxygen content (wt %)	TUS (ksi)	TYS (ksi)	RA (%)	Elong. (%)	Fatigue life* (cycles)		K_{IC} (ksi$\sqrt{in.}$)
							Notch	Lap splice	
Plate	1900° F/20 min./AC + 1350° F/2 hrs./AC	0.08	125-126	113-115	26-31	10-13	52,000	98,000	82.7**
		0.11	134-138	124-128	17-20	8-10	39,000	70,000	87.3**
		0.13***	135	124	17-19	8-10	65,000	145,000	80.4
		0.18	142-145	131-133	17-24	10-12	36,000	85,000	77.9
Sheet	1785° F/30 min./AC + 1350° F/2 hrs./AC	0.15	130-139	128-134	--	16	57,000	185,000	--

*Log average life at:

Center hole notch: σ_g = 50 ksi, R = 0.05, K_t = 2.53, f = 1800 cpm

Lap splice: σ_g = 30 ksi, R = 0.05, f = 1800 cpm

**K_{IC} invalid due to ASTM E399 thickness criterion.

***Beta annealed plate from Phase I included for comparison.

Table 3.—Prior Beta Grain Size and Alpha Colony Packet Size for Phase II Plate

Oxygen content, weight %	Prior beta grain size, $\bar{\ell}_\beta$, in μm	Packet size, $\bar{\ell}_\beta$, in μm
0.08	562	47
0.11	620	74
0.18	671	48

NOTE: Prior beta grain size determined in accordance with ASTM E112 except that the fields of view did not contain 50 grains. Three randomly selected fields of view were used, providing a total of about 50 prior beta grains in the determination. Packet size was determined using the linear intercept technique.

The lower yield strength of the P08 material (i.e., 114 versus 126 ksi) results in greater invalidity and a more conservative value. Linear regression analyses using data from numerous heats of the various product forms (sheet, plate, extrusions, and bar and forging stock) all indicate a negative oxygen effect on K_{IC} (and K_{ISCC}), i.e., increasing oxygen decreases the toughness and stress-corrosion resistance (refs. 1, 2). Regression analyses of the air toughness were only run on extrusions and bar and forging stock. These analyses did show a negative oxygen coefficient for both product forms (beta-annealed condition). It seems reasonable to assume that the same trends would occur for the plate product. K_{ISCC} data for SST plate (fig. 26) shows a definite trend with oxygen. The DOT-SST follow-on program data are considered important to this program, to aid in selection of a maximum oxygen content for the specifications, due to the number of heats involved. Use of these data aids in smoothing out effects due to data scatter, which cannot be assessed when evaluating only three or four heats of material as in this study.

A pronounced drop in K_{IC} as oxygen was increased from about 0.12 to 0.18 weight percent was observed by Chesnutt (ref. 9) for beta-quenched Ti-6A1-4V. The fracture toughness dropped from 90-100 ksi$\sqrt{\text{in.}}$ at the lower oxygen level to 62 at the higher oxygen content. Similar behavior was observed for RA materials.

The da/dN testing in this phase of the program was conducted in the ΔK range of approximately 15-30 ksi$\sqrt{\text{in.}}$ at a frequency of 1 Hz and R = 0.05. Only the T-L specimen orientation was tested. Initial testing of the plate material was done using DCB specimens. These data showed considerable scatter in the 10-20 ΔK range (these data are contained in the appendix). This is attributed to the difficulty of accurately measuring the crack length in the side groove of the DCB specimen. Compact tension specimens were machined and the specimens retested.

The FCP data also exhibited erratic behavior as a function of oxygen content (fig. 27). The P11 material had the slowest crack growth rate, in both air and salt. P08 and P18 displayed similar crack growth behavior in air, and P18 had the fastest growth rate in salt water. Yoder et al. (ref. 10) also studied the crack growth rate in air of beta-annealed Ti-6A1-4V as a function of oxygen content and reported similar results with regard to oxygen, i.e., no trend. They were, however, able to establish a correlation of the FCP rate to packet size; as the alpha packet size decreased, the crack propagation rate increased. They also reported a knee in their da/dN curves related to the transition from microstructurally sensitive crack growth below the transition from microstructurally insensitive growth above the transition point. They observed that this transition occurred at the point where the reversed plastic zone size approximated the Widmanstatten packet size. This will be discussed more fully later in conjunction with the Phase III data. The FCP rate-packet size relationship derived by Yoder et al. does appear to apply to the Phase II data (compare fig. 27 and table 3). P11 has the largest packet size and lowest growth rate. P08 and P18 have similar packet sizes and exhibit similar FCP rates in air.

The Phase I FCP plate data fell within the scatter band of the Phase II data.

No significant effects of the basal plane texture of the sheet evaluated in this phase of the program were observed. The properties were very similar to those observed in Phase I

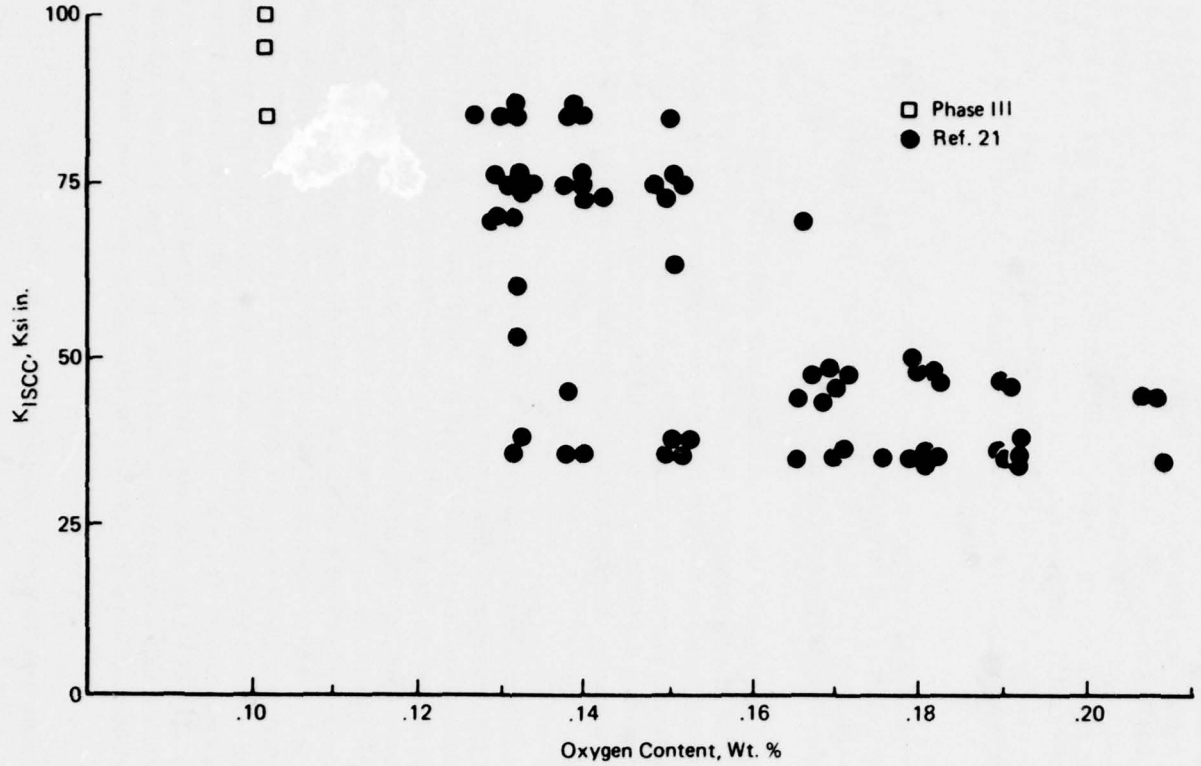

Figure 26.—K_{ISCC} of Beta Annealed Ti-6A1-4V Plate as a Function of Oxygen Content.

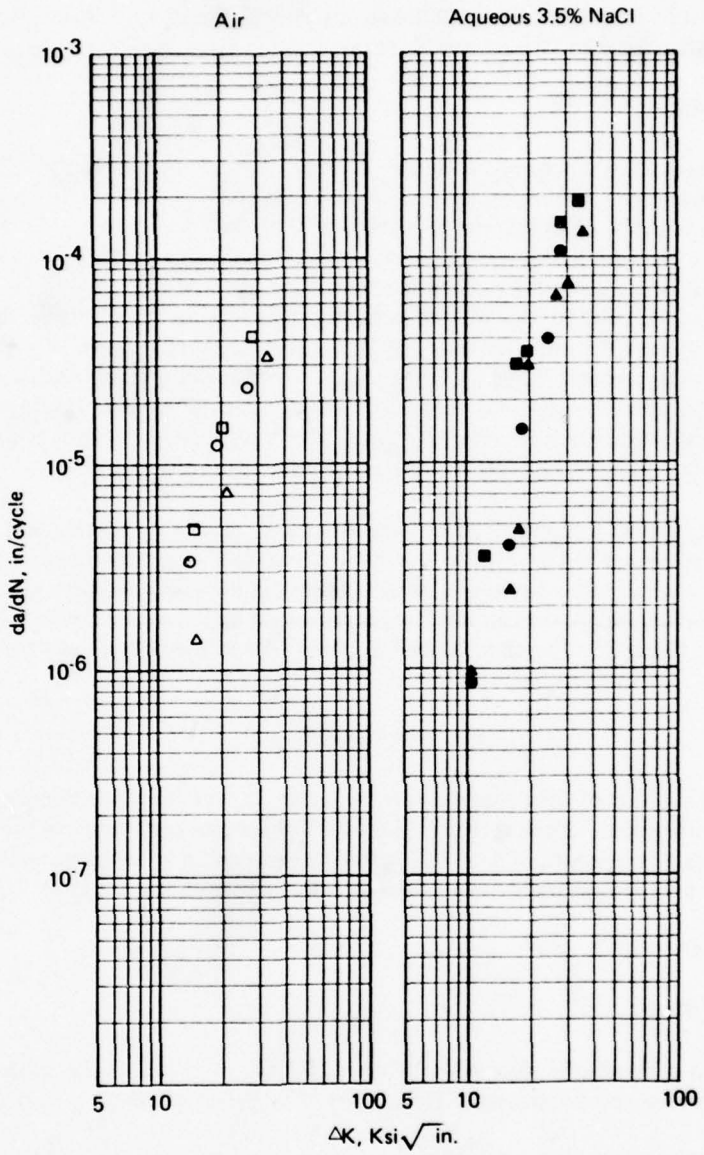

Figure 27.—Fatigue Crack Growth Rate in Air and Aqueous 3.5% NaCl as a Function of ΔK for Phase II Plate Material (T-L Orientation).

○ *P08*
△ *P11*
□ *P18*
Open Symbols = Air
Solid Symbols = 3.5% NaCl

(table 4 and fig. 28). The lower strength of the Phase II sheet can be related to the lower oxygen and aluminum contents of this material as opposed to the Phase I sheet. Again, the Phase II data fell within the Phase I scatter band.

4.2.3 CONCLUSIONS

Based on the data generated in this phase of the program, there was no basis for selecting a maximum oxygen level for premium-quality, damage-tolerant Ti-6A1-4V. The decision (to require super ELI quality, 0.11 maximum oxygen) was therefore based on previous data generated during the DOT-SST follow-on program (refs. 1 and 2) where data from a larger number of heats with widely varying oxygen contents were available. Rockwell International (ref. 11) also reported decreasing K_{IC} with increasing oxygen levels. In addition, there is a general feeling throughout the industry that higher oxygen contents are generally associated with poorer fracture properties. While a slight drop in strength is attendant with a super-ELI material, it is felt that there is sufficient data that indicate that the greatest assurance of achieving the maximum fracture properties requires specifying super-ELI material. This is particularly applicable if environmental factors are taken into consideration.

With this in mind, first drafts of specifications for sheet and plate were written and sent out for coordination throughout the aerospace industry. These specifications also contained cross-rolling requirements to minimize texture effects, making the products as isotropic as is feasible. A piece of plate was then ordered from RMI to be processed in accordance with this specification for testing in Phase III. The sheet tested in Phase III was sheet produced for the SST program.

4.3 PHASE III

The objectives of this phase of the program were twofold: (1) provide specifications for procurement of premium-grade damage-tolerant Ti-6A1-4V sheet and plate (the proposed specifications are contained in appendix C), and (2) produce material in accordance with the proposed specification and demonstrate the damage-tolerant nature of the material.

4.3.1 MATERIALS

4.3.1.1 Ti-6A1-4V Plate

The plate material was purchased from RMI. They had available a 4.75- x 26- x 63-inch slab of Ti-6A1-4V containing approximately 0.1% oxygen. The process history to this stage was as follows:

1. Thirty-inch-diameter ingot was upset at 2100°F.
2. The upset ingot was forged into a slab in three stages:
   - First, at 1925°F, it was forged to 16 x 16 inches in length.
   - Second, at 1925°F, it was forged to 8 x 16 inches in length, cooled, and conditioned.
   - Third, it was forged to 4.75 x 26 x 63 inches at 1750°F, cooled, and conditioned.

Table 4.—Comparison of Phase I and Phase II Sheet Data

1st anneal* temp., °F	Test direc.	TUS ksi	TYS, ksi	Elong., %	Fatigue life,** cycles x 10^3
β_T-70 (Phase I)	T	140.5	136	14	454.5
β_T-50 (Phase II)	T	134.5	131	16	57
β_T-35 (Phase I)	T	143	136	13	50.8

*Anneal time 30 minutes followed by an air cool and a 1350°F/2 hr./AC age.

**Log average life for center-hole-notched fatigue specimens, σ_g = 50 ksi, K_t = 2.53, R = 0.05.

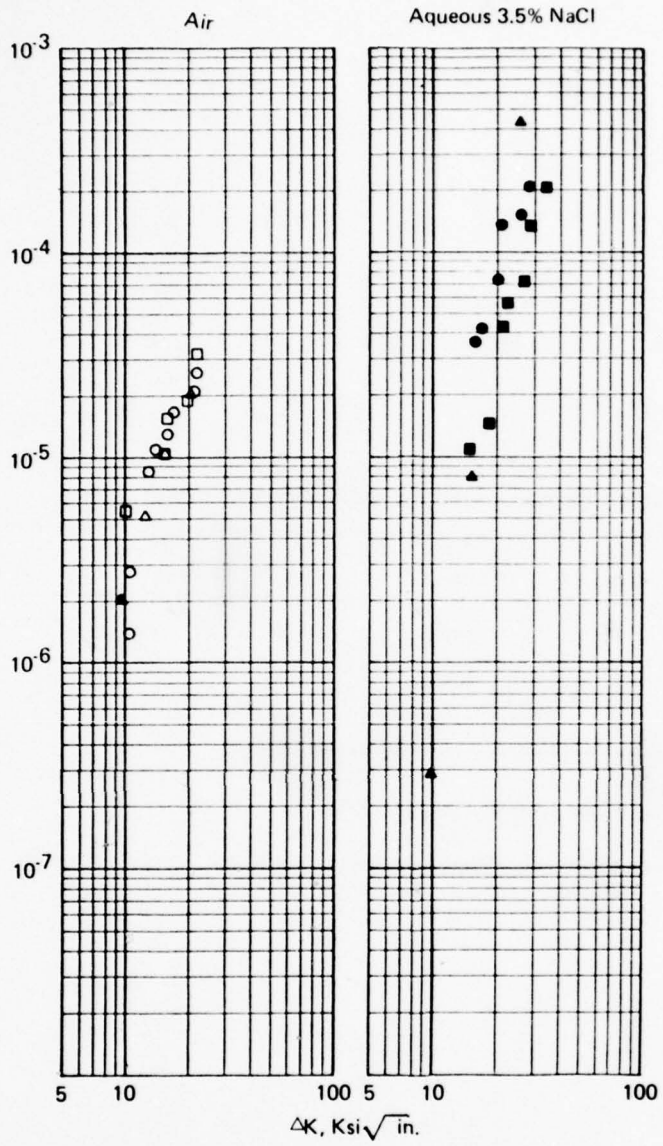

Figure 28.—Phase I and Phase II Sheet Fatigue Crack Propagation Rates in Air and Aqueous 3.5% NaCl (T-L Orientation). Open Symbols = Air, Solid Symbols = 3.5% NaCl.

Ann. Temp.: ○ *Phase I, 1735° F*
□ *Phase I, 1770° F*
△ *Phase III, 1785° F*

The billet was then rolled, per our instructions, as outlined below:

1. The billet was preheated at 1725°F. Before start of rolling, the billet temperature was 1630°F. The billet was reduced from 4.75 to 2.65 inches in seven passes. The finish temperature was 1480°F.

2. The billet was recharged into a 1725°F furnace for 15 minutes.

3. The billet was turned 90 degrees and finish rolled to 1.58 inch thickness in four passes. Starting temperature was 1600°F and finish temperature was 1500°F.

4. The plate was roll-leveled in three passes and air cooled to room temperature. The final cleaned-up dimensions were 1.50 x 48.00 x 95.94 inches.

5. The plate was beta annealed at 1845°F, 20 minutes, air cooled, and aged at 1350°F, 2 hours, air cooled.

The beta annealing temperature was dropped to beta transus plus 50°F (1845°F) from the 1900°F temperature used in Phases I and II in the interest of minimizing grain growth and contamination losses. The RMI-supplied certification data for this material are contained in tables 5 and 6. The microstructure and crystallographic texture of this material are illustrated in figures 28 and 29.

4.3.1.2 Ti-6Al-4V Sheet

The sheet material used in this phase of the program was material previously purchased by Boeing (for the SST program) with a nominal oxygen content of 0.11%. Even though the processing history is not well defined, this material was used because the chemistry was close to that desired and funding to purchase the custom-processed sheet was not required. This sheet (0.128 x 28 x 203 inches in size) was conventionally alpha-beta rolled and duplex annealed at 1675°F/10 minutes/AC + 1350°F/4 hours/AC. The rolling temperatures and amount of cross-rolling are not known. The RMI-supplied certification data for the as-received sheet are presented in tables 7 and 8. For this program, the material was again duplex annealed at 1730°F (beta transus minus 50°F)/10 minutes/AC + 1350°F/2 hours/AC. The resulting mechanical properties data are also included in table 8. The small difference in strength between the longitudinal and transverse directions suggests that the sheet was not strongly textured, which was as desired. The microstructures of this material as received and after re-heat-treatment are presented in figure 31. The basal plane pole figure for the Phase III sheet after heat treatment is illustrated in figure 32.

4.3.2 RESULTS AND DISCUSSION

The properties evaluated during this phase of the program included:

1. Tensile properties

2. Fracture properties–K_C, K_{IC}, K_{SCC}, K_{ISCC}

Table 5.—Chemical Composition of Phase III Plate Material

	Alloying elements, weight percent							
	O_2	Al	V	Fe	N_2	C	H_2	Y
1.5-inch plate	0.102	6.1	4.0	0.15	0.010	0.02	0.048	<0.005
Proposed specification	0.11 max.	5.7-6.2	3.6-4.4	0.25 max.	0.03 max.	0.05 max.	0.0125 max.	0.005 max.

NOTE: Beta transus was 1795°F.

Table 6.—Mechanical Properties of Phase III Plate Material

	UTS, ksi		TYS, ksi		Elong., %	
	L	T	L	T	L	T
1.5-inch plate	134.6, 135.9	134.1 136.7	120.8, 121.8	121.1, 122.5	14, 14	12, 15
Proposed specification requirement*	125 min.		112 min.		8 min.	

*The average results of the tensile tests for each lot shall show a maximum difference between the longitudinal and transverse directions of 4.0 ksi for the ultimate tensile strength and 5.0 ksi for the yield strength.

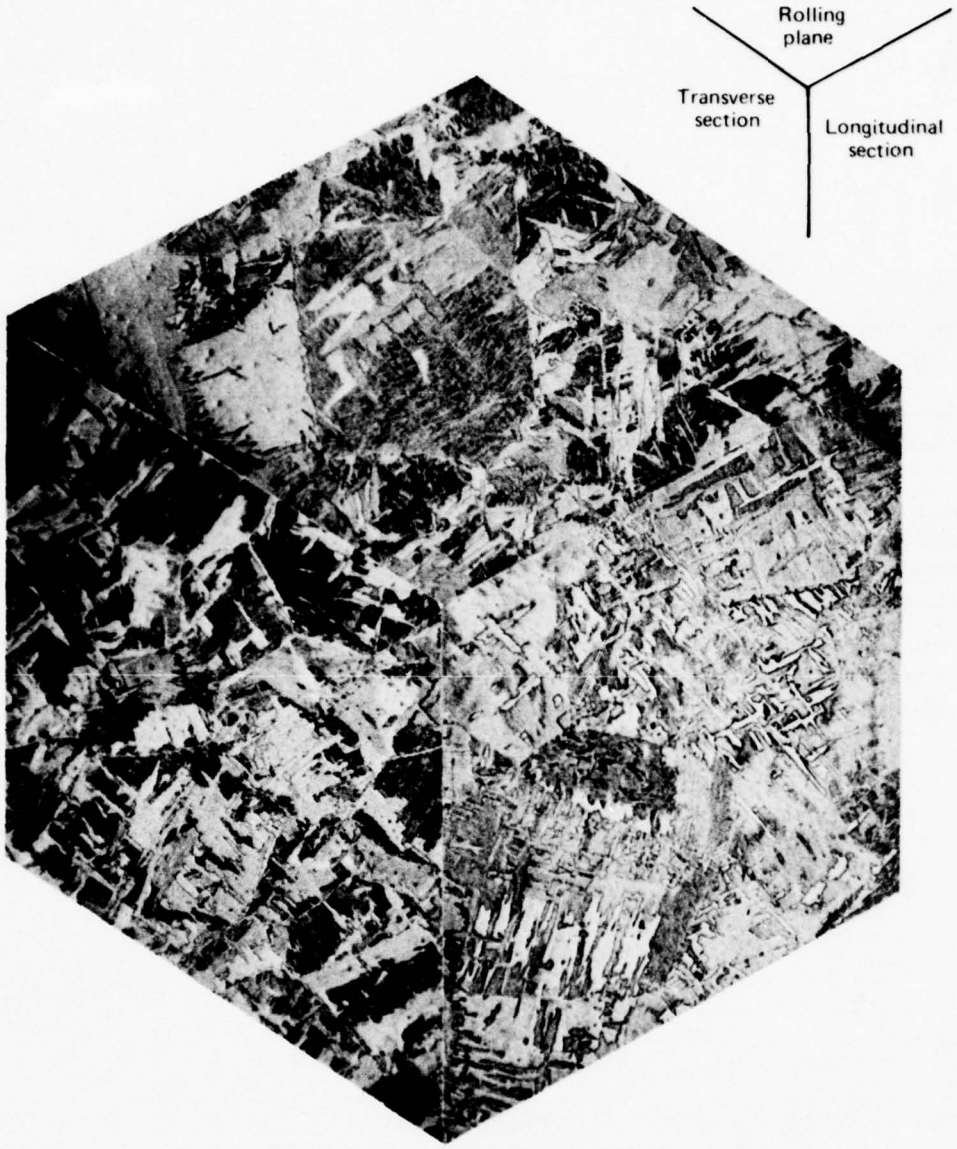

a.) 40x

Figure 29.--Microstructure of Phase III Beta Annealed Plate.

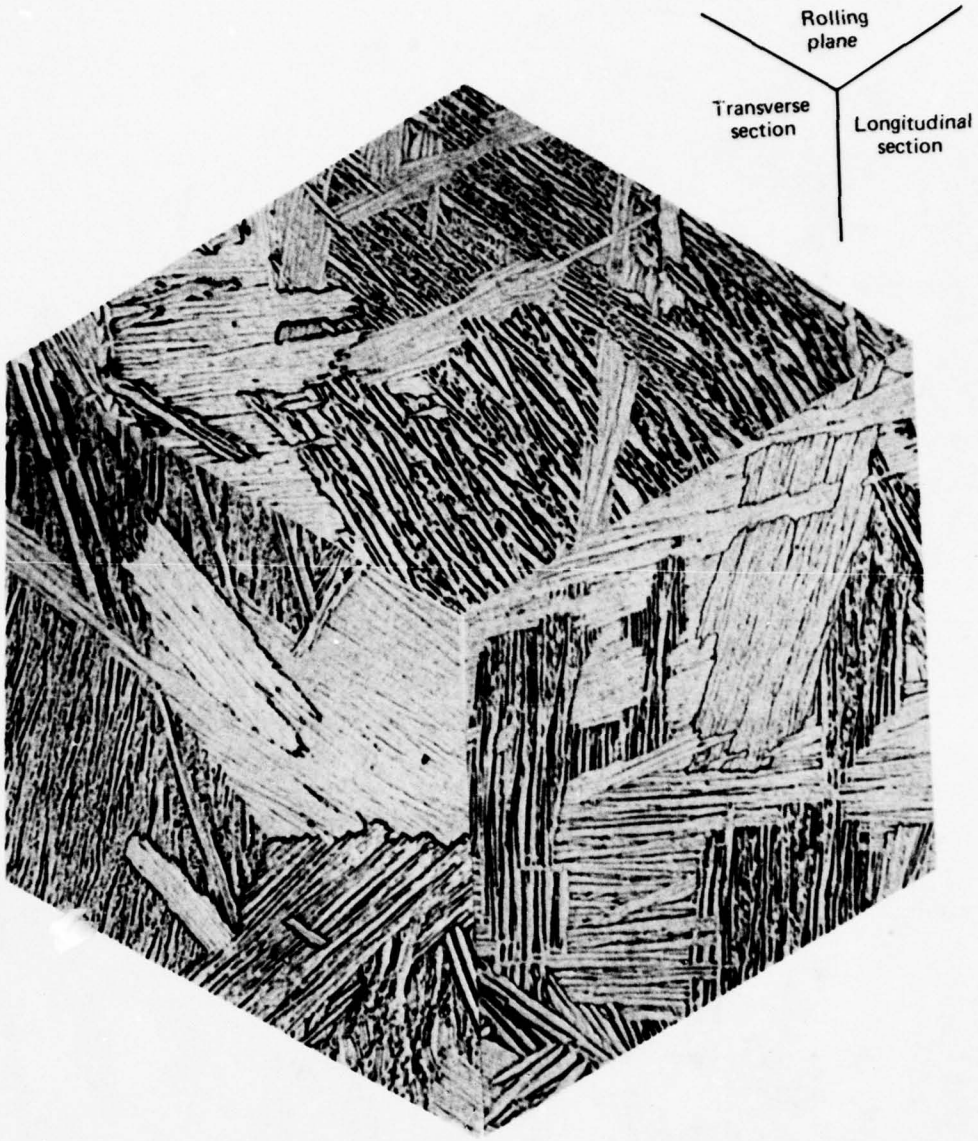

b.) 500x

Figure 29.—(Concluded).

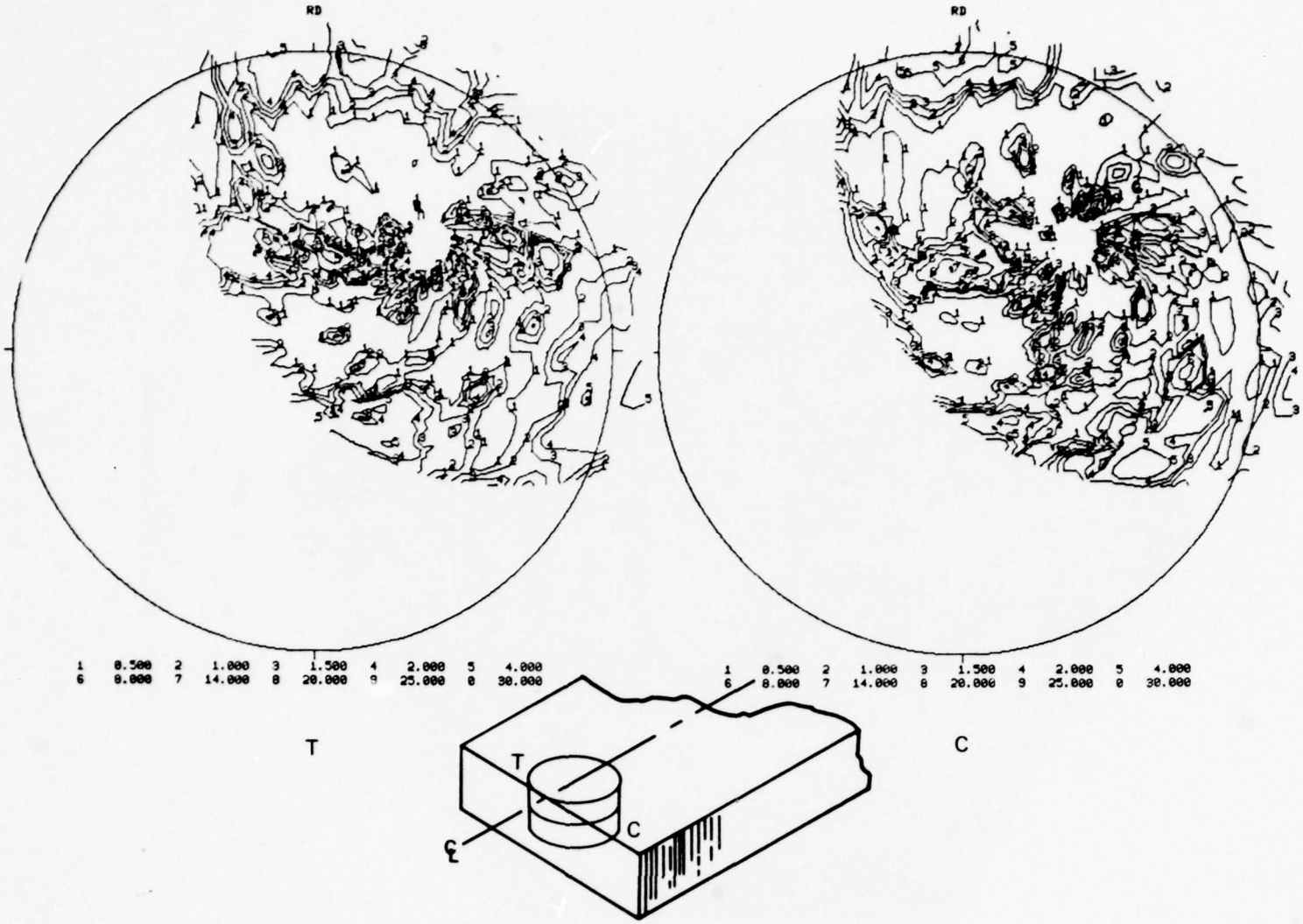

Figure 30.—Basal Plane Pole Figures of Phase III Beta-annealed Plate (T-Top Third, C-Middle Third Section From the End of the Plate)

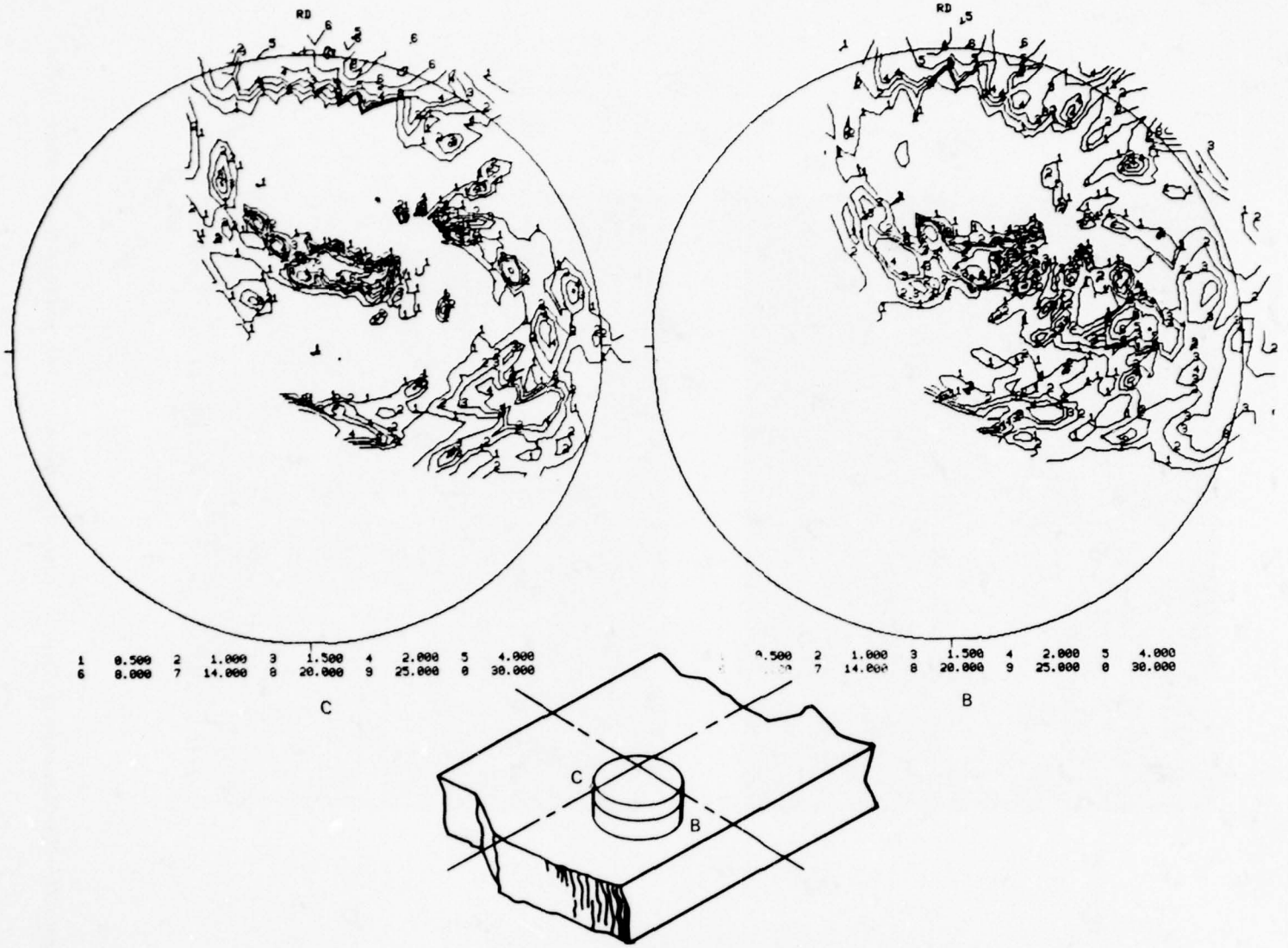

Figure 30.—(Concluded)—Basal Plane Pole Figures of Phase III Beta-annealed Plate (C-middle Third, B-bottom Third Section From the Center of the Plate).

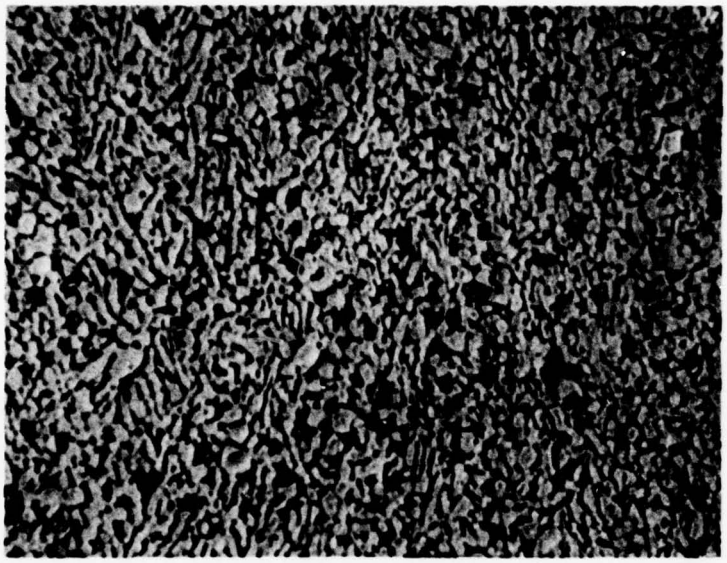

a) 500x

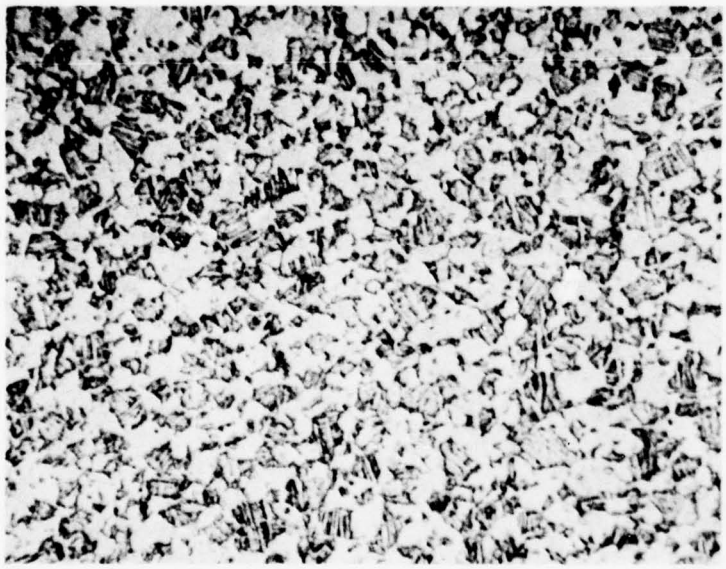

b) 500x

Figure 31.—Microstructure of Phase III Sheet (a) As-received (DA), and (b) After the Phase III DA.

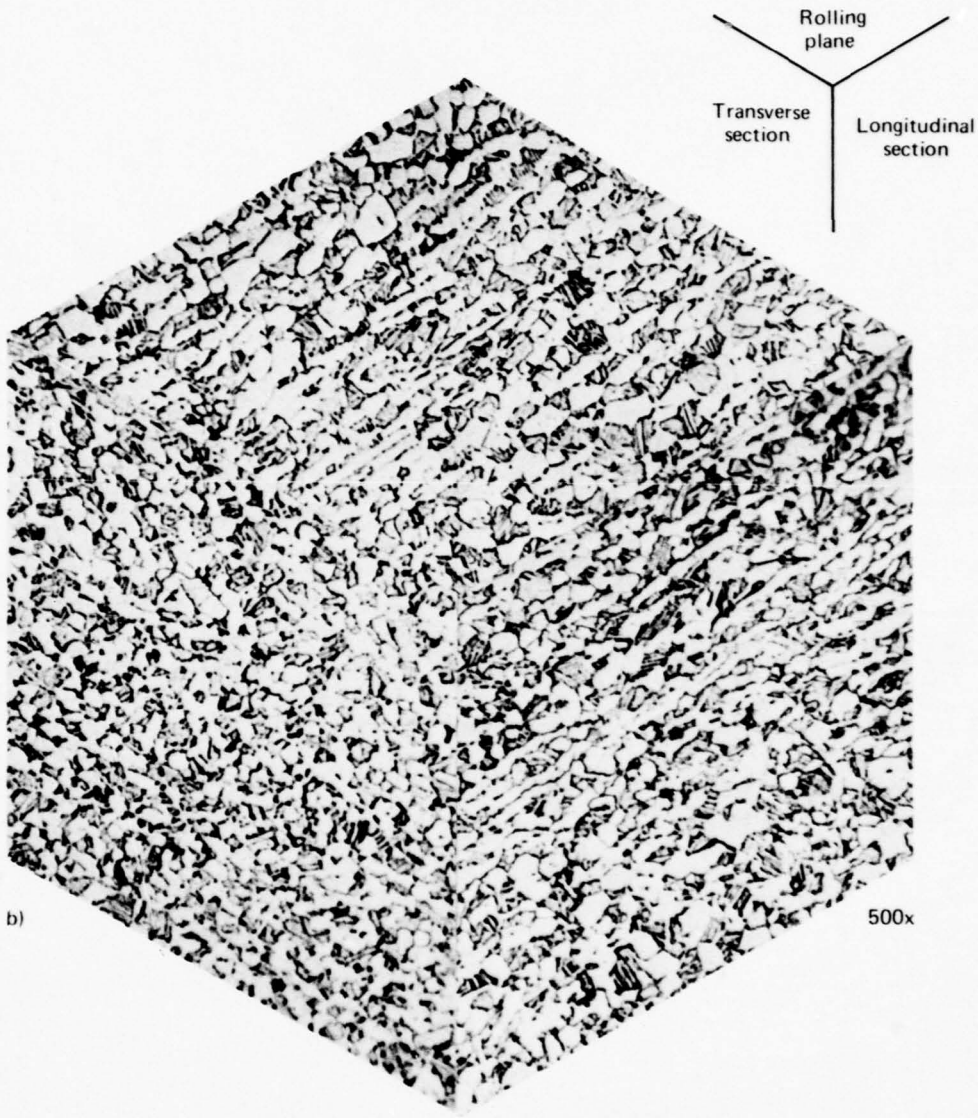

Figure 31.—(Concluded).

Table 7.—Chemical Composition of Phase III Sheet Material

	Alloying elements, weight percent							
	O_2*	Al	V	Fe	N_2	C	H_2	Y
0.128-inch sheet	0.111	6.0	4.0	0.19	0.01	0.02	0.0034	--
Proposed specification	0.11 max.	5.7-6.2	3.6-4.4	0.25 max.	0.03 max.	0.05 max.	0.0125 max.	0.005 max.

*Boeing conducted three oxygen analyses which yielded 0.1017, 0.0911, and 0.0963.
NOTE: Beta transus was 1780°F.

Table 8.—As-Received Mechanical Properties of Phase III Sheet Material

	UTS, ksi		TYS, ksi		Elong., %	
	L	T	L	T	L	T
As-received sheet	135.3, 135.3	134.0, 135.6	125.1,	127.8, 126.8	15, 15	15, 15
Duplex-annealed	136-137	135-138	129-130	131-133	15-17	13-15
Proposed specification requirement*	130 min.		120 min.		10 min.	

*The average results of the tensile tests for each lot shall show a maximum difference between the longitudinal and transverse directions of 4.0 ksi for the ultimate tensile strength and 5.0 ksi for the yield strength.

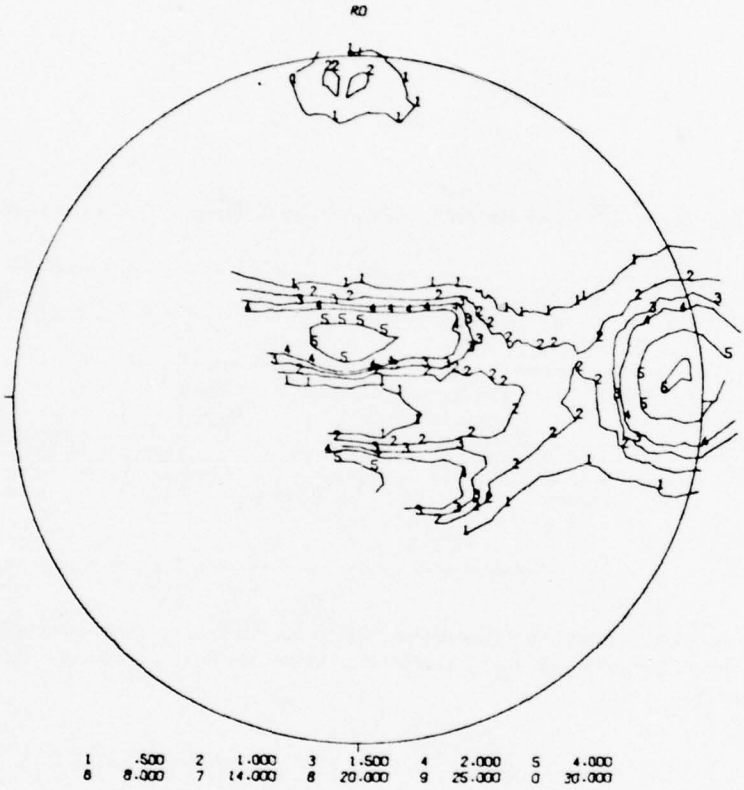

Figure 32.—Basal Plane Pole Figures of Phase III Sheet.

3. Fatigue properties–S-N curves and Constant Life Diagrams were developed using smooth and center-notched specimens (K_t = 1 and 2.53, respectively) at R ratios of 0.5, 0.05, and -1 (all testing in air).

4. Fatigue crack propagation rates over a ΔK range from about 10 to 50 ksi$\sqrt{\text{in.}}$ at R ratios of 0.05 and 0.5 in both air and 3.5% NaCl, using both compact tension and surface-flaw specimens were developed.

4.3.2.1 Tensile Properties

The tensile data for the sheet material is presented in table 8. In addition to the plate vendor certification data, three longitudinal and three transverse tensile tests were conducted. The minimum tensile strength obtained was 131 ksi, minimum yield strength was 119 ksi, and minimum elongation was 10% (the tabulated data are contained in appendix B). Both the sheet and plate materials used in Phase III exceeded the strength requirements and met the isotropy requirements of the proposed specifications.

4.3.2.2 Fracture Properties

4.3.2.2.1 Plate.–Three K_{IC} tests were conducted in both the T-L and L-T orientations. The values for the former ranged from 86.5 to 92 ksi$\sqrt{\text{in.}}$ and for the latter ranged from 89.5 to 101.9 ksi$\sqrt{\text{in.}}$ The K_{IC} values are only valid to 95.5 ksi$\sqrt{\text{in.}}$, due to the ASTM E399 thickness criterion. These values exceed the proposed specification minimum of 85 ksi$\sqrt{\text{in.}}$ The 85 ksi$\sqrt{\text{in.}}$ minimum fracture toughness value may appear tenuous based on a minimum value of this material of 86.5 ksi$\sqrt{\text{in.}}$ There is, however, a much larger data base that indicates this goal is attainable. In 1965, Lockheed (ref. 12) listed the fracture toughness of beta-annealed Ti-6A1-4V as 96 ksi$\sqrt{\text{in.}}$ A substantial data base was established in the DOT-SST follow-on program (refs. 1, 4). In that program, the K_{IC} of beta-annealed material generally exceeded 90 ksi$\sqrt{\text{in.}}$ McDonnell Aircraft Company (St. Louis) has purchased beta-annealed plates from four heats of Ti-6A1-4V (ELI grade) for the F-18. Three heats from one supplier had K_Q values (due to the thickness criterion) of 104, 108, and 114 ksi$\sqrt{\text{in.}}$ The plate from the second supplier had a K_Q of 84 ksi$\sqrt{\text{in.}}$ (ref. 13). In addition, General Dynamics–Convair (ref. 14) also performed extensive testing of beta-annealed ELI Ti-6A1-4V plate on an Air Force ADP program, contract AF33615-73-C-3001. They obtained fracture data from nearly 30 heats of plate. No K_{IC} values below 90 ksi$\sqrt{\text{in.}}$ were observed. These values compare to a specification minimum K_{IC} of 70 ksi$\sqrt{\text{in.}}$ requirement for RA plate by Rockwell International (ref. 11) and a minimum K_{IC} for MA plate purchased per MIL-T-9046, which would be about 40 ksi$\sqrt{\text{in.}}$

The stress-corrosion resistance of the Phase III material far exceeded the proposed specification minimum of 60 ksi$\sqrt{\text{in.}}$ The values ranged from 85 to 100 ksi$\sqrt{\text{in.}}$ for the T-L orientation; three values of 95 ksi$\sqrt{\text{in.}}$ for the T-L orientation were obtained (three tests in each orientation). Referring again to the General Dynamics-Convair program, they conducted their K_{SCC} tests at a maximum stress intensity of 62 ksi$\sqrt{\text{in.}}$ No crack growth was observed at this stress level on any of the specimens. Stress corrosion thresholds down to 22 ksi$\sqrt{\text{in.}}$ have been observed for MA plate (ref. 4). There is not much salt water K_{ISCC} data for RA plate,

but the threshold for ELI RA plate was reported as 45 ksi$\sqrt{\text{in.}}$ by Hall et al. (ref. 23).

4.3.2.2.2 Sheet.—The fracture toughness of the sheet material ranged from 147.3 to 173.6 ksi$\sqrt{\text{in.}}$ in the transverse test direction and 166.3 to 170.1 ksi$\sqrt{\text{in.}}$ in the longitudinal test direction, exceeding the proposed specification minumum of 140 ksi $\sqrt{\text{in.}}$ Again referring to DOT-SST follow-on program data, valid K_C data were developed on 14 heats of DA Ti-6A1-4V sheet. There was one value of 137.1 ksi$\sqrt{\text{in.}}$ and the remaining data ranged from 141.6 to 182 ksi $\sqrt{\text{in.}}$ The average longitudinal and transverse values from that program were 157.3 and 168.7 ksi $\sqrt{\text{in.}}$ respectively.

The stress-corrosion threshold for this sheet was 120 ksi$\sqrt{\text{in.}}$ (three tests, all the same value) in the transverse direction, and ranged from 120 to 154 ksi$\sqrt{\text{in.}}$ in the longitudinal test direction. This property, along with environmental crack growth, is one that clearly justifies the requirement for super-ELI material. A strong correlation between oxygen content and the stress-corrosion threshold has been demonstrated (refs. 1, 2, 16). Linear regression analyses correlating the stress-corrosion threshold of 46 heats of DA sheet to metallurgical and compositional parameters indicated that oxygen played a strong role in the value of this property. The best fit obtained of over 100 analyses was:

$$\text{Trans. } K_{SCC}\ (\text{ksi}\sqrt{\text{in.}}) = 321.9 - 714\ (\text{wt \% } O_2) - 228\ (\text{wt \% Al}) - 274\ (\Delta\text{TYS in ksi}) - 2.95\ (\text{O.F.}) - 0.224\ (\text{ppm } H_2)$$

where:

ΔTYS = transverse-longitudinal yield strength

O.F. = a factor quantifying the ordering ($\alpha \rightarrow d + Ti_3Al$) effects

The correlation coefficient for this equation was 0.88. It can be seen that on a statistical basis, dropping the oxygen 0.1% (from 0.2 to 0.1%) could increase K_{SCC} over 70 ksi$\sqrt{\text{in.}}$ Ninety percent of the data used in that analysis fell within a ±15 ksi$\sqrt{\text{in.}}$ scatterband. That is a very significant effect and one of the driving forces for specifying super-ELI material.

4.3.2.3 Fatigue Properties

4.3.2.3.1 Plate.—The data from the notched and smooth fatigue specimens can be seen in figures 33 and 34. The data behaved as would be anticipated with the fatigue life at a constant maximum stress increasing as R increases. No significant difference in fatigue behavior between the longitudinal and transverse test orientations was observed, so the trend lines drawn in are meant to be representative of both test directions.

It has been difficult to locate comparable data on standard grade mill-annealed Ti-6A1-4V to make a comparison between this product and the most commonly used grade and heat treatment. The only comparable data for smooth specimens ($K_t = 1$) found was for RA plate (ref. 17). These data have been superimposed on figure 33. The RA material has a fatigue strength about % higher than the BA treatment in the low-cycle regime with an

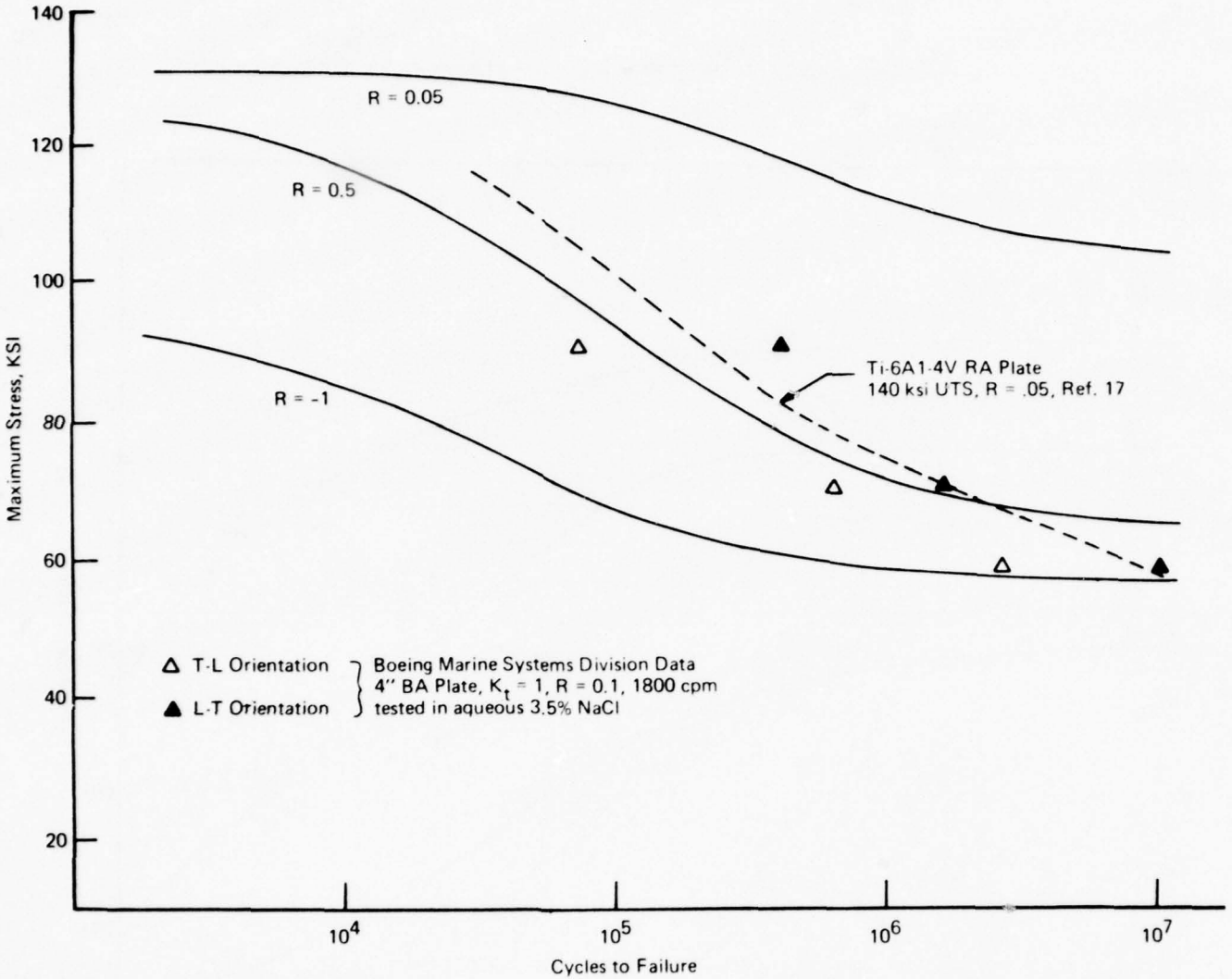

Figure 33.—Fatigue Life Vs. Maximum Net Area Stress for Phase III BA Plate Tested at 3 R Ratios, in Air, K_t = 1

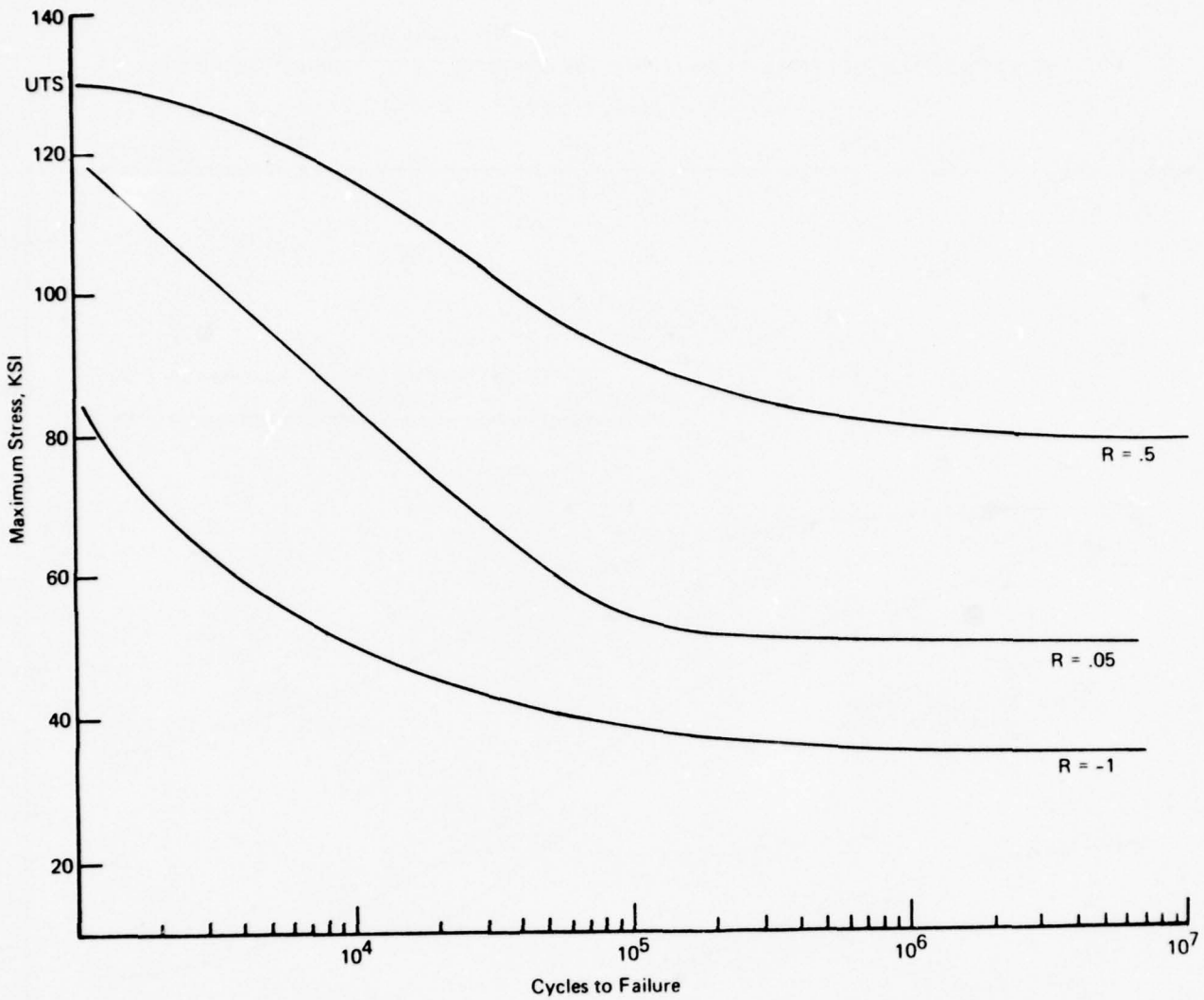

Figure 34.—Fatigue Life Vs. Maximum Net Area Stress for Phase III BA Plate Tested at 3 R Ratios, $K_t = 2.53$

apparent crossover at lives between 10^6 and 10^7 cycles, with the BA then being slightly superior. Also included are some data generated by the Boeing Marine Systems Division on 4-inch-thick beta-annealed ELI plate. This material was tested in salt water (aqueous 3.5% NaCl). The specimen surfaces were face milled. It appears that there is no effect of salt water on smooth specimen fatigue life.

No suitable comparative data could be located with which to compare the notched data. The little data available were obtained from tests at a different K_t value. Attempts were made to normalize the data using $K_t - K_f$ curves, but they were unsuccessful.

The S/N curves were converted to constant life diagrams for 10^4, 10^5, and 10^6 cycles, which are presented in figures 35 and 36.

4.3.2.3.2 Sheet.—The S/N curves for the sheet material are contained in figures 37 and 38 and the constant life diagrams in figures 39 and 40. Generally, the fatigue lives of the sheet were superior to those of the plate. However, at an R of -1, K_t = 1, the fatigue lives of the sheet and plate are almost identical in the range of 10^6 to 10^7 cycles.

The smooth fatigue properties of the DA sheet were superior to MA material at all three R ratios (fig. 36) in comparison to the data referenced. Almost no comparative notched fatigue data, K_t = 2.53, could be found. One notched fatigue set of data (ref. 21) at an identical K_t for 0.1-inch standard grade MA Ti-6Al-4V sheet was obtained. The scatterband is indicative of as-received and chem-milled surface finishes. Comparison with those data indicates that DA exhibits better high-cycle properties. In Phase I of this program, notched fatigue specimens of each heat treatment were run at 50 ksi gross area stress (K_t = 2.53). The MA sheet in that phase exhibited a range in log average life which is included in figure 38 (the 50 ksi gross area stress is equivalent to about 61 ksi maximum net area stress). These data indicate a MA fatigue strength at 10^6 cycles which is about 12 ksi higher than the DA, and about 16 ksi higher than the Boeing MA "typical" data.

4.3.2.4 Fatigue Crack Propagation Rate

Fatigue crack propagation rate data were developed in both air and salt water (aqueous 3.5% NaCl) at frequencies of 0.1 and 1 Hz and R ratios of 0.05 and 0.5.

4.3.2.4.1 Plate.—Plate FCP rate data were obtained using both compact tension and surface flaw specimens. The individual curves and tabulated data are contained in appendix B.

Figure 41 indicates the scatterband of the transverse (the only orientation tested in all three phases) da/dN data generated on material meeting or nearly meeting the specification chemistry requirements. This includes the textured plate from Phase I, P08 and P11, and the Phase III material. The dashed lines represent the scatterband when all the beta-annealed material evaluated in this program is included.

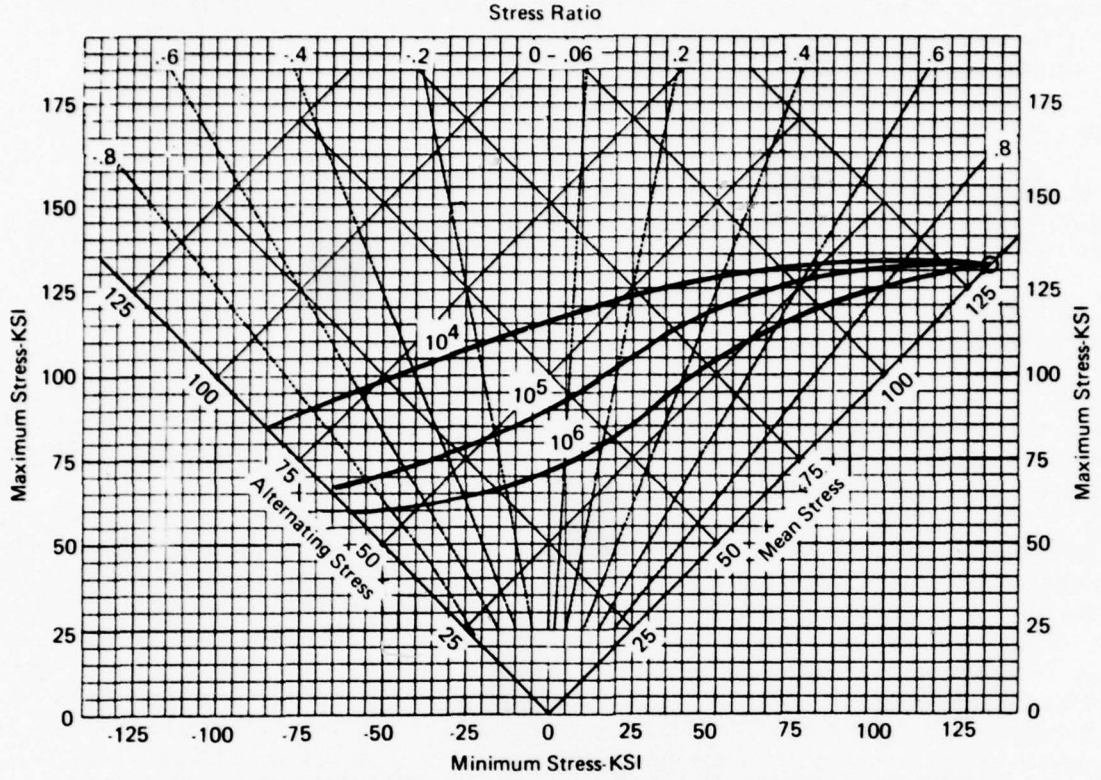

Figure 35.—Constant-life diagram for Phase III BA Plate Tested at Room Temperature, $K_t = 1$, $f = 1800$ cpm.

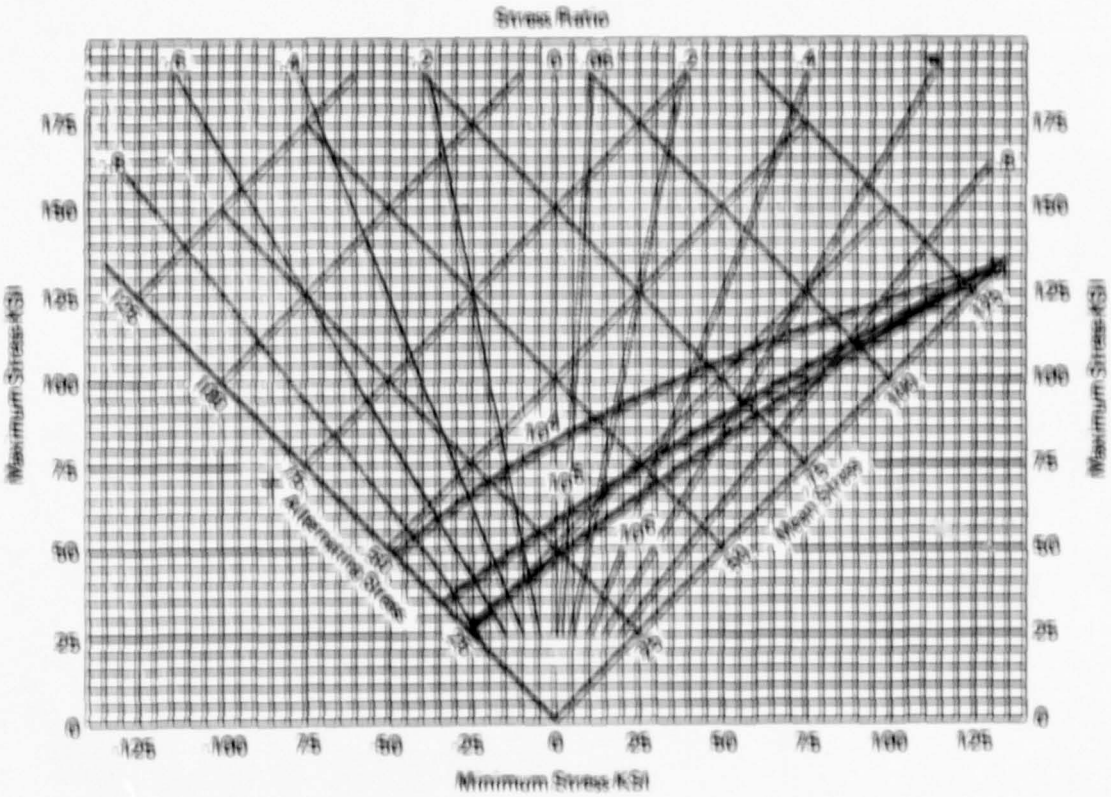

Figure 36. – Constant life Diagram for Phase III BA Plate Tested at Room Temperature, K_t = 2.53, f = 1800 cpm.

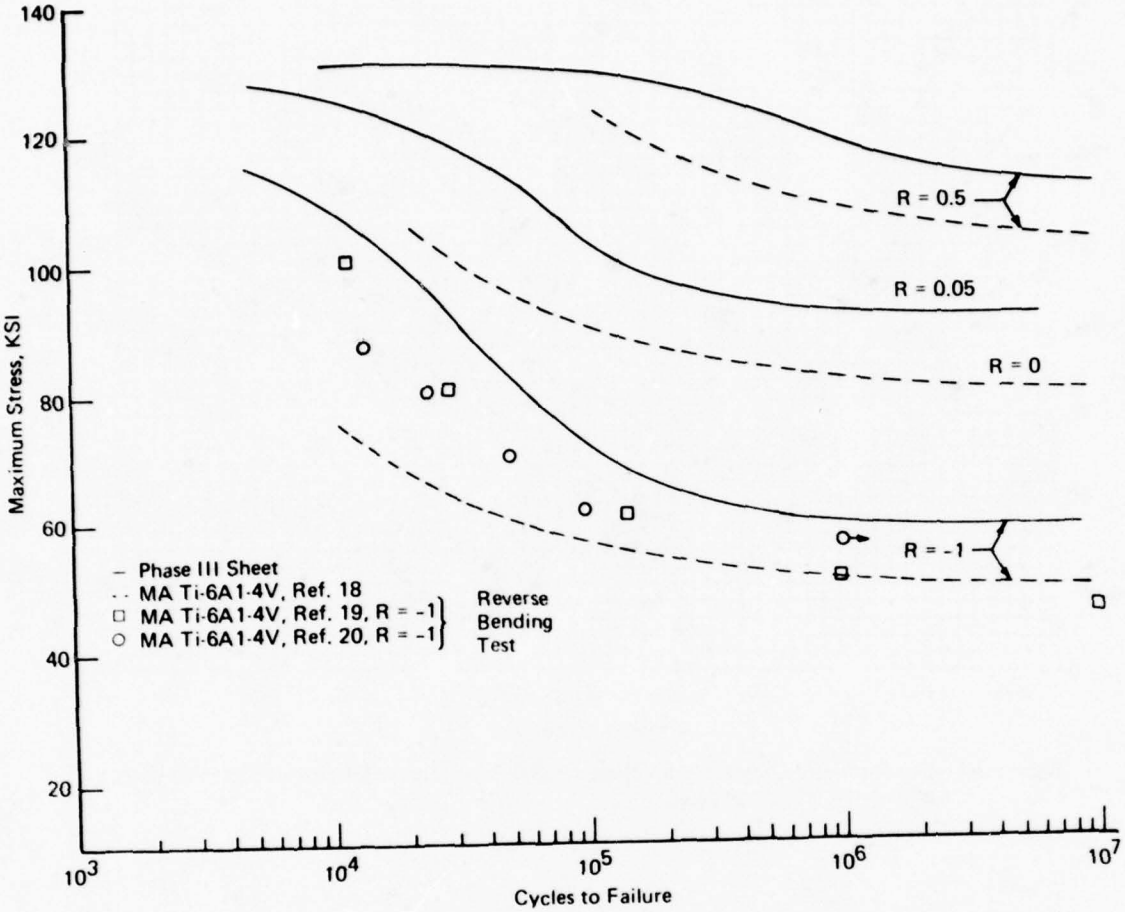

Figure 37.—Fatigue Life Vs. Maximum Net Area Stress for Phase III DA Sheet Tested at 3 R Ratios, $K_t = 1$.

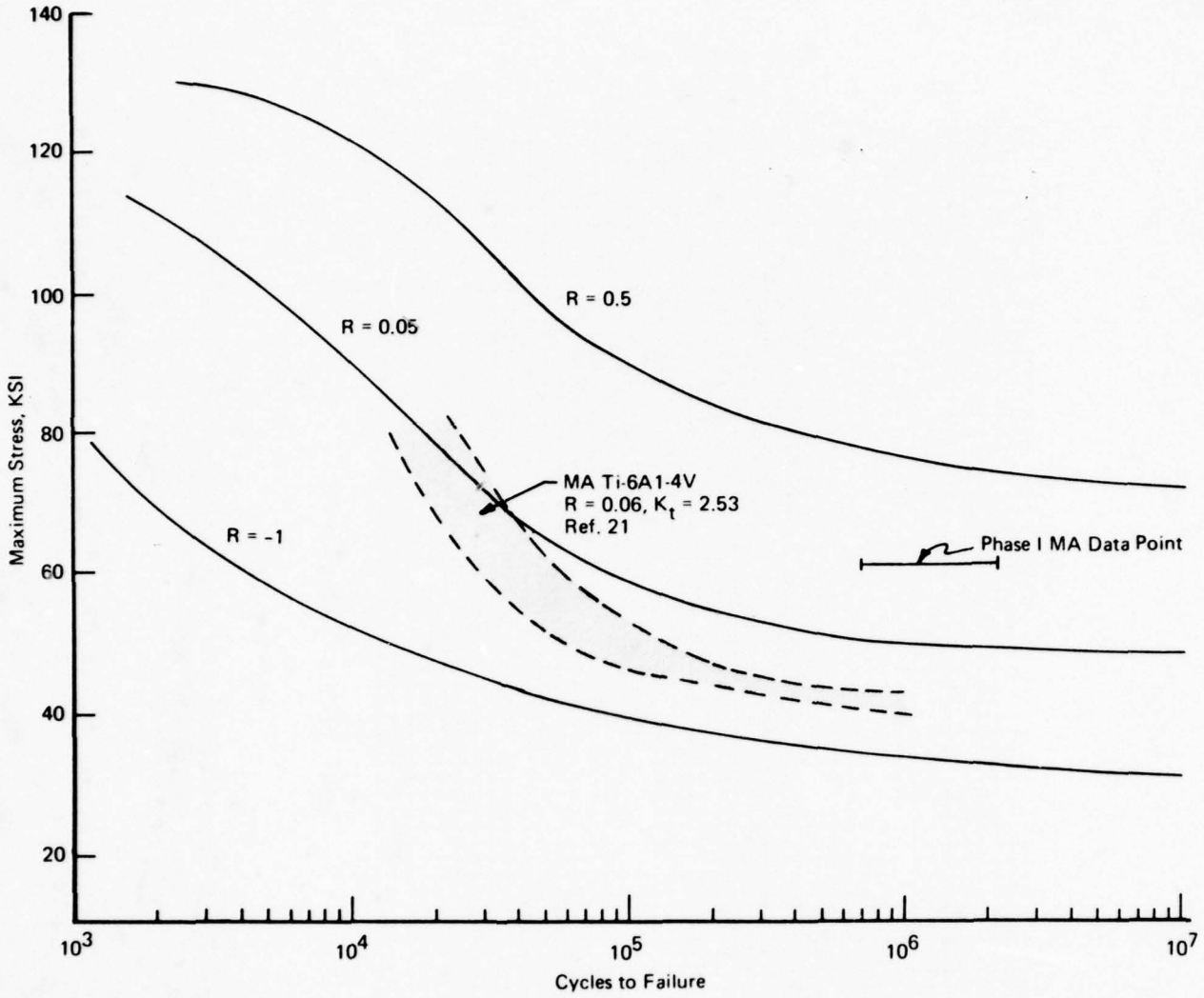

Figure 38.—Fatigue Life Vs. Maximum Net Area Stress for Phase III DA Sheet Tested at Three R Ratios, K_t = 2.53

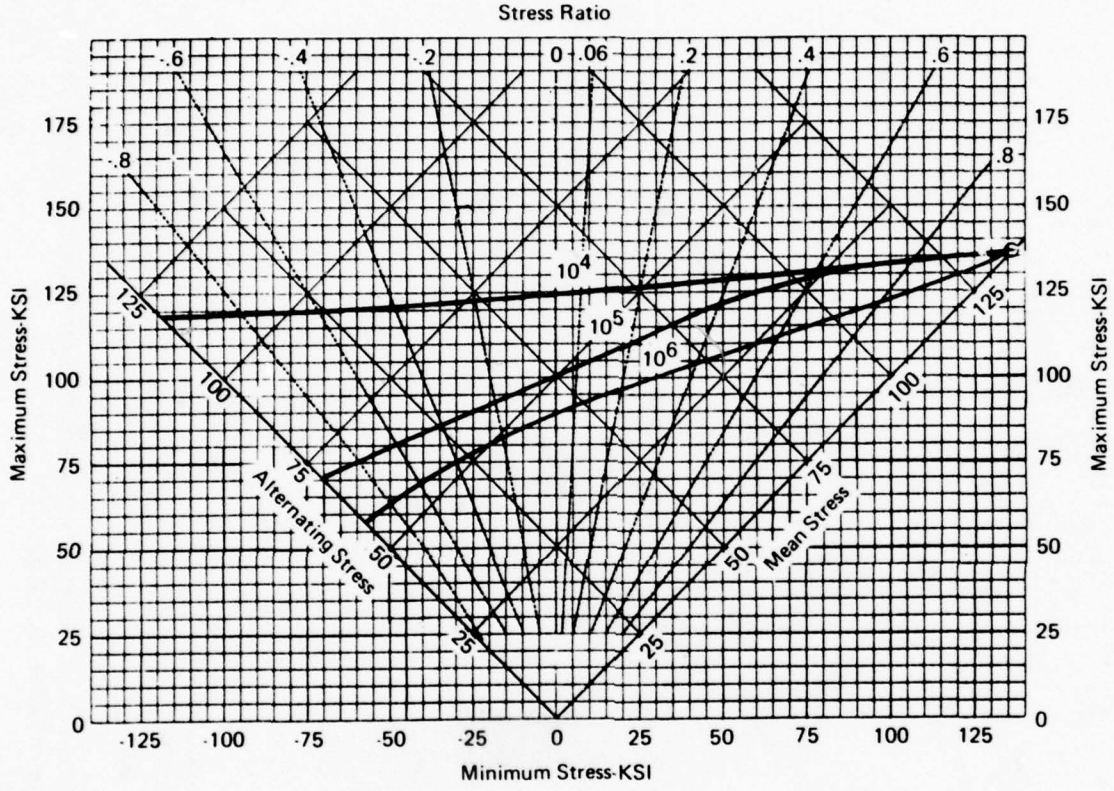

Figure 39.—Constant-life Diagram for Phase III DA Sheet Tested at Room Temperature, $K_t = 1$, $f = 1800$ cpm.

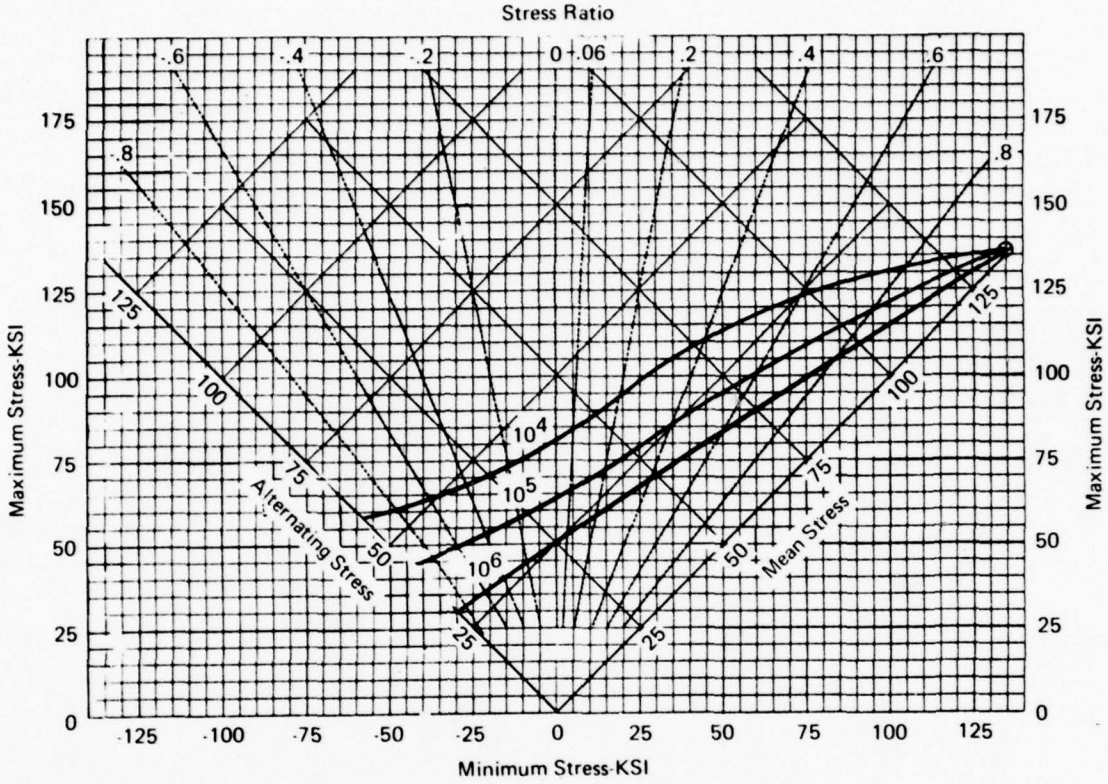

Figure 40.—Constant-life Diagram for Phase III DA Sheet Tested at Room Temperature, K_t = 2.53, f = 1800 cpm.

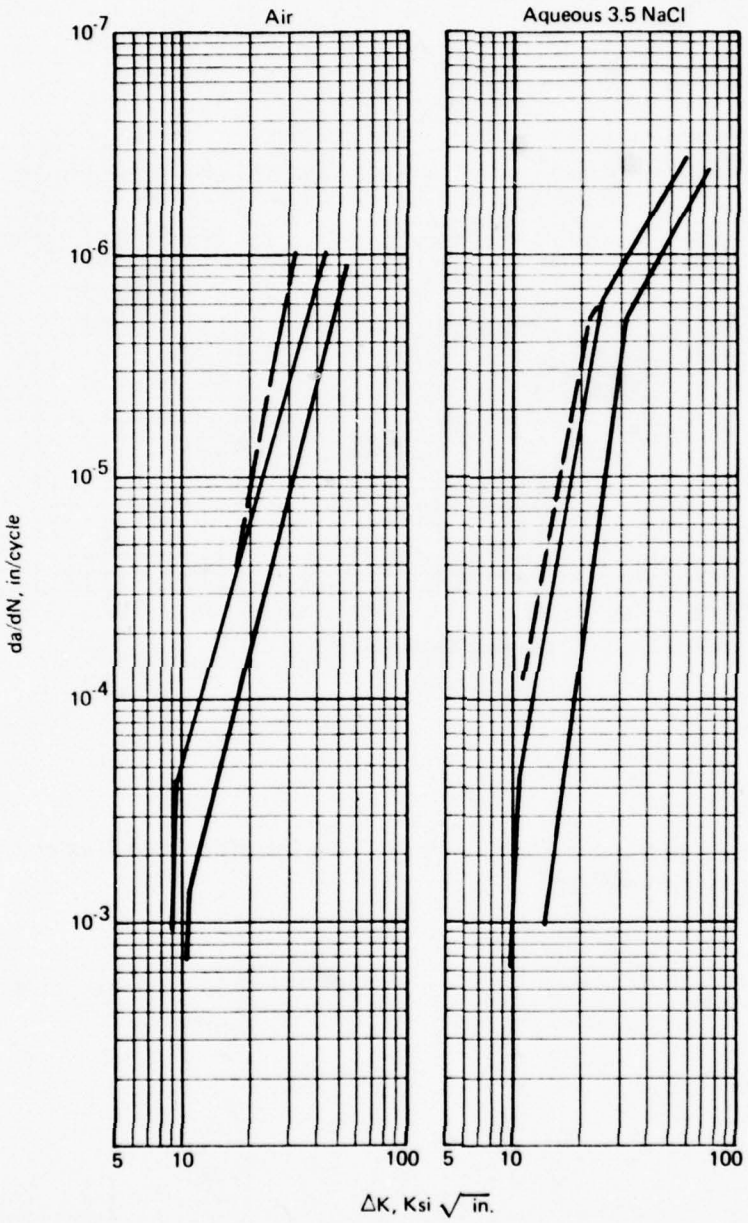

Figure 41.—FCP Rate Versus ΔK Scatterband for All BA Plates Tested in Phases I, II, and III (T-L Orientation, R = 0.05, f = 60 cpm).

——— *Scatterband For Plate Meeting Chemistry Requirements of Proposed Specification*

- - - *Scatterband For All Plate.*

A comparison to RA and MA Ti-6A1-4V is made in figure 42. The solid lines represent the scatterband of data obtained in this program of material that nominally meets the proposed specification chemistry requirements. It can be seen that in air the BA condition is slightly superior to the RA condition, although they fall pretty much in the same scatterband. The BA (and RA) are much superior to the MA data. The upper end of the scatterband of the BA material almost coincides with the lower portion of the scatterband for MA plate. The mid-point of the BA scatterband exhibits a growth rate about an order of magnitude slower than that of the MA condition at given ΔK's. The MA tests are for the L-T orientation. The comparison is, however, valid since the growth rates of the T-L and L-T specimens for the BA product are essentially identical (fig. 43).

The comparison of environmental crack growth rates between RA, MA, and BA material again indicates that the BA condition is superior. The increased severity of aqueous 3.5% NaCl (as opposed to sump tank water) is indicated in figure 42. Sump tank water (STW) tests were also performed by Hall et al. (ref. 23) on the same material. These data fell within the STW scatterband established in reference 11. Comparison to MA plate is presented in figure 44. The only suitable da/dN comparison for the plate material in salt water was at 0.1 Hz. Beta annealing obviously produces environmental crack growth resistance much superior to mill annealing.

The frequency effect in air is very minor, as reported elsewhere (res. 9, 23). Data obtained at 0.1 and 1 Hz are presented in figure 45. The transverse orientation consistently exhibits slightly faster growth rates at 1 Hz than at 0.1 Hz, while the longitudinal data are comparable at both frequencies (within the limits of data scatter).

The frequency effect in salt water shows no orientation dependence (fig. 46). Both orientations exhibit faster growth rates at 0.1 Hz in the slower and faster growth rate regimes, and slower growth rates in the intermediate ΔK regime. Faster growth at the lower frequency could be expected since the environment has more time to act on the crack front during each cycle, allowing the environment to have a more significant effect. The process is not that simple, however, as pointed out by Dawson and Pelloux (ref. 24). There are competing processes occurring: (1) cyclic stress-corrosion cracking (SCC), and (2) repassivation of the freshly created surface at the crack tip. They concluded that above the cyclic stress-corrosion threshold (ΔK_{SCC}), repassivation can no longer suppress cleavage fracture and crack growth occurs by cyclic SCC; hence, in this region, the crack would be expected to grow faster at lower frequency. Below ΔK_{SCC}, the FCP rate is determined by the rate of repassivation and the load rise time. In this region, cracks would be expected to grow slower at lower frequencies as repassivation could play a more prominent role.

These data were not consistent with the proposed mechanism. The differences in microstructure may contribute to the differences in observed results.

The effect of R ratio is demonstrated in figures 47 and 48. The results are similar to those reported by Chesnutt et al. (ref. 9), in that increasing the R ratio from a low value (such as 0.05–0.1) to an intermediate value (0.3–0.7) increases the crack growth rate. This was observed in both air and salt water. (Their data also indicated that in the range of R =0.3 to 0.7 the crack growth rates all fall within the same scatterband for BA material.) The air data at the two R ratios at 1 Hz merge or cross over at about 40 ksi$\sqrt{\text{in}}$. Although the data trend line of Chesnutt et al. is not clear cut, a similar thing could be occurring with their data at a

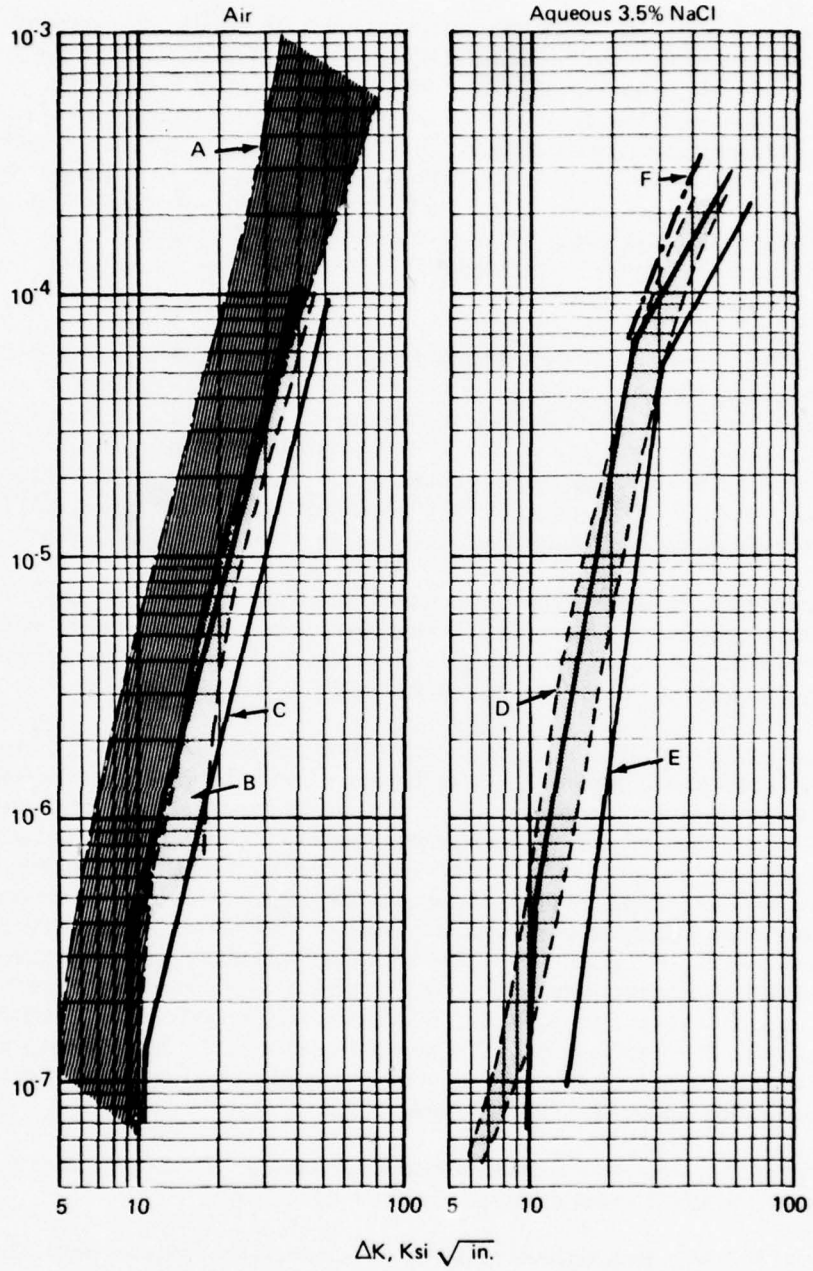

Figure 42.—Comparison of BA and RA Plate FCP Behavior.
A — MA Plate, R = .08, f = 60-1500 cpm, L-T - Orient, Air, Ref. 22, pp. 8.44, 5, 7, 8
B — RA Plate, R = .08, F = 360 cpm, T-L Orient, Air, Ref. 11, p. 8-398
C — Phase III BA Plate, R = .05, f = 60 cpm, T-L Orient, Air
D — RA Plate, R = .08, f = 60 cpm, T-L Orient, Sump Tank Water, Ref. 11, p. 8-403
E — Phase III BA Plate, R = .05, f = 60 cpm, T-L Orient, 3.5% NaCl
F — RA Plate, R = .1, f = 6 cpm, T-L Orientation, Ref. 23

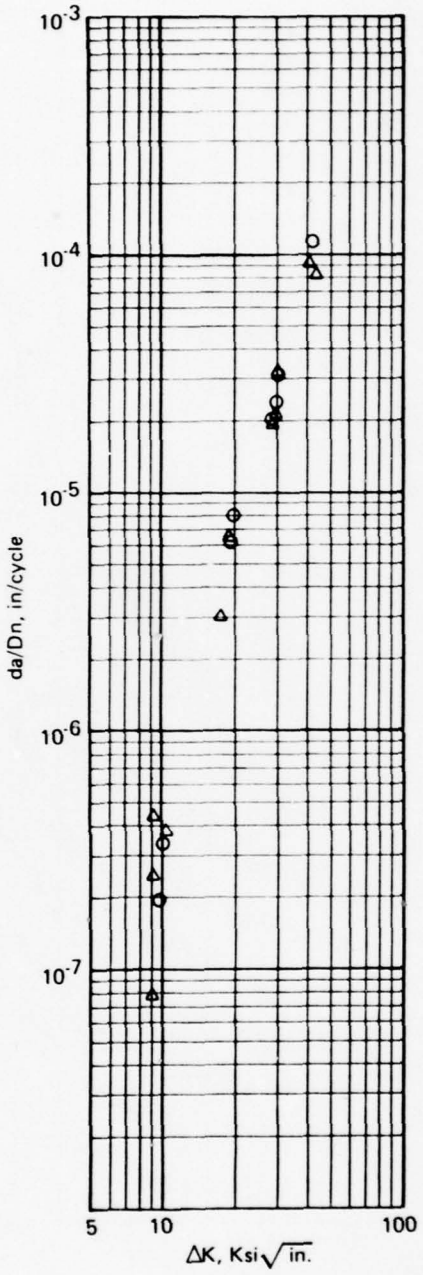

Figure 43.—Comparison of the T-L and L-T Orientation FCP Behavior for Phase III BA Plate, In Air, R = .05, f = 60 cpm.

△ *L-T*
○ *T-L*

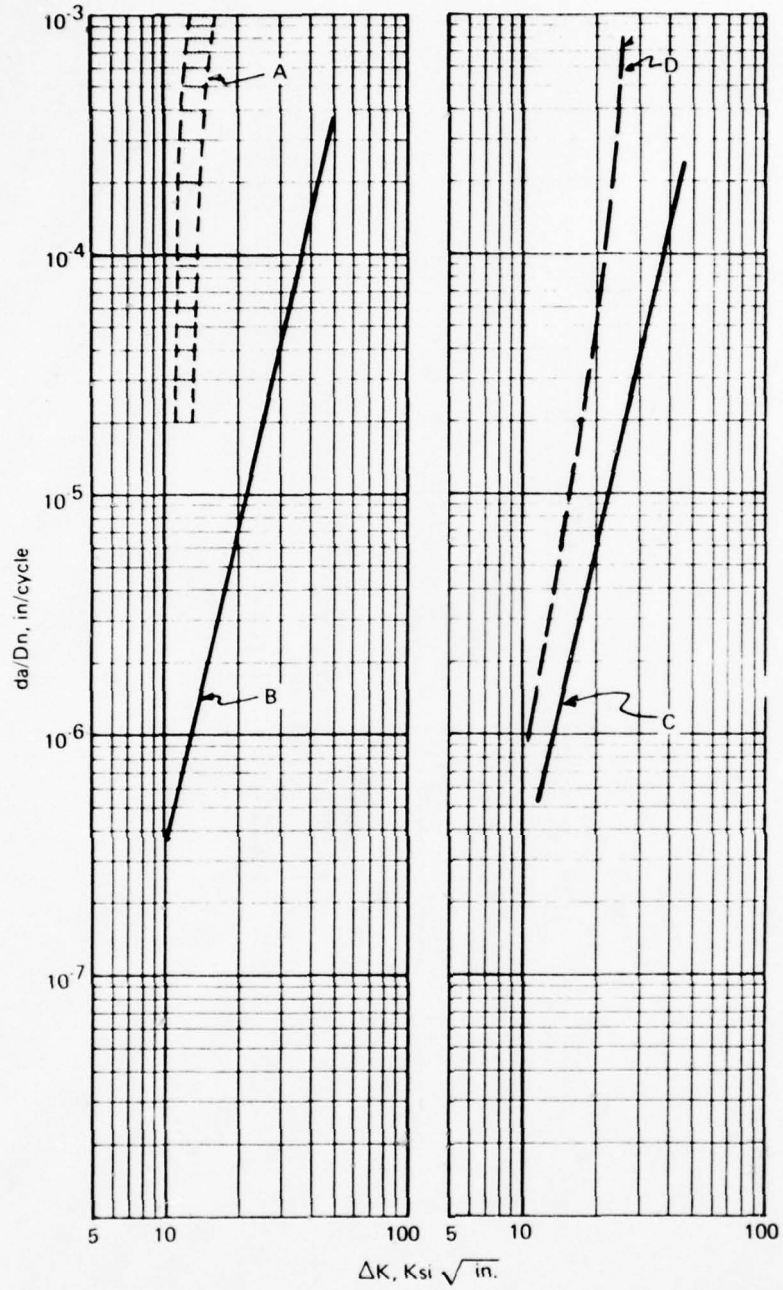

Figure 44.—Comparison of 3.5% NaCl FCP Behavior of BA, MA & RA Plate Tested at 6 cpm, T-L Orientation.

A – MA Plate, R = .1, f = 6 cpm, Ref. 22, pg. 8.4-102

B – BA Phase III Plate, R = .05, f = 6 cpm

C – Phase III, Plate, 6 cpm, R = .5

D – RA Plate, R = .5, f = 6 cpm, Ref. 23, pg. 120

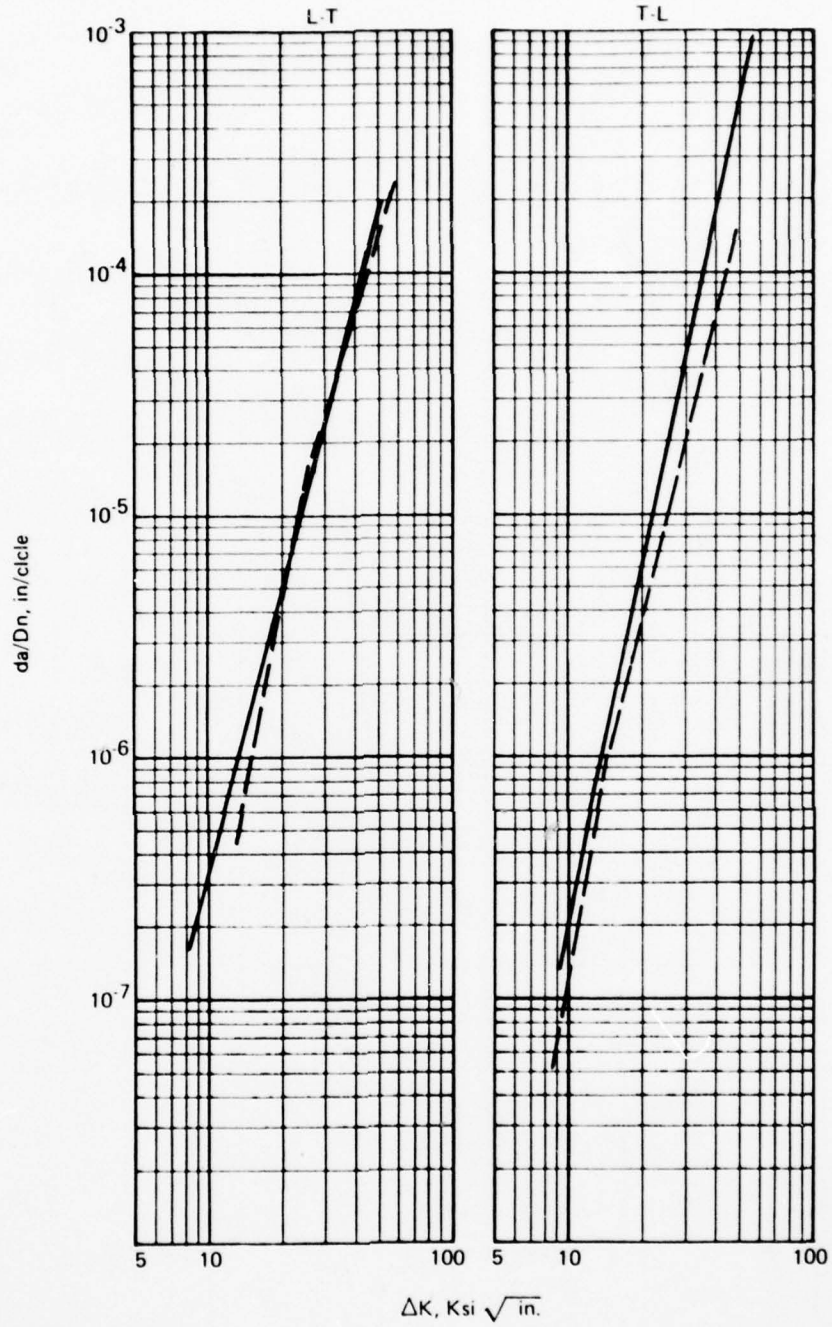

Figure 45.—Comparison of FCP Behavior of BA Plate in Air at 6 and 60 cpm, Tested at R = 0.05.
— 60 cpm
- - 6 cpm

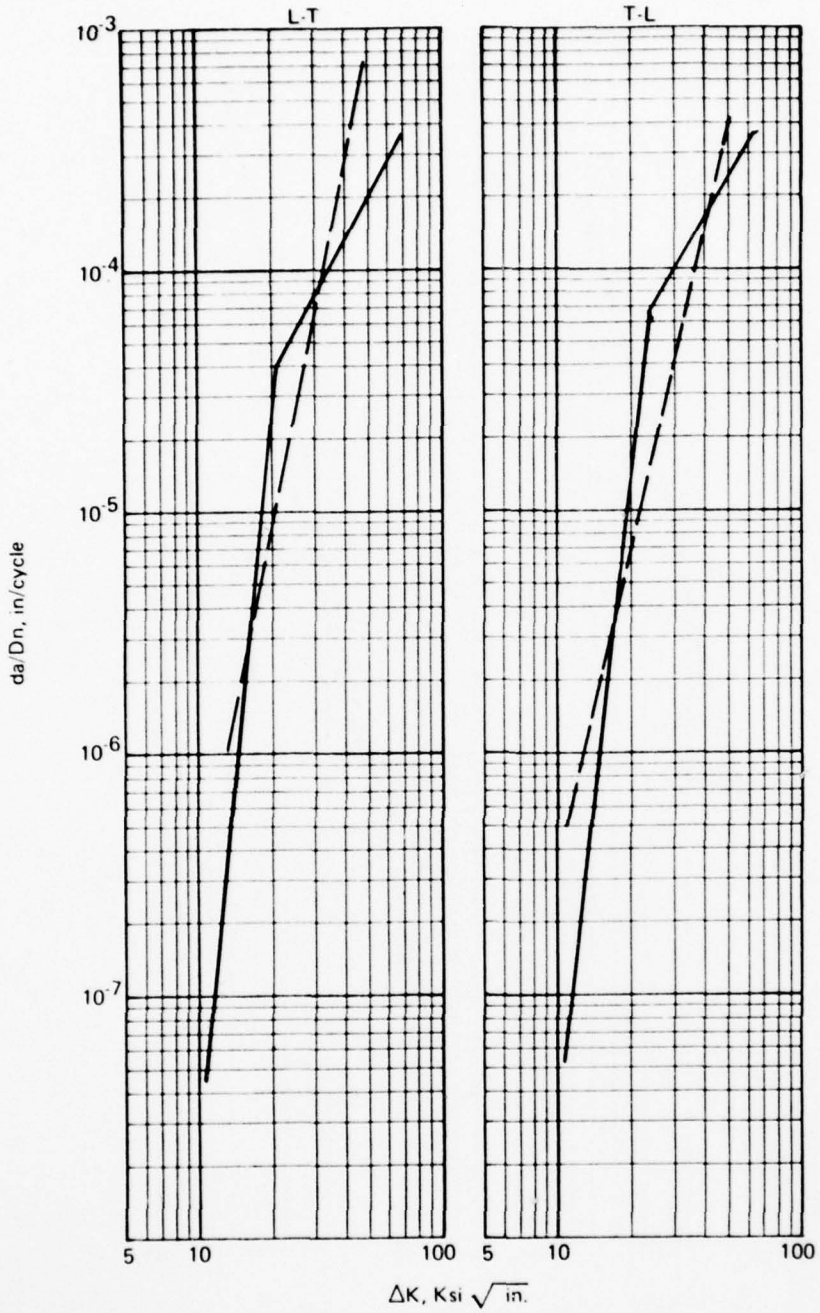

Figure 46.—Comparison of FCP Behavior of BA Plate in 3.5% NaCl at 6 and 60 cpm, Tested at R = 0.05.

— 60 cpm
·· 6 cpm

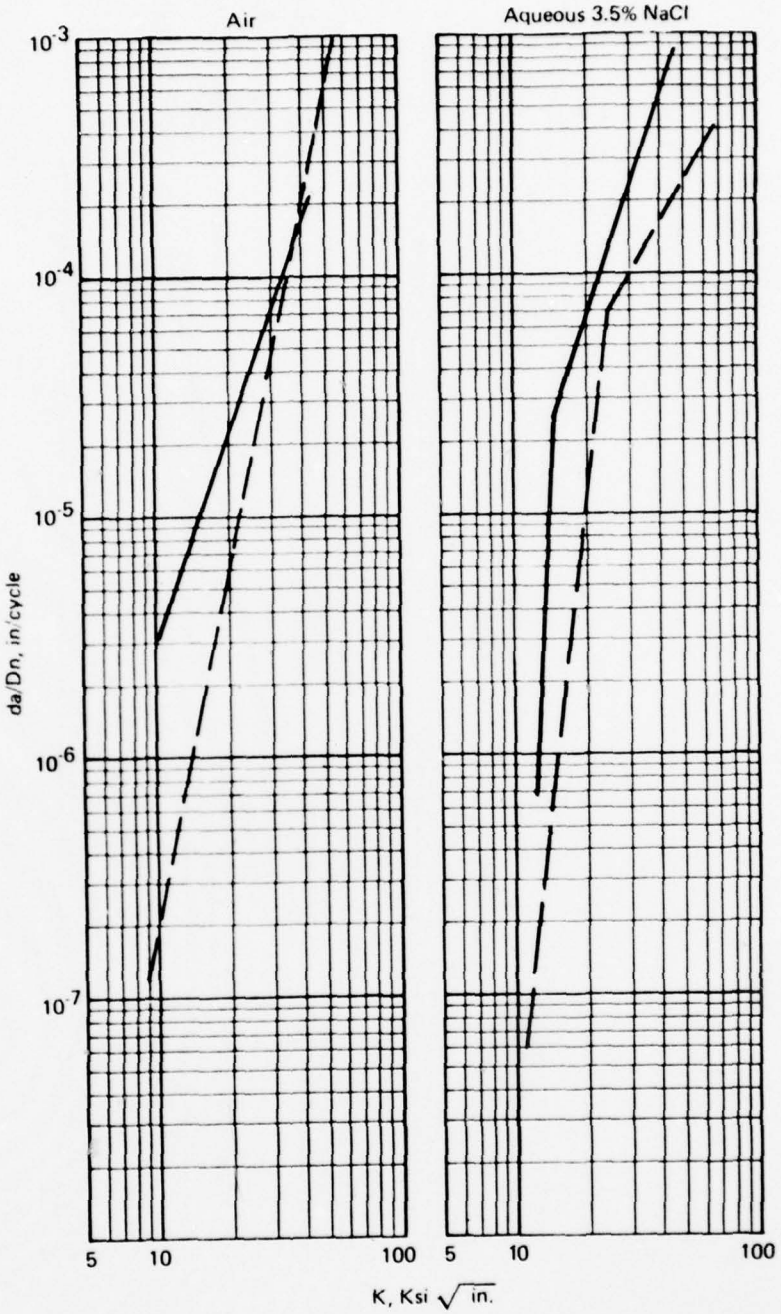

Figure 47.—Comparison of FCP Behavior of BA Plate at R = 0.05 and 0.5 in Air and Salt Water, f = 60 cpm, T-L Orientation.

- - *R = .05*
— *R = .5*

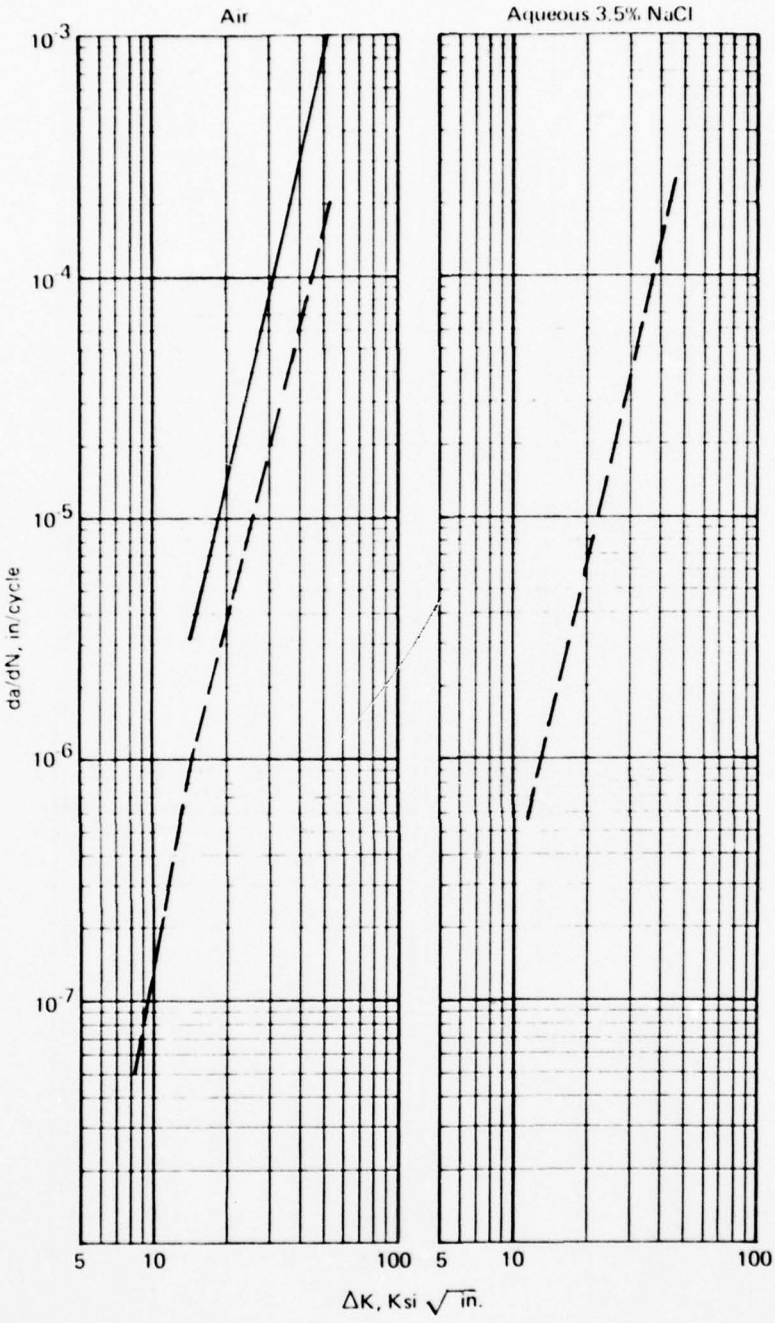

Figure 48.—Comparison of FCP Behavior of BA Plate at R = 0.05 and 0.5 in Air and Salt Water, f = 6 cpm, T-L Orientation.

- - - *R = .05*
— *R = .5*

ΔK of 30-40 ksi$\sqrt{in}$. Their data did not merge at a frequency of 6 cpm, also in agreement with these data.

The relationship of the FCP test results and the microstructure did not correlate to the theory proposed by Yoder et al. (refs. 10, 25) regarding the relationship of alpha colony packet size and FCP characteristics. They proposed that (1) a change in slope (on a logarithmic plot of da/dN versus ΔK) occurrs when the reversed plastic zone size corresponds to the colony size, and (2) the FCP rate decreases as the colony size increases.

The first point hinges on a transition from microstructurally sensitive propagation (below the transition) to microstructurally insensitive fracture. At low ΔK's, when the reversed plastic zone size is smaller than the colony size, crack bifurcation within the colonies (and through them) occurs, reducing the effective ΔK by dispersing the strain field of energy of the microscopic cracks among multiple crack fronts. A transition in the da/dN versus ΔK plot would then be expected when the reversed plastic zone size exceeded the colony size, reducing or eliminating the amount of crack bifurcation within the packets. This transition from bifurcation within the packets was observed metallographically by them and confirmed in this program. In fact, at ΔK's significantly above the reversed plastic zone size, very little bifurcation was observed at all.

Analyzing all the plate air da/dN data from Phases II and III (contained in appendices A and B), it is difficult to assign a clear transition point to most of the data. If a transition point were to be established by these plots, it would be in the neighborhood of ΔK of 20 ksi$\sqrt{in}$. or lower except for the FCP-3-L specimen, where it would be at a ΔK of about 25 ksi$\sqrt{in}$. The mean colony size of this material was 55.25 microns. The equation used by Yoder et al. was:

$$r_y^c = 0.132 \left(\frac{\Delta K}{2\sigma_y}\right)^2$$

where:

r_c^y = reversed plastic zone size, meters

ΔK = stress intensity range, MPa$\sqrt{m}$

σ_y = yield strength, MPa

Solving for ΔK results in:

$$\Delta K_T = 5.5\, \sigma_y\, r_y^c$$

Using a packet size of 55.25 microns (and assuming r_y^c = packet size at the transition) and a yield strength of 122.3 ksi (842.9 MPa) and solving for ΔK at the transition point yields a ΔK_T of 31.3 ksi$\sqrt{in}$. This does not correspond to the indicated transition points of the data. Admittedly, more data points would be desirable to more clearly define the transition.

However, we wish to take issue with an aspect of the proposed relationship. It is based upon a transition from microstructurally sensitive to microstructurally insensitive crack propagation. In the microstructurally sensitive region, crack growth is retarded by crack bifurcation within the colonies (as well as transcolony bifurcation). Using this rationale in conjunction with the proposed colony size-reversed plastic zone size relationships suggests that at the transition,

the growth rate should accelerate, not slow down as it in fact occurs.

The work by Thompson et al. (ref. 7) does not support this theory either. They present da/dN curves for BA and RA Ti-6A1-4V (among other treatments). The RA material indicates a transition at about 17 ksi$\sqrt{\text{in.}}$ and the BA at about 20 ksi$\sqrt{\text{in.}}$ Solving then for r_y^c, hence the colony (or critical microstructural dimension) size, yields 23.1 microns for the RA structure and 26.7 microns for the BA material. Yet the packet size of the BA microstructure must be an order of magnitude larger than the transformed beta grain size in the RA material, which is the largest microstructural dimension it seems reasonable to use. The primary alpha grain size is a possible dimension to use, but its relevance does not appear justifiable since bifurcation into or within the alpha phase occurs at a much reduced frequency compared to a transformed structure, and its effects would be minor in comparison.

Their second point, increased packet size associated with greater FCP resistance, could be borne out in this program, as already discussed Phase II and further illustrated in figure 49, which combines the Phase II and Phase III data. The P08, P18, and Phase III materials all have similar packet sizes and their growth rates are quite similar. P11 has a significantly larger mean packet size, and its FCP rate is significantly slower. This part of the theory seems reasonable. The larger the packet size (or key microstructural dimension) in relationship to the reversed plastic zone size, the more extensive the amount of intra- and inter-colony bifurcation is possible below ΔK_T and the more inter-colony bifurcation above ΔK_T, hence the greater the reduction in the effective ΔK. This is supported indirectly by the grain size fatigue life relationship; generally, the smaller the grain size the greater the fatigue life (ref. 25). With Ti-6A1-4V, increased fatigue life generally implies poorer da/dN characteristics. Hence, if increasing grain size is associated with poorer fatigue life, it probably implies better da/dN properties. The grain size, or in this case colony size, does display an inverse relationship with da/dN except for the P18 material. The notched fatigue lives, in kilocycles in ascending order of packet size (see fig. 49) are 52, 36, 46, and 39. The spread in packet size is much too small and the data too limited to generalize this relationship, however.

4.3.2.4.2 Sheet.—The FCP rate data for sheet were generated using center-cracked panels. The individual curves and tabulated data are contained in appendix B. There was very little data available to permit direct comparison of the sheet produced in accordance with the proposed specification and sheet produced per MIL-T-9046. Comparisons of MA sheet in the longitudinal (L-T) and transverse (T-L) orientations to DA data in air are presented in figure 50. The FCP resistance of the DA condition is superior to the MA material in both instances. The only environmental comparison available was to sump tank water (fig. 51). The DA material again exhibits better FCP characteristics. It should be reiterated that sump tank water is not as aggressive as 3.5% NaCl, so the difference should be even greater (ref. 23). Also included in figure 51 is the scatterband obtained from Phase I MA material. This scatterband was obtained (from the single sheet of material) by employing the various annealing schedules allowed for MA sheet in accordance with MIL-H-81200A. At low ΔK values, the lower portion of the MA scatterband is slightly superior to the Phase III material. The high side of the scatterband is, however, much inferior. The extent of the scatterband of the Phase I data clearly indicates that sheet produced per MIL-T-9046 and MIL-H-81200 is not sufficient for damage-tolerant structure. First, the range of permissible heat treatment conditions is too broad to produce consistent properties, and secondly, at the low annealing temperatures utilized, the heat

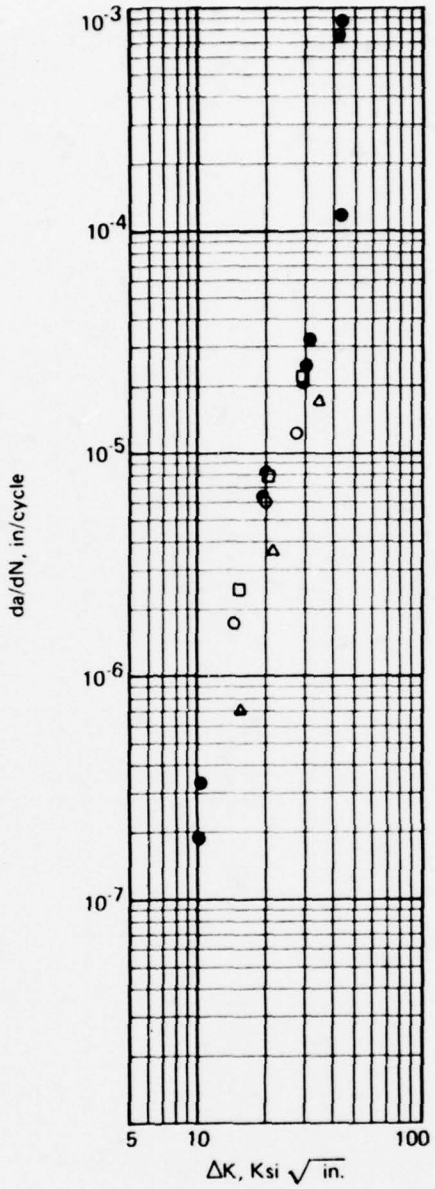

Figure 49.—FCP Behavior of BA Plate (Phases II and III) With Corresponding Packet Size and K_t Values, Tested at R = 0.05, f = 60 cpm in Air, T-L Orientation.

	Packet Size (μm)	K_t (Ksi $\sqrt{\text{in.}}$)
○ P08	47	27
□ P18	48	32
△ P11	74	31
● Phase III	55	37

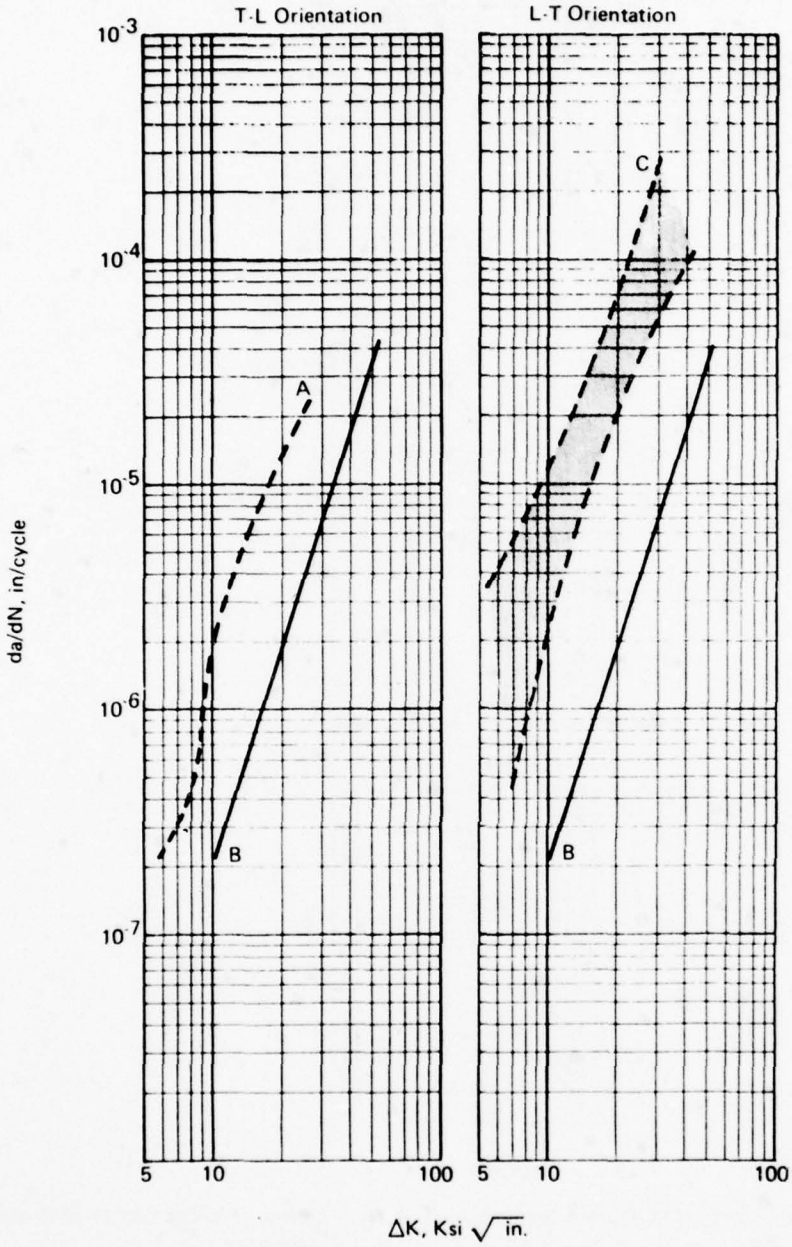

Figure 50.—Comparison of FCP Behavior of Phase III DA Sheet to MA Sheet In Air.

A — MA Sheet, R = .08, f = 60 cpm, Ref. 11, Pg. A-108

B — Phase III, D.A. Sheet, R = .05, f = 60 cpm

C — MA Sheet, R = .08, f = 60 to 360 cpm, Ref. 22, pp. 8.4-94, 98, 100

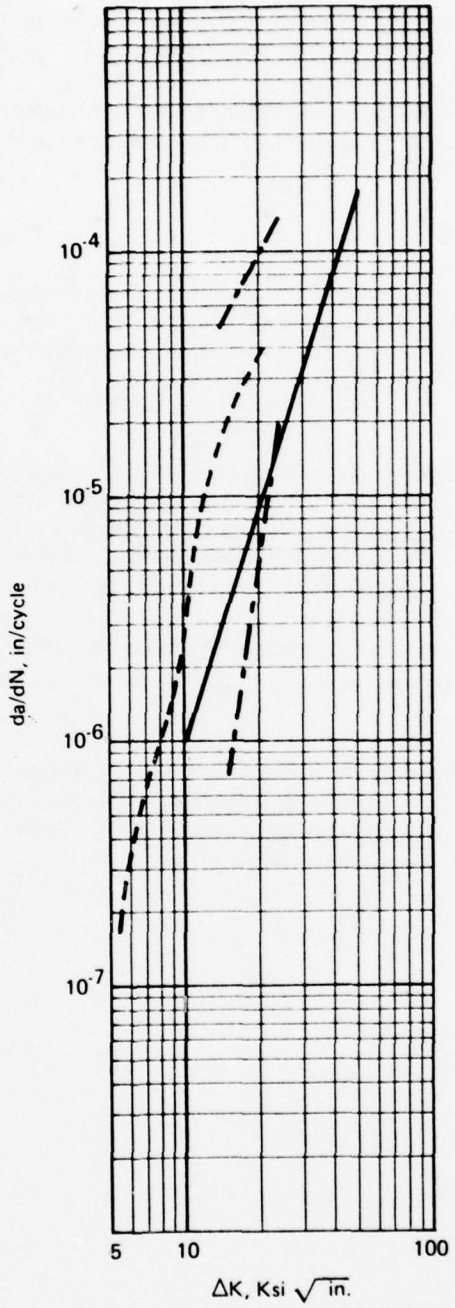

Figure 51.—Comparison of Environmental FCP Behavior of Phase III DA Sheet to MA Sheet.

— *Phase III DA Sheet, R = .05, f = 60 cpm, T-L Orient, 3.5% NaCl*

–·– *MA Sheet, R = .08, f = 60 cpm, T-L Orient, Sump Tank Water, Ref. 11, pg. A-113*

- - - - *Phase I MA Sheet, R = .05, f = 60 cpm, T-L Orient, 3.5% NaCl*

treatment responses can be markedly different depending on prior processing histories. This was clearly demonstrated for plate material in Phase I (ref. 3).

The effect of R ratio on FCP behavior was as anticipated, higher da/dN values at R = 0.5 than at R = 0.05 (fig. 52). All testing of the sheet material was conducted at 1 Hz, so the frequency effect was not evaluated.

4.3.2.5 Proposed Specification

The first drafts of a sheet and a plate specification for premium-grade damage-tolerant Ti-6Al-4V were drafted in Phase II and sent out for comments. Copies of these specifications were routed to 34 firms. Comments were received from 10 sources, including 3 suppliers. Pertinent applicable comments were incorporated in the final draft of these specifications, contained in appendix C.

These specifications were basically patterned after the AST (Advanced Supersonic Transport) specifications written during the DOT-SST follow-on program (ref. 16). The General Dynamics-Convair beta-annealed plate specification (FMS 1109), which they are using the purchase material for the F-16, was also derived from the AST specification. The main alterations of the AST specifications for this program were the inclusion of cross-rolling to reduce anisotropy, the addition of fracture toughness testing, and more stringent stress-corrosion resistance requirements. Data generated during this program and, for plate, data obtained from present users of beta-annealed plate, make the requirements of these specifications appear reasonable and attainable.

The Boeing Marina Systems Division has released an initial specification for beta annealed damage tolerant Ti-6Al-4V alloy plate, bar and forgings. This specification was patterned after the proposed plate specification written for this program. The plate and forging suppliers have agreed to provide material per this specification.

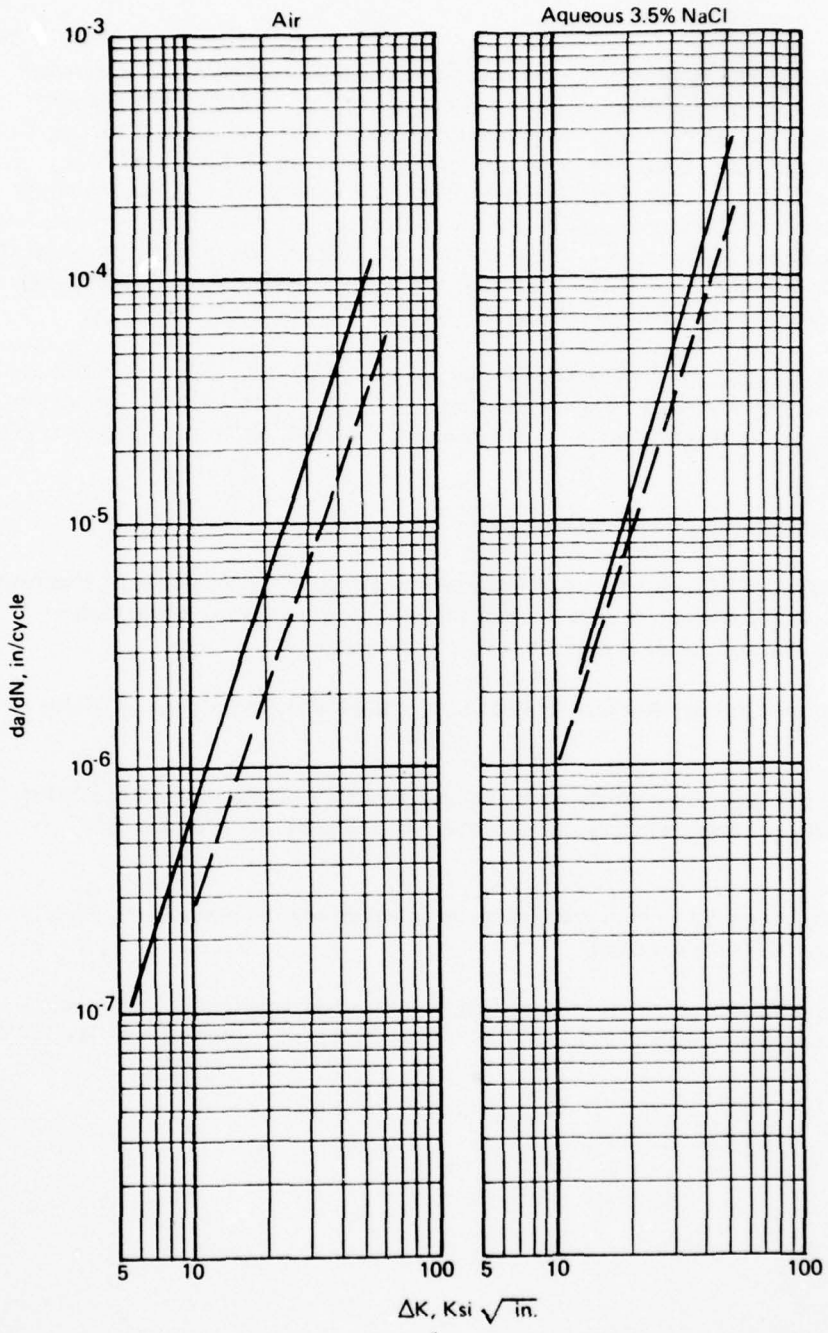

Figure 52.—Comparison of FCP Behavior of Phase III DA Sheet as a Function of R Ratio, f = 60 cpm, Tested in Transverse Direction.

--- *R = .05*

— *R = .5*

5.0 SUMMARY AND CONCLUSIONS

The data generated in Phases II and III were as anticipated based on Phase I. The damage-tolerant properties of the beta-annealed plate and duplex-annealed sheet were superior to those obtained by alternate heat treatment conditions of the respective product forms. These were obtained with a slight drop in tensile and fatigue strengths for the plate (no reduction in sheet). This compromise in plate is offset by a very substantial improvement in fracture properties over conventional mill-annealed material and a significant improvement over recrystallized annealed material. The benefits of the beta anneal are even more dramatic in an aggressive environment, especially for corrosion fatigue at higher stress ratios. Comparative data are presented in the form of a bar graph in figure 53.

The data generated during this program justify the selection of beta-annealed plate and duplex-annealed sheet for premium-grade, damage-tolerant Ti-6A1-4V. These data, in conjunction with that from other sources, also indicate that the property goals of the proposed specifications are realistic.

The conclusions drawn from this program include:

1. Maximum damage tolerance for plate material is obtained by beta annealing. Fracture toughness, stress corrosion threshold, and fatigue crack growth rate, particularly in aggressive environments are superior to other heat treatments.

   This higher damage tolerance is accompanied by a slight drop in tensile and fatigue strengths.

2. Duplex annealing provides the optimum damage tolerance practically obtainable for sheet material. Considerations such as formability and grain size preclude beta annealing.

3. A super low interstitial oxygen grade of material is necessary to provide consistently high damage-tolerant properties.

4. Plate and sheet produced in accordance with the proposed specifications will more reliably produce a consistent and superior product than is now possible with MIL-T-9046 materials.

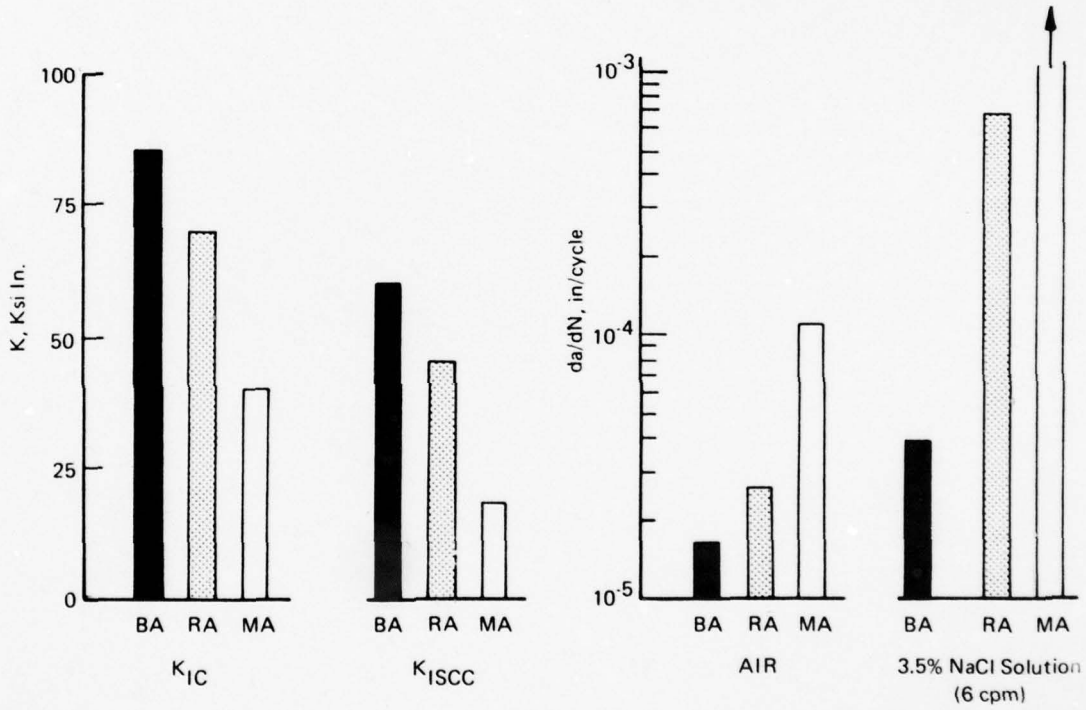

FCP Rates At ΔK = 30 KSI $\sqrt{\text{in.}}$, R = .05

Figure 53.—Comparison of Damage Tolerant Properties of Beta Annealed, Mill Annealed and Recrystallization Annealed Ti-6A1-4V Plate.

AD-A071 542 BOEING COMMERCIAL AIRPLANE CO SEATTLE WASH F/G 11/6
STANDARDIZATION OF TI-6AL-4V PROCESSING CONDITIONS.(U)
SEP 78 R R BOYER, R BAJORAITIS F33615-74-C-5176
UNCLASSIFIED D6-48016 AFML-TR-78-131 NL

2 OF 2
AD
A071542

END
DATE
FILMED
8-79
DDC

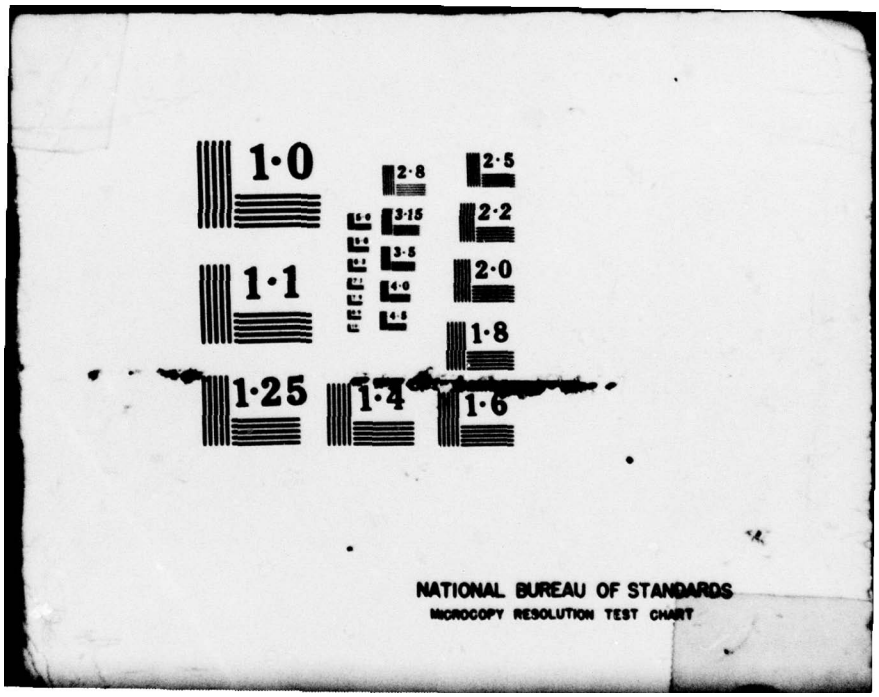
1·0
1·1
1·25
2·8
3·15
3·5
4·0
1·4
2·5
2·2
2·0
1·8
1·6
NATIONAL BUREAU OF STANDARDS
MICROCOPY RESOLUTION TEST CHART

6.0 RECOMMENDATIONS REFERENCES

1. We recommend that for fracture-critical hardware, the use of beta annealing be expanded to other product forms, such as forgings.

2. A comprehensive search for additional mill-annealed data should be initiated to establish data scatterbands typical of MIL-T-9046 products suitable for insertion into MIL-H-5. These are commonly used product forms, and yet there are no handbook data available.

3. A similar search for applicable beta-annealed data should be instituted to provide scatterbands for fatigue life and fatigue crack propagation characteristics to compliment data generated in this investigation.

REFERENCES

1. F. L. Parkinson and W. F. Spurr, SST Technology Follow-on Program - Phase I, "Titanium Allou Ti-6A1-4V Mechanical-Metallurgical Testing," Report No. FAA-SS-72-13, Boeing Document D6-60213, July 1972.

2. R. R. Boyer and W. F. Spurr, "Effect of Composition, Microstructure, and Texture on Stress-Corrosion Cracking in Ti-6A1-4V Sheet," accepted for publication in Met. Trans.

3. W. F. Spurr, R. R. Boyer, R. Bajoraitis, and D. C. Engdahl, Phase I Interim Technical Report on "Standardization of Ti-6A1-4V Processing Conditions," Contract F33615-75-C-5176, Boeing Document D6-44167, December 1976.

4. F. L. Parkinson, SST Follow-on Program - Phase I, "Beta Processed Titanium Alloy Ti-6A1-4V Plate," Report No. FAA-SS-72-00, Boeing Document D6-60200, July 1972.

5. D. Eylon and C. M. Pierce, "Effect of Microstructure on Notch Fatigue Properties of Ti-6A1-4V," Met. Trans. A, vol. 7A, Jan. 1976, pp. 111-120.

6. H. A. Wood, R. M. Engle, J. Gallagher, and J. M. Potter, "Current Practice on Estimating Crack Growth Damage Accumulation with Specific Application to Structural Safety, Durability and Reliability," AFFDL-TR-75-32, Jan. 1976.

7. A. W. Thompson, J. C. Williams, J. D. Frandsen, and J. C. Chesnutt, "The Effect of Microstructure on Fatigue Crack Propagation Rate in Ti-6A1-4V," Proc. Third International Conference on Titanium, Moscow, Russia, Plenum Press (not yet released).

8. S. F. Frederick, "Manufacturing Methods for Production Process for Titanium Sheet with Controlled Texture," Technical Report AFML-TR-73-265, USAF Contract F33615-71-C-1543, McDonnell Douglas Astronautics Company, Nov. 1973.

9. J. C. Chesnutt, A. W. Thompson, and J. C. Williams, "Influence of Metallurgical Factors on the Fatigue Crack Growth Rate in Alpha-Beta Titanium Alloys," Technical Report AFML-TR-78-68, USAF Contract F33615-74-C-5067, Rockwell International Science Center, March 1978.

10. G. R. Yoder, L. A. Cooley, and T. W. Crooker, "Fatigue Crack Propagation Resistance of Beta Annealed Ti-6A1-4V Alloys of Differing Interstitial Oxygen Contents," NRL Report 8166, Oct. 1977.

11. R. R. Ferguson and R. C. Berryman, "Fracture Mechanics Evaluation of B-1 Materials," vol. 1, Technical Report AFML-TR-76-137, USAF Contract F33657-70-C-0800, Rockwell International, B-1 Division, Oct. 1976.

12. "Primary Structure Material Selection Report Supersonic Transport," Lockheed Report No. LR19150, Oct. 1965.

13. Private communications with Bob Newcomer, McDonnall Aircraft Company (St. Louis).

14. Private communication with Jim Shults, General Dynamics-Convair (Ft. Worth).

16. W. F. Spurr and D. T. Lovell, SST Technology Follow-on Program–Phase II, "Development of Improved Titanium 6A1-4V Mill Products," FAA-SS-73-4, Boeing Document D6-60276, May 1974.

17. B-1 Airframe Material Fatigue Design Properties Manual, Technical Report NA-72-1088, Los Angeles Division, Rockwell International, Aug. 1975.

18. J . K. Childs and M. M. Lem Coe, "Determination of Materials Design Criteria for 6A1-4V Titanium Alloy at Room and Elevated Temperatures," WADC Technical Report 58-246, Contract AF33(616)-3348, Southwest Research Institute, Aug. 1958.

19. R. J. Favor, D. N. Gideon, H. J. Grover, J. E. Hayes, and G. M. McClure, "Investigation of Fatigue Behavior of Certain Alloys in the Temperature Range Room Termperature to -423F," WADD Technical Report 61-132, Contract AF33(616)-6888, Battelle Memorial Institute, March 1961.

20. T. R. Kramer and A. Kumar, "Study of Effects of Diffused Layers on the Fatigue Strengths of Commercial Titanium Alloys," Technical Report AFML-TR-70-185, Contract F33615-69-C-1573, Martin Marietta Corporation, Sept, 1970.

21. Unpublished Boeing Data, circa 1970.

22. Damage Tolerant Design Handbook, Part 2, MCIC-HB-01, Jan. 1975.

23 L. R. Hall, R. W. Finger, and W. F. Spurr, "Corrosion Fatigue Crack Growth in Aircraft Structural Materials," Report AFML-TR-73-204, Contract F33615-71-C-1687, Boeing Aerospace Company, Sept. 1973.

24. D. B. Dawson and R. M. Pelloux, "Corrosion Fatigue Crack Growth of Titanium Alloys in Aqueous Environments," Met. Trans., vol. 5, 1974, pp. 723-731.

25. G. R. Yoder, L. A. Cooley, and T. W. Crooker, "Observations of Microstructurally Sensitive Fatigue Crack Growth in a Widmanstatten Ti-6A1-4V Alloy," Met. Trans. A, vo. 8A, 1977, pp. 1737-1743.

26. N. E. Paton, J. C. Williams, J. C. Chesnutt, and A. W. Thompson, "The Effects of Microstructure on the Fatigue and Fracture of Commercial Titanium Alloys," Alloy Design for Fatigue and Fracture Resistance, Agard Conference Proc. No. 185, 92200 Neiully-Sur-Seiner, France April 1975, pp. 4-1 to 4-14.

APPENDIX A

TEST DATA--PHASE II

This appendix contains all the detailed test data generated during Phase II of this program. Included are tensile properties, fatigue crack propagation (FCP) rates in air and aqueous 3.5% NaCl solution using double cantilever beam and compact tension type specimens, notched fatigue and lap splice fatigue properties, and fracture toughness (K_{IC}) of plate.

Table A.1.—Tensile Properties of Ti-6A1-4V Sheet and Plate (Phase II Material)

Form	Heat Treatment	Nominal Oxygen Content (wt %)	TUS (ksi)	YTS (ksi)	RA (%)	Elong. (%)	Fatigue Life (cycles) [1] Notch	Fatigue Life (cycles) [1] Lap Splice	K_{IC} (ksi$\sqrt{in.}$)
Plate	1900°F/20 min./AC + 1350°F/2 hrs./AC	0.08	126	114	31	12	52,000	98,000	82.7 [2]
			125	115	31	13			
		[4]	126	113	26	11			
			125	115	28	10			
		0.11	134	125	18	10	39,000	70,000	87.3 [2]
			134	124	20	10			
		[4]	137	126	18	9			
			138	128	17	8			
		0.13 [3]	135	124	19	10	65,000	145,000	80.4
			135	124	17	8			
		0.18	142	132	24	12	36,000	85,000	77.9
			142	132	24	11			
		[4]	144	131	17	10			
			145	133	21	10			
Sheet	1785°F/30 min./AC + 1350°F/2 hrs./AC	0.15	139	134	--	16	57,000	185,000	--
			130	128	--				

[1] Log average life at:

Center hole notch: σ_g = 50 ksi, R = 0.05, K_t = 2.53, f = 1800 cpm

Lap splice: σ_g = 30 ksi, R = 0.05, f = 1800 cpm

[2] $K_{IC} \neq K_Q$ (Conservative values. Highest toughness anticipated with 0.08% O_2 material.)

[3] Beta annealed, textured plate (Phase I material).

[4] Tensile properties from heat treat blanks for retest of fatigue crack propagation rates.

Table A.2.—Fatigue Properties of Ti-6A1-4V Plate and Sheet (Phase II Material)

Form	Heat Treatment	Nominal Oxygen Content (wt %)	Center Hole Notch* (cycles)	Lap Splice** (cycles)
Plate	1900°F/20 min./AC + 1350°F/2 hrs./AC	0.08	45,000 89,000 55,000 42,000 41,000	74,000 137,000 111,000 81,000
			log avg.: 52,000	log avg.: 98,000
		0.09***		71,000 72,000 59,000 73,000
				log avg.: 68,000
		0.11	49,000 39,000 34,000 40,000 34,000	84,000 65,000 65,000 68,000
			log avg.: 39,000	log avg.: 70,000
		0.13***		118,000 59,000 49,000 71,000
				log avg.: 70,000
		0.18	43,000 29,000 37,000 33,000 42,000	74,000 74,000 101,000 94,000
			log avg.: 36,000	log avg.: 85,000
Sheet	1785°F/30 min./AC + 1350°F/2 hrs./AC	0.15	34,000 73,000 48,000 82,000 64,000	201,000 396,000 182,000 174,000
			log avg.: 57,000	log avg.: 185,000

*Center hole notch: σ_g = 50 ksi, R = 0.05, K_t = 2.53, f = 1800 cpm.

**Lap splice: σ_g = 30 ksi, R = 0.05, f = 1800 cpm

***Heat treated and tested as a separate lot. Material with O_2 content of 0.13% is textured plate from Phase I.

Table A.3.—Fatigue Crack Propagation Rates for Ti-6A1-4V Plate and Sheet (Phase II Material)*

Oxygen Content (wt %)	Air***		3.5% NaCl***	
	$\Delta K_{avg.}$	da/dN	$\Delta K_{avg.}$	da/dN
0.08 (Plate)	12.3	3.3×10^{-6}	10.3	2.4×10^{-6}
	15.1	4.7×10^{-6}	14.1	4.5×10^{-6}
	16.1	4×10^{-6}	19.5	5.4×10^{-6}
	20.1	4.6×10^{-6}	20.9	1.4×10^{-5}
	26.5	1.4×10^{-5}	24.4	2×10^{-5}
	30.8	2.8×10^{-5}	33.8	3.8×10^{-5}
0.11 (Plate)	14.8	1.5×10^{-6}	8.8	3×10^{-6}
	19.2	2.3×10^{-6}	8.9	2.2×10^{-6}
	23.5	6×10^{-6}	10	2.7×10^{-6}
	28.3	8×10^{-6}	12.8	2.8×10^{-6}
	37.5	5×10^{-5}	14.4	5.2×10^{-6}
			17.5	5×10^{-6}
			21.5	9×10^{-6}
			26.8	2×10^{-5}
			37.3	8×10^{-5}
0.13** (Plate)	15	4.7×10^{-7}	15	5.5×10^{-7}
	20	3.2×10^{-6}	20	3×10^{-6}
	25	1.4×10^{-5}	25	1.1×10^{-5}
0.18 (Plate)	15.1	1.2×10^{-6}	10.7	9.1×10^{-7}
	18.1	5.8×10^{-6}	14.1	2.4×10^{-6}
	23.7	1.2×10^{-5}	19.9	7.2×10^{-6}
	28.5	2.3×10^{-5}	25.4	2.1×10^{-5}
0.15 (Sheet)	10	2×10^{-6}	10.1	3.9×10^{-7}
	12.5	5.2×10^{-6}	15.1	8.8×10^{-6}
	15.5	1.1×10^{-5}	25.0	4.1×10^{-4}
	20.2	2.1×10^{-5}		

*Sheet: Duplex annealed at 1785°F/30 min./AC and 1350°F/2 hr./AC.
Plate: Beta annealed at 1900°F/20 min./AC and 1350°F/2 hr./AC.

**Textured plate -- data reported in Phase I report.

***$\Delta K_{avg.}$ is average ΔK obtained at a given load range over the crack length through which it is cycled; da/dN -- inches per cycle; ΔK -- ksi-in.$^{1/2}$; R = 0.05; f = 60 cpm. Specimen type - DCB (Fig. 6)

Table A4

FATIGUE CRACK GROWTH RATES FOR
Ti-6Al-4V ALLOY PLATE, BETA-ANNEALED

(PHASE II MATERIAL)

R = 0.05, 60 cpm

Air		3.5% NaCl	
ΔK (ksi$\sqrt{in.}$)	da/dN (inch/cycle)	ΔK (ksi$\sqrt{in.}$)	da/dN (inch/cycle)
	Specimen No. 08-2-T (O_2 = 0.08)		
14.6	1.7×10^{-6}	11.4	4.3×10^{-7}
19.5	6.1×10^{-6}	16	2×10^{-6}
26.5	1.2×10^{-5}	17.9	7.3×10^{-6}
		24.3	2×10^{-5}
		26.9	5.3×10^{-5}
	Specimen No. 11-2-T (O_2 = 0.11)		
15.5	7.1×10^{-7}	11.7	4.8×10^{-7}
21.5	3.7×10^{-6}	16.6	1.2×10^{-6}
33.4	1.7×10^{-5}	18.1	2.4×10^{-6}
		20.5	1.5×10^{-5}
		27.6	3.2×10^{-5}
		30.9	3.7×10^{-5}
		35.9	6.6×10^{-5}
	Specimen No. 18-2-T (O_2 = 0.18)		
15	2.4×10^{-6}	12.4	1.8×10^{-6}
20.8	7.6×10^{-6}	17.3	1.5×10^{-5}
28.7	2.1×10^{-5}	19.6	1.7×10^{-5}
		28.6	7.3×10^{-5}
		33.6	9×10^{-5}

NOTE: ΔK is an average value obtained at a given load range over the crack length through which it is cycled; da/dN--inches per cycle; ΔK--ksi$\sqrt{in.}$; R = 0.05; f = 60 cpm; specimen type--CT (fig. 7).

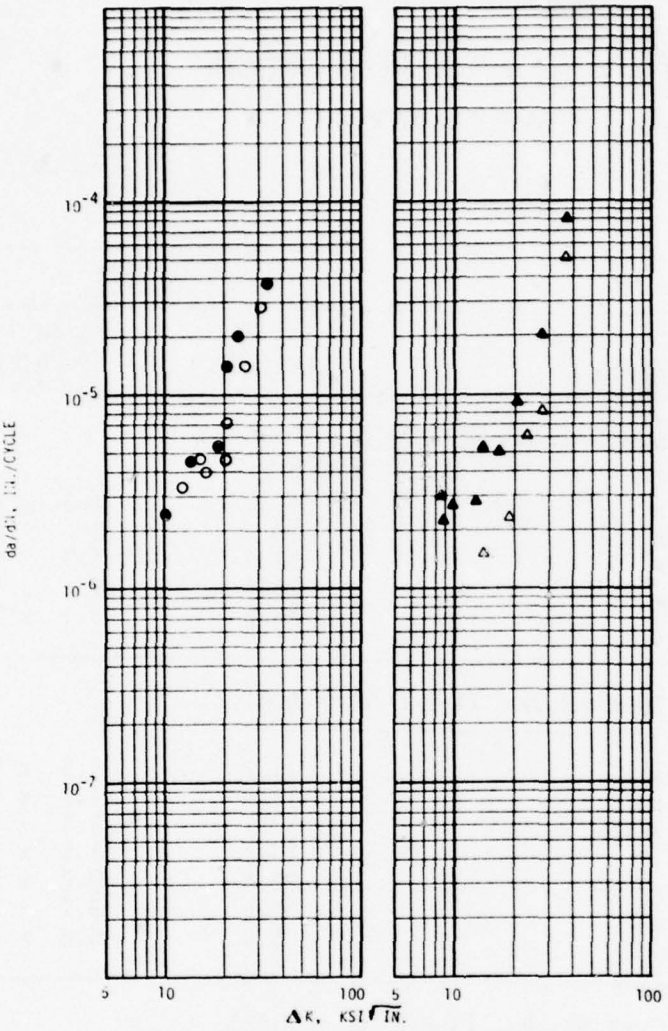

Figure A1.—Fatigue Crack Propagation Rate in Air and Aqueous 3.5% NaCl as a Function of ΔK for Phase II Material. T-L Orientation, Specimen Type—DCB (Figure 6) for Plate, Center Notch (Figure 9) For Sheet.

○ *Plate, P08*
△ *Plate, P11*
□ *Plate, P18*
⬡ *Sheet, S15*
Open Symbols - Air
Solid Symbols - 3.5% NaCl

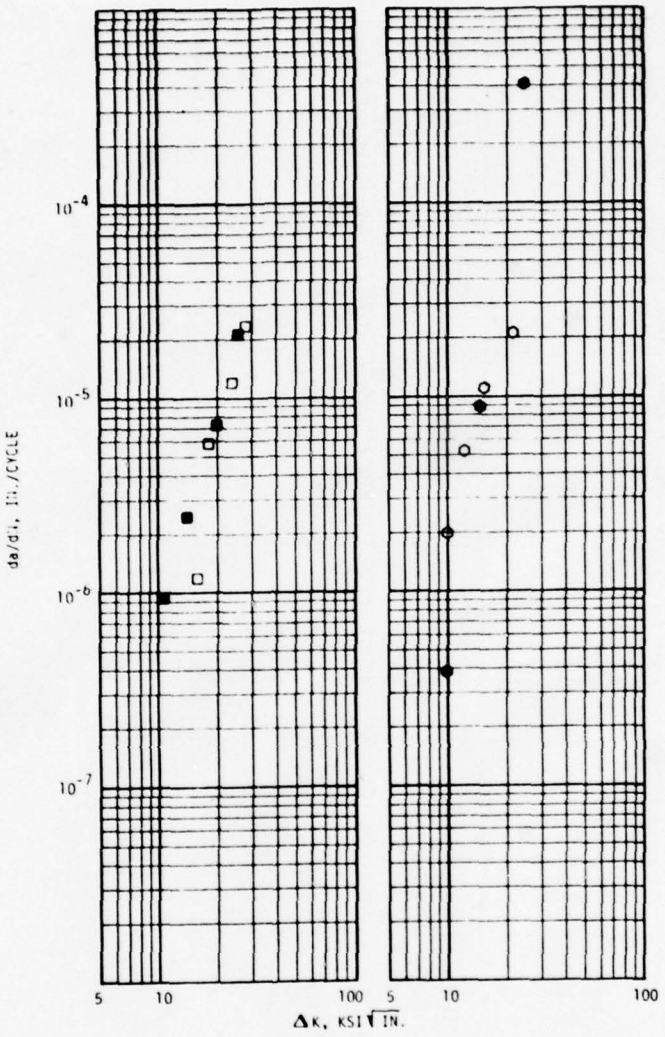

Figure A1.—(Concluded).

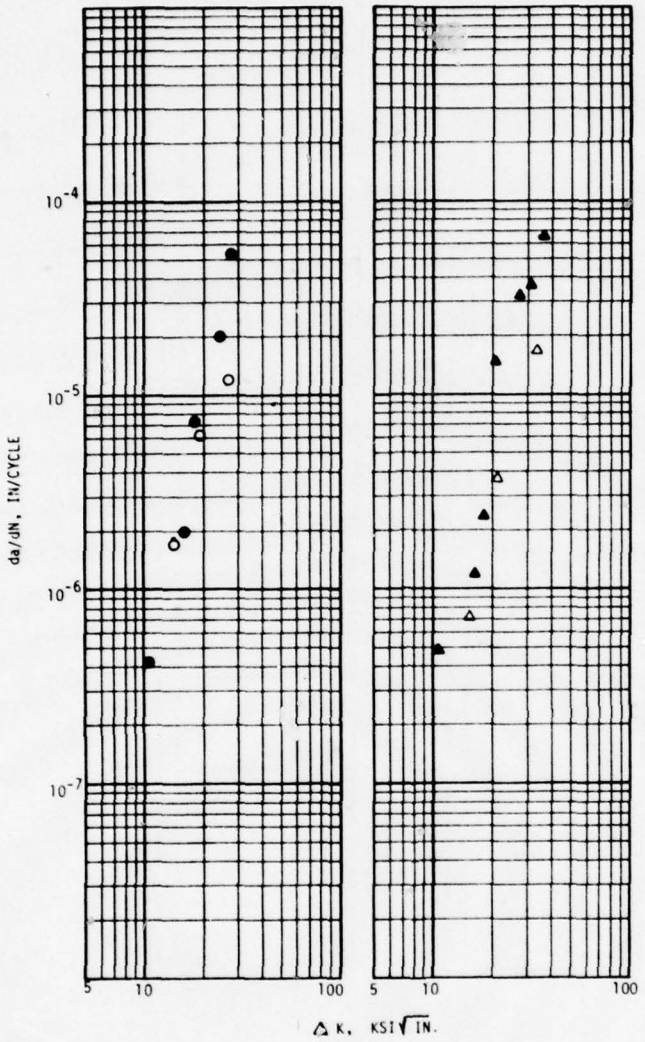

Figure A2.—Fatigue Crack Propagation Rate in Air and Aqueous 3.5% NaCl as a Function of K for Phase II Plate Material. T-L Orientation, Specimen Type—CT (Figure 7).

○ *Plate, P08*
△ *Plate, P11*
□ *Plate, P18*
Open Symbols - Air
Solid Symbols - 3.5% NaCl

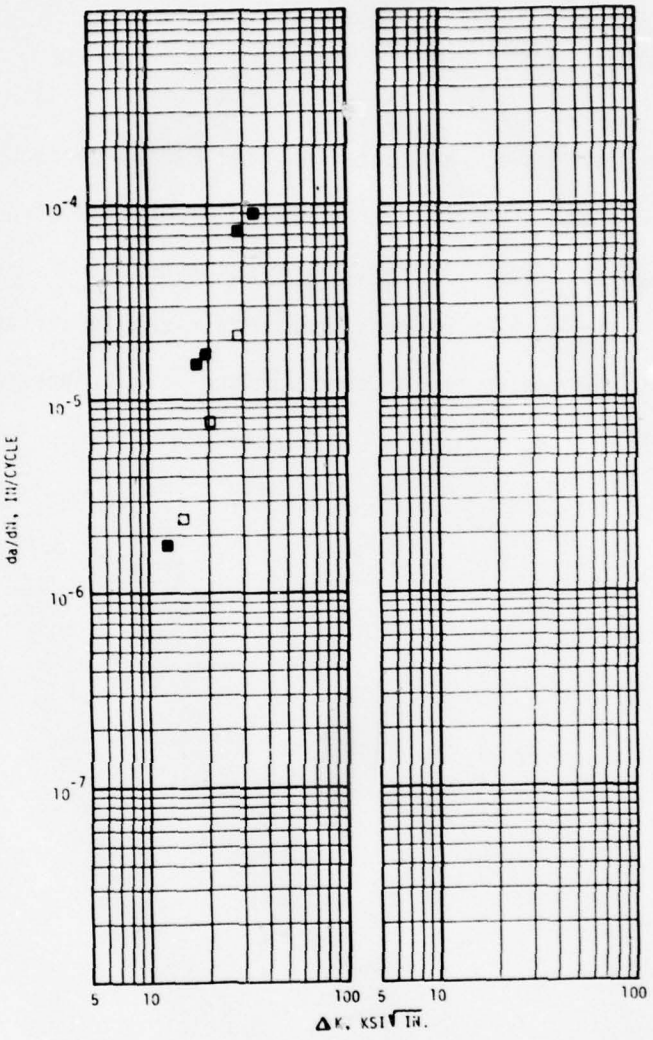

Figure A2.—(Concluded).

APPENDIX B

TEST DATA--PHASE III

This appendix contains all the detailed test data generated during Phase III of this program. Included are tensile properties, fracture toughness properties (K_{IC} and K_C), stress-corrosion cracking threshold (K_{ISCC} and K_{SCC}), fatigue crack propagation (FCP) rates in air and aqueous 3.5% NaCl solution, and smooth and notched fatigue life properties.

Table B1.—Tensile and Fracture Properties of Ti-6A1-4V Sheet and Plate (Phase III Material)

Form	Heat Treatment	Nominal Oxygen Content (wt %)	Testing Direction	TUS (ksi)	YTS (ksi)	RA (%)	Elongation (%)	K_{IC}	K_{ISCC}** (ksi$\sqrt{in.}$)	K_C	K_{SCC}**
Plate 1.5 inch	1845°F/20 min./AC + 1350°F/2 hrs./AC	0.10	T	133	123	22	10	86.5	85	---	---
			T	132	121	24	10	89.4	85	---	---
			T	134	123	22	12	92.0	100	---	---
	(Beta transus - 1795°F)		L	131	119	16	11	98.0*	95	---	---
			L	134	125	22	11	101.9*	95	---	---
			L	132	123	22	11	89.5	95	---	---
Sheet 0.128 inch	1730°F/10 min./AC + 1350°F/2 hrs./AC	0.11	T	138	133	15	15	---	--	154.4	120
			T	138	133	21	16	---	--	147.3	120
			T	135	131	14	13	---	--	173.6	120
	(Beta transus - 1780°F)		L	136	129	23	17	---	--	170.1	142
			L	137	130	21	15	---	--	166.3	120
			L	136	129	25	15	---	--	---	154

*$K_Q \neq K_{IC}$ due to thickness criteria of ASTM E399-72.

**Estimated K_{ISCC} and K_{SCC}.

Table B2

FATIGUE CRACK GROWTH RATES FOR
Ti-6Al-4V ALLOY PLATE, BETA-ANNEALED

R = 0.05, 60 cpm

Air		3.5% NaCl	
ΔK (ksi$\sqrt{in.}$)	da/dN (inch/cycle)	ΔK (ksi$\sqrt{in.}$)	da/dN (inch/cycle)
	Specimen No. FCP-1-L		
9.1	7.8×10^{-8}	10	6.6×10^{-8}
9.3	2.4×10^{-7}	10.1	7.8×10^{-8}
9.7	4.3×10^{-7}	14.8	9.5×10^{-8}
10	2×10^{-7}	15	2.7×10^{-7}
10.2	3.9×10^{-7}	16	2.1×10^{-6}
18.2	3×10^{-6}	23.5	3.5×10^{-5}
19.8	6.2×10^{-6}	23.9	4.6×10^{-5}
20.8	8.1×10^{-6}	24.3	5.7×10^{-5}
29	1.8×10^{-5}	24.6	6.2×10^{-5}
30.7	3.1×10^{-5}	31.4	7.4×10^{-5}
31.7	2×10^{-5}	32.3	8.3×10^{-5}
43.3	8.9×10^{-5}	42.2	1.5×10^{-4}
45.3	8×10^{-5}	43.8	1.4×10^{-4}
		55.2	2.5×10^{-4}
		59.3	2.7×10^{-4}
	Specimen No. FCP-5-T		
9.9	1.9×10^{-7}	10.1	8.9×10^{-8}
10.4	3.4×10^{-7}	15.2	2.6×10^{-7}
19.8	6.1×10^{-6}	16.4	4×10^{-6}
21	8×10^{-6}	21.4	3×10^{-5}
29.2	2.1×10^{-5}	21.7	4.5×10^{-5}
30.4	2.4×10^{-5}	22	6.4×10^{-5}
31.4	3.2×10^{-5}	22.3	7×10^{-5}
43	1.1×10^{-4}	28.4	9.1×10^{-5}
44.2	7.6×10^{-4}	28.6	8.2×10^{-5}
45.5	8.5×10^{-4}	29	8×10^{-5}
		29.4	9×10^{-5}
		37.9	1.3×10^{-4}
		38.6	1.29×10^{-4}
		39	1.37×10^{-4}
		39.6	1.75×10^{-4}
		48.7	2.3×10^{-4}
		49.9	2.3×10^{-4}
		52.8	2.7×10^{-4}

Table B3

FATIGUE CRACK GROWTH RATES FOR
Ti-6Al-4V ALLOY PLATE, BETA-ANNEALED

R = 0.05, 6 cpm

Air		3.5% NaCl	
ΔK (ksi$\sqrt{\text{in.}}$)	da/dN (inch/cycle)	ΔK (ksi$\sqrt{\text{in.}}$)	da/dN (inch/cycle)
	Specimen No. FCP-3-L		
9.4	9.6×10^{-8}	13.5	1.4×10^{-6}
14.9	8.2×10^{-7}	13.7	1.3×10^{-6}
15.2	9.4×10^{-7}	13.9	2×10^{-6}
15.3	1.3×10^{-6}	18.9	4.2×10^{-6}
18	2.4×10^{-6}	19.6	5.2×10^{-6}
18.6	4.1×10^{-6}	25	1.2×10^{-5}
23.2	1.2×10^{-5}	25.2	9.4×10^{-6}
23.5	1.1×10^{-5}	25.6	1.2×10^{-5}
23.8	1.5×10^{-5}	33.3	1.2×10^{-4}
28.8	1.8×10^{-5}	40	2.7×10^{-4}
29.7	2.1×10^{-5}	42.6	3.2×10^{-4}
34.3	3.5×10^{-5}	45	4×10^{-4}
34.8	4.7×10^{-5}	46.1	4.9×10^{-4}
35.2	5.6×10^{-5}	48.5	6.7×10^{-4}
41	5.7×10^{-5}		
41.5	6.7×10^{-5}		
42.7	8.3×10^{-5}		
42.8	8.8×10^{-5}		
43.5	1×10^{-4}		
48.7	1.15×10^{-4}		
49.1	1.2×10^{-4}		
49.7	1.3×10^{-4}		
50.2	1.4×10^{-4}		
50.7	1.5×10^{-4}		

Table B4

FATIGUE CRACK GROWTH RATES FOR
Ti-6Al-4V ALLOY PLATE, BETA-ANNEALED

R = 0.05, 6 cpm

Air		3.5% NaCl	
ΔK (ksi$\sqrt{\text{in.}}$)	da/dN (inch/cycle)	ΔK (ksi$\sqrt{\text{in.}}$)	da/dN (inch/cycle)
	Specimen No. FCP-7-T		
9	6.1×10^{-8}	12.4	9.8×10^{-7}
9.1	1×10^{-7}	12.6	1.2×10^{-6}
14.3	9.9×10^{-7}	12.7	1.6×10^{-6}
14.5	1.2×10^{-6}	17.3	3.7×10^{-6}
14.7	1.1×10^{-6}	17.7	5.1×10^{-6}
17.3	2.8×10^{-6}	22.7	5.3×10^{-6}
17.7	4.6×10^{-6}	22.9	7.6×10^{-6}
22.4	6.5×10^{-6}	23.1	1×10^{-5}
22.5	8.2×10^{-6}	28.3	1.4×10^{-5}
22.5	8.7×10^{-6}	28.8	2.8×10^{-5}
27.2	1.2×10^{-5}	31.7	1.7×10^{-4}
27.8	1.8×10^{-5}	41.5	2.5×10^{-4}
33.1	4.1×10^{-5}	44.4	2.7×10^{-4}
33.8	5×10^{-5}		
38.8	6.6×10^{-5}		
40	7.2×10^{-5}		
40.5	8.2×10^{-5}		
45.3	1×10^{-4}		
46.1	1.2×10^{-4}		
46.4	1.25×10^{-4}		

Table B5

FATIGUE CRACK GROWTH RATES FOR
Ti-6Al-4V ALLOY PLATE, BETA-ANNEALED

R = 0.5, 60 cpm

Air		3.5% NaCl	
ΔK (ksi$\sqrt{in.}$)	da/dN (inch/cycle)	ΔK (ksi$\sqrt{in.}$)	da/dN (inch/cycle)
	Specimen No. FCP-4-L		
10.8	3.96×10^{-6}	14.75	5.4×10^{-6}
14.2	5.4×10^{-6}	15.5	7.2×10^{-6}
14.7	6.9×10^{-6}	16.2	1×10^{-5}
18.7	1.5×10^{-5}	17	2×10^{-5}
23.1	2.5×10^{-5}	18.4	3.3×10^{-5}
23.8	4.3×10^{-5}	20.7	6.5×10^{-4}
28.4	4.5×10^{-5}	24.1	1.1×10^{-4}
23.6	9.2×10^{-5}	30.7	2.1×10^{-4}
34.8	1.25×10^{-4}	38.9	4.6×10^{-4}
Specimen No. FCP-8-T		Specimen No. FCP-5-T	
10.8	4.2×10^{-6}	13.6	6.9×10^{-7}
11	5.7×10^{-6}	14.4	2.4×10^{-5}
14.5	6.2×10^{-6}	16.7	5.2×10^{-5}
15	6.5×10^{-6}	19.6	7.6×10^{-5}
18.5	1.4×10^{-5}	22.6	8.7×10^{-4}
19.4	1.9×10^{-5}	26.1	1.3×10^{-4}
24.1	3.1×10^{-5}	31.5	1.8×10^{-4}
25	5.3×10^{-5}	39.3	8.75×10^{-4}
36.6	1.3×10^{-4}		

Table B6

FATIGUE CRACK GROWTH RATES FOR
Ti-6Al-4V ALLOY PLATE, BETA-ANNEALED

R = 0.5, 6 cpm

Air	
ΔK (ksi$\sqrt{in.}$)	da/dN (inch/cycle)
Specimen No. FCP-8-T	
14.6	2.8×10^{-6}
16	8.6×10^{-6}
26.3	3.8×10^{-5}
36.3	1.1×10^{-4}
37.8	1.6×10^{-4}
47.8	1.1×10^{-3}
Specimen No. FCP-4-L	
12.9	9.1×10^{-7}
13.1	1×10^{-6}
20.2	2.7×10^{-5}
21.7	2.8×10^{-5}
25.5	3.4×10^{-5}
25.8	4.4×10^{-5}
26.5	5.2×10^{-5}
35.3	1×10^{-4}
44.7	3.4×10^{-4}
44.9	5.2×10^{-4}

Table B7

FATIGUE CRACK GROWTH RATES FOR
Ti-6Al-4V ALLOY SHEET, DUPLEX-ANNEALED

R = 0.05, 60 cpm

Air		3.5% NaCl	
ΔK (ksi$\sqrt{in.}$)	da/dN (inch/cycle)	ΔK (ksi$\sqrt{in.}$)	da/dN (inch/cycle)
Specimen No. S-3-5-T		Specimen No. SC-3-2-T	
10.4	3.28×10^{-6}	10.2	9.2×10^{-6}
10.8	2.5×10^{-6}	11.6	1.4×10^{-5}
11.2	3.92×10^{-6}	13.0	2×10^{-5}
16.4	1.2×10^{-5}	14.5	3×10^{-4}
17.2	2×10^{-5}	21	1×10^{-4}
17.9	1.8×10^{-5}	22.4	1.25×10^{-4}
18.1	1.67×10^{-5}	23.2	2×10^{-4}
21.9	2.3×10^{-5}	30	4.4×10^{-4}
22.2	2.5×10^{-5}	31.3	5.2×10^{-4}
23.1	2.75×10^{-5}	32.8	5.7×10^{-4}
24.3	4×10^{-5}	36.5	4.9×10^{-4}
30.1	6.97×10^{-5}	37.5	6.9×10^{-4}
30.8	8×10^{-5}	39	8.3×10^{-4}
31.8	7.49×10^{-5}	43.1	1.1×10^{-3}
37.7	1.5×10^{-4}	45.6	1.2×10^{-3}
38.4	1.4×10^{-4}	50	1.4×10^{-3}
39.3	1.47×10^{-4}	50.9	1.5×10^{-3}
43.5	2×10^{-4}	52.8	1.5×10^{-3}
44.2	2.4×10^{-4}		
47.7	3×10^{-4}		
48.6	2.8×10^{-4}		
50.6	3.55×10^{-4}		
51.3	4.2×10^{-4}		

Table B8

FATIGUE CRACK GROWTH RATES FOR
Ti-6Al-4V ALLOY SHEET, DUPLEX-ANNEALED

R = 0.05, 60 cpm

Air		3.5% NaCl	
ΔK (ksi$\sqrt{in.}$)	da/dN (inch/cycle)	ΔK (ksi$\sqrt{in.}$)	da/dN (inch/cycle)
Specimen No. SC-3-1-L		Specimen No. SC-3-6-L	
10.5	2.8×10^{-6}	9.7	2.7×10^{-6}
10.9	2×10^{-6}	10.3	4.6×10^{-6}
11.3	4×10^{-6}	11.6	5.6×10^{-6}
11.9	5.2×10^{-5}	11.9	5.6×10^{-6}
16.9	1.25×10^{-5}	12.4	6.9×10^{-6}
17.9	1.76×10^{-5}	14.8	1.3×10^{-5}
18.6	2.13×10^{-5}	15.2	1.4×10^{-5}
19	2.6×10^{-5}	15.7	1.5×10^{-5}
22.1	2.6×10^{-5}	16.8	1.8×10^{-5}
22.5	2.7×10^{-5}	19.9	3.7×10^{-5}
23.5	3.4×10^{-5}	21.2	4.4×10^{-5}
24.8	4.2×10^{-5}	21.7	5.4×10^{-5}
31.7	6.9×10^{-5}	23	7.5×10^{-5}
32.3	7.8×10^{-5}	23.4	8.4×10^{-4}
33	6.7×10^{-5}	26.3	1.2×10^{-4}
33.6	7.9×10^{-4}	27.5	1.3×10^{-4}
37.1	1.5×10^{-4}	32.2	1.8×10^{-4}
37.6	1.3×10^{-4}	33.5	2.3×10^{-4}
38.5	1.4×10^{-4}	39.6	6.6×10^{-4}
39.6	1.8×10^{-4}	41.1	7.4×10^{-4}
44.8	3.3×10^{-4}	43	9.04×10^{-3}
45.5	2.4×10^{-4}	45	1×10^{-3}
46.4	2.6×10^{-4}	49.7	1.1×10^{-3}
48.7	3.8×10^{-4}	50.9	1.26×10^{-3}
49.5	3.8×10^{-4}		
50.2	4×10^{-4}		
50.6	3.5×10^{-4}		

Table B9

FATIGUE CRACK GROWTH RATES FOR
Ti-6Al-4V ALLOY SHEET, DUPLEX-ANNEALED

R = 0.5, 60 cpm

Air		3.5% NaCl	
ΔK ($ksi\sqrt{in.}$)	da/dN (inch/cycle)	ΔK ($ksi\sqrt{in.}$)	da/dN (inch/cycle)
Specimen No. S-3-4-L		Specimen No. SC-3-5-L	
10.5	7.6×10^{-6}	10.5	4.8×10^{-6}
10.7	8.5×10^{-6}	11	6.3×10^{-6}
11.5	9×10^{-6}	11.5	7.4×10^{-6}
19.1	2.9×10^{-5}	12.2	9.3×10^{-6}
27.6	8.7×10^{-5}	13.1	1.3×10^{-5}
33	1.6×10^{-4}	14.2	1.8×10^{-5}
38.1	1.9×10^{-4}	17.4	2.8×10^{-5}
45.2	3.1×10^{-4}	18.3	3.2×10^{-5}
46.8	4×10^{-4}	19.9	5×10^{-5}
49.9	5.1×10^{-4}	24.4	1.9×10^{-4}
		25.9	2.2×10^{-4}
		27.7	2.7×10^{-4}
		31.5	6.1×10^{-4}
		33	7×10^{-4}
		34	8×10^{-4}
		38	1.2×10^{-3}
		39.3	1.5×10^{-3}
		40	1.2×10^{-3}
		43.8	2.1×10^{-3}
		45.5	2×10^{-3}
		47.1	2.3×10^{-3}
		49.6	2.5×10^{-3}
		51.5	2.7×10^{-3}

Table B10

FATIGUE CRACK GROWTH RATES FOR
Ti-6Al-4V ALLOY SHEET, DUPLEX-ANNEALED

R = 0.5, 60 cpm

Air		3.5% NaCl	
ΔK (ksi$\sqrt{in.}$)	da/dN (inch/cycle)	ΔK (ksi$\sqrt{in.}$)	da/dN (inch/cycle)
Specimen No. S-3-3-T		Specimen No. SC-3-3-T	
5.2	1×10^{-6}	14.6	5.3×10^{-5}
5.5	1.35×10^{-6}	16.7	4.6×10^{-5}
5.7	1.4×10^{-6}	26.3	2.6×10^{-4}
10.1	4.7×10^{-6}	27.9	3.6×10^{-4}
10.6	7.5×10^{-6}	29.4	4.8×10^{-4}
11.3	8×10^{-6}	36.7	9.7×10^{-3}
12	8.5×10^{-6}	38	1.1×10^{-3}
15.6	2.8×10^{-5}	43.9	2.2×10^{-3}
17	3.4×10^{-5}	45.1	2.1×10^{-3}
18.5	4.6×10^{-5}	48.7	2×10^{-3}
24	9×10^{-4}		
25.1	1.1×10^{-4}		
30.5	1.8×10^{-4}		
31.3	2.1×10^{-4}		
32.1	2.7×10^{-4}		
36.4	3.1×10^{-4}		
37.2	3.4×10^{-4}		
38	5×10^{-4}		
43.5	5×10^{-4}		
48.9	8.4×10^{-4}		

Table B11

FATIGUE DATA FOR Ti-6Al-4V ALLOY PLATE
AT ROOM TEMPERATURE AND 1800 cpm

Smooth Specimen - $K_t = 1$

Specimen Number	Test Direction	Maximum Gross Stress (x 1000)	R	Cycles to Failure (x 1000)
FP-19	T	125	0.05	2
-13		120		17
-8		110		42
-7		100		42
-2		90		1,725
-14		90		74
-20		80		232
-23		80		2,814
-1	T	50		4,890*
FP-28	L	100		64
-25		80		164
-26		60		10,347*
-27	L	59	0.05	641
FP-21	T	130	0.50	64
-22		130		104
-3		120		743
-4		120		89
-15		120		131
-16		120		131
-9		110		1,359
-10		110	0.50	1,406
FP-5		80	-1.0	1**
-17		80		32
-6		70		66
-11		70		36
-12		60		156
-18		60		116
-24	T	60	-1.0	2,806

*No failure
**Grip failure

Table B12

FATIGUE DATA FOR Ti-6Al-4V ALLOY PLATE
AT ROOM TEMPERATURE AND 1800 cpm

Notched Specimen - $K_t = 2.53$

Specimen Number	Test Direction	Maximum Gross Stress (x 1000)	R	Cycles to Failure (x 1000)
CHFP-19	T	82.5	0.05	6
-2		80		4
-7		62.9		18
-13		62.7		20
-1		60		16
-14		42		81
-8		41.8		800
-20	T	41.8		2,639
CHFP-26	L	104.5		4
-25		83		4
-27		62.8		18
-28	L	42	0.05	1,579
CHFP-22	T	104.7	0.50	1
-9		104.4		7
-15		101.7		2
-16		83.7		31
-10		83.6		24
-4		80		39
-21		72		3,713
-3		55	0.50	841
CHFP-12		62.8	-1.0	1
-5		60		2
-11		41.8		7
-18		41.6		10
-6		40		13
-17		31.5		73
-23		31.1		69
-24	T	20.9	-1.0	5,041*

*No failure

Table B13

FATIGUE DATA FOR Ti-6Al-4V ALLOY SHEET
AT ROOM TEMPERATURE AND 1800 cpm

Smooth Specimen - $K_t = 1$

Specimen Number	Test Direction	Maximum Gross Stress (x 1000)	R	Cycles to Failure (x 1000)
SFS-19	T	130	0.05	1
-8		120		43
-13		120		53
-2		110		24
-7		110		134
-14		110		134
-20		110		5,033*
-1	T	90		302
SFS-26	L	120		38
-28		110		68
-27		100		522
-25	L	90	0.05	4,739
SFS-22	T	130	0.50	329
-16		125		836
-3		120		176
-4		120		1,795
-9		120		1,985
-15		120		1,522
-10		110		2,888
-21		110		2,473
-E3		130		119
-E5		120	0.50	2,255
SFS-24		90	-1.0	1
-X1		90		36
-17		86		78
-5		80		1
-12		80		35
-6		70		1
-18		70		4,028
-X2		70		181
-23		64.2		72
-11		60		2,028*
-E10	T	50	-1.0	7,470*

*No failure

Table B14

FATIGUE DATA FOR Ti-6Al-4V ALLOY SHEET
AT ROOM TEMPERATURE AND 1800 cpm

Notched Specimen - K_t = 2.53

Specimen Number	Test Direction	Maximum Gross Stress (x 1000)	R	Cycles to Failure (x 1000)
CHF-1	T	80	0.05	7
-8		80		1
-13		80		1*
-2		60		1,130
-7		60		23
-14		60		27
-19		60		26
-20		40		1,895
-24	T	40		1,741
CHF-26	L	100		3
-25		80		7
-27		60		28
-28	L	40	0.05	2,796
CHF-9	T	100	0.50	14
-22		100		12
-10		80		38
-15		80		1
-16		80		43
-21		80		43
-3		80		1,526
-4		60	0.50	1,247
CHF-5		60	-1.0	1
-12		60		2
-6		40		19
-11		40		18
-17		30		484
-23		30		444
-18	T	20	-1.0	9,273

*Grip failure

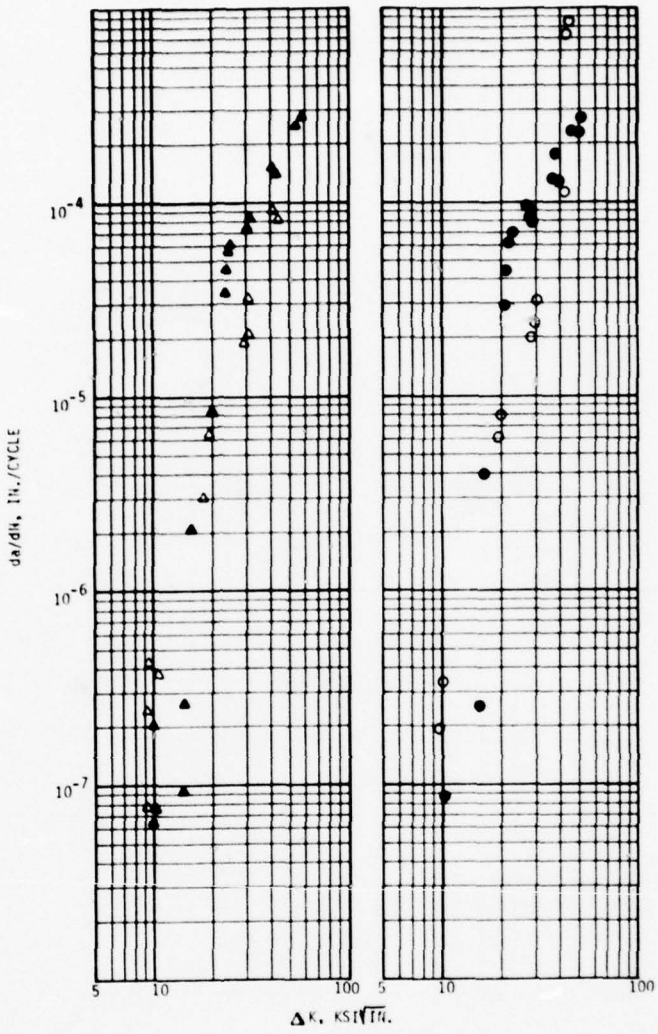

Figure B1.—Fatigue Crack Propagation Vs. Stress Intensity Range for Ti-6A1-4V Plate (Phase III Material).
Annealing: 1845° F, 20 Min,. Ac + 1350° F, 2 Hrs., AC.
Test Conditions: f - 60 cpm; R - .05
Symbols: o = Crack Plane Transverse to Rolling Direction
Δ = Crack Plane Parallel to Rolling Direction
Open = Air
Solid = 3.5% NaCl

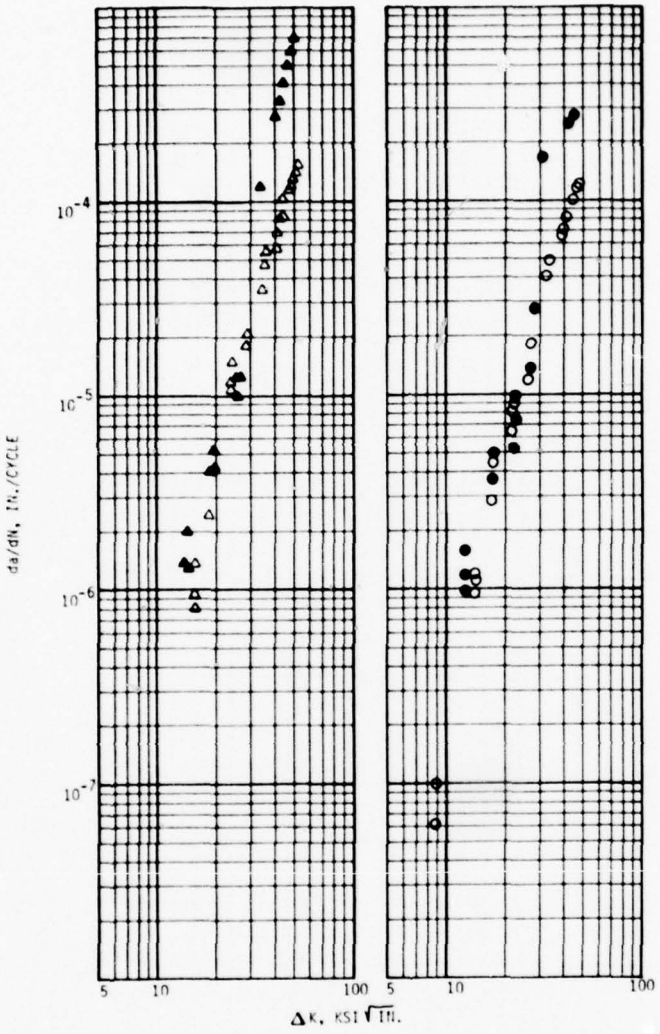

Figure B2.—Fatigue Crack Propagation Vs. Stress Intensity Range for Ti-6A1-4V Plate (Phase III Material).
Annealing: 1845° F, 20 Min., Ac + 1350° F, 2 Hrs., AC.
Test Conditions: f - 6 cpm; R - .05.
Symbols: o = Crack Plane Transverse to Rolling Direction
Δ = Crack Plane Parallel to Rolling Direction
Open = Air
Solid = 3.5% NaCl

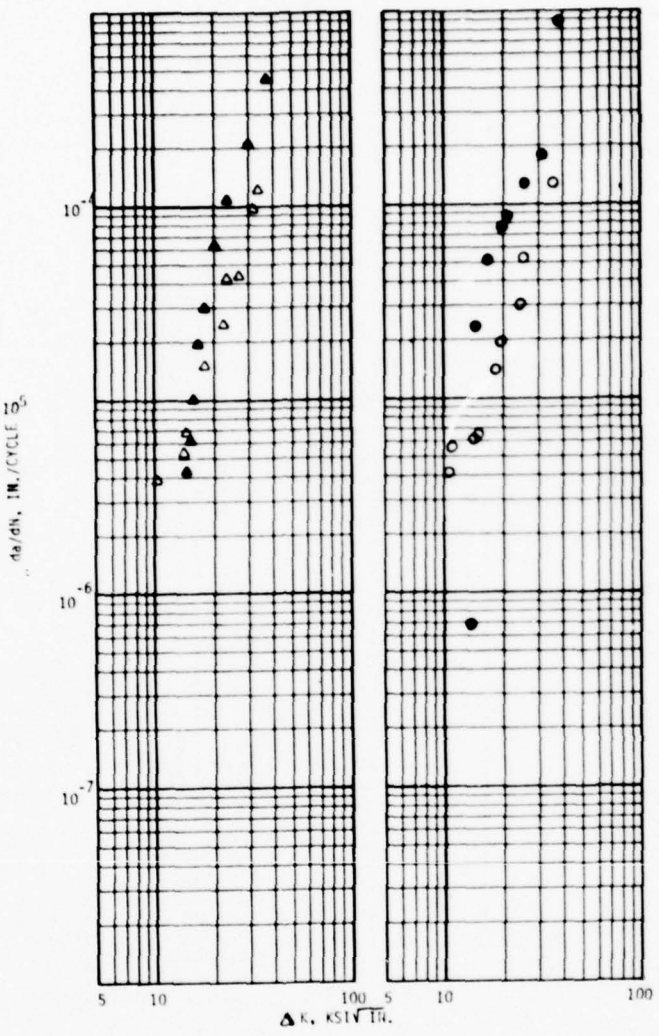

Figure B3.—Fatigue Crack Propagation Vs. Stress Intensity Range for Ti-6A1-4V Plate (Phase III Material).
Annealing: 1845° F, 20 Min., Ac + 1350° F, 2 Hrs., AC.
Test Conditions: f - 60 cpm; R - .5.
Symbols: o = Crack Plane Transverse to Rolling Direction
Δ = Crack Plane Parallel to Rolling Direction
Open = Air
Solid = 3.5% NaCl

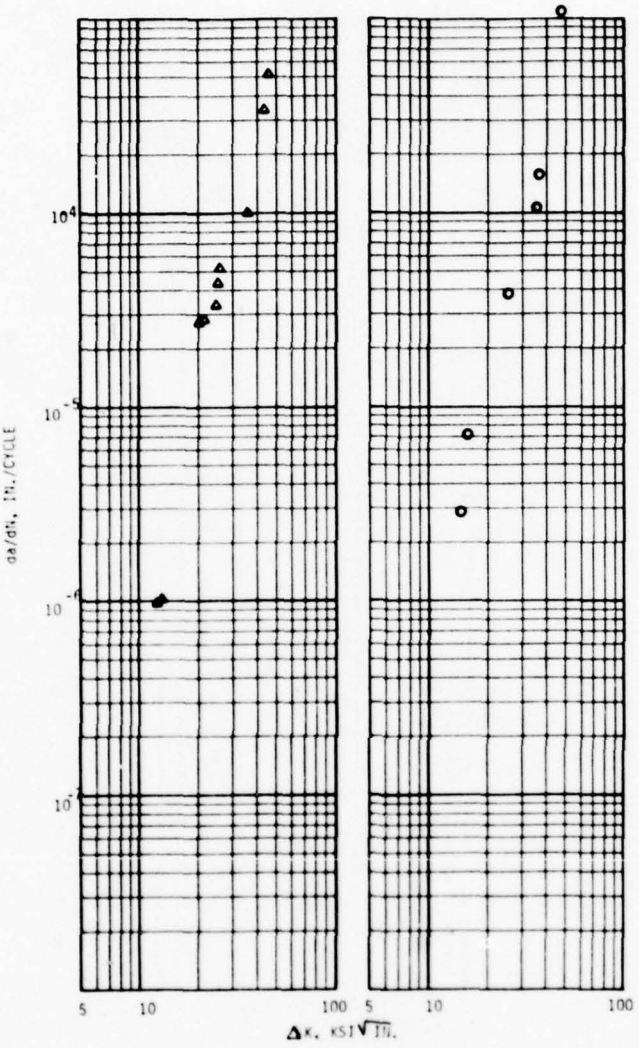

Figure B4.—Fatigue Crack Propagation Vs. Stress Intensity Range for Ti-6A1-4V Plate (Phase III Material).
Annealing: 1845° F, 20 Min., Ac + 1350° F, 2 Hrs., AC.
Test Conditions: f - 6 cpm; R - .5.
Symbols: o = Crack Plane Transverse to Rolling Direction
Δ = Crack Plane Parallel to Rolling Direction
Open = Air

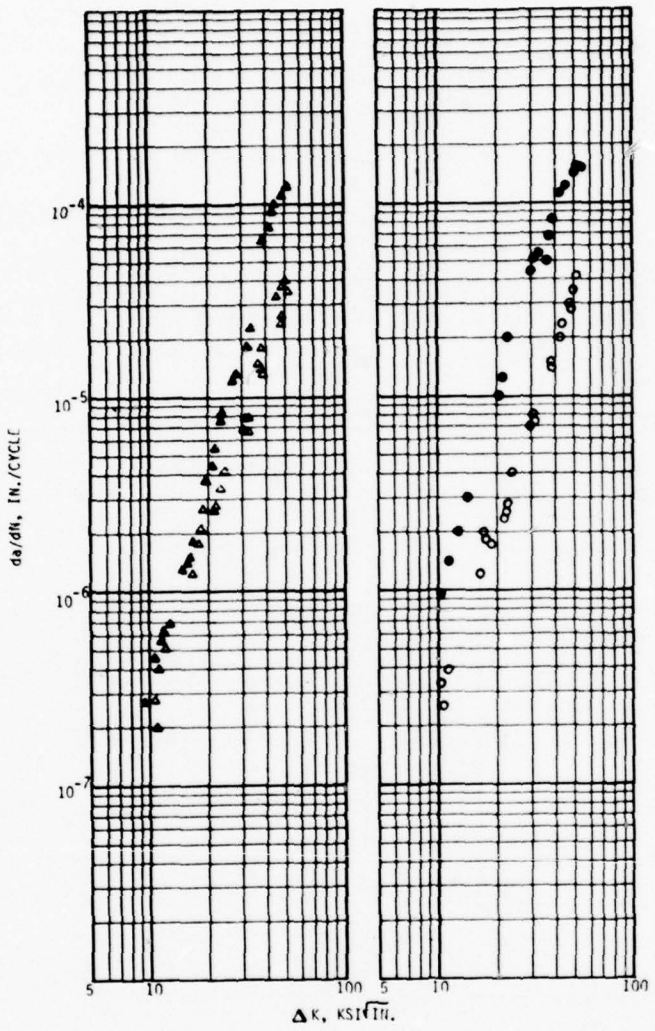

Figure B5.—Fatigue Crack Propagation Rate Vs. Stress Intensity Range for Ti-6A1-4V Sheet (Phase III Material).
Annealing: 1730° F, 10 Min., AC + 1350° F, 2 Hrs., AC.
Test Conditions: f - 60 cpm; R - .05.
Symbols: o = Crack Plane Transverse to Rolling Direction
Δ = Crack Plane Parallel to Rolling Direction
Open = Air
Solid = 3.5% NaCl

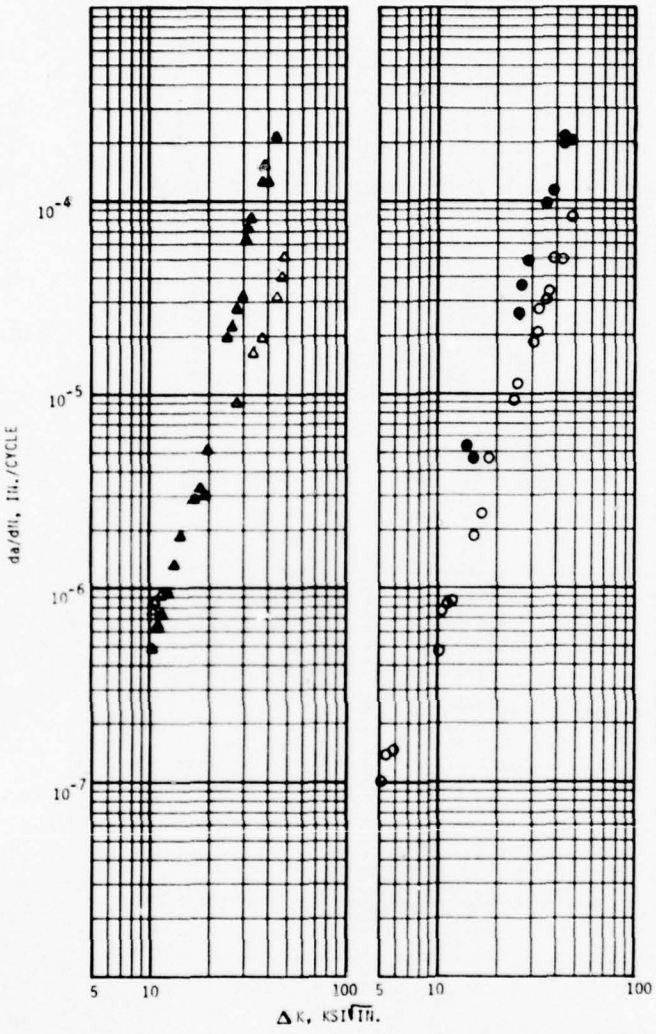

Figure B6.—Fatigue Crack Propagation Rate Vs. Stress Intensity Range for Ti-6A1-4V Sheet (Phase III Material).
Annealing: 1730° F, 10 Min., AC + 1350° F, 2 Hrs., AC.
Test Conditions: f - 60 cpm; R - .5
Symbols: o = Crack Plane Transverse to Rolling Direction
Δ = Crack Plane Parallel to Rolling Direction
Open = Air
Solid = 3.5% NaCl

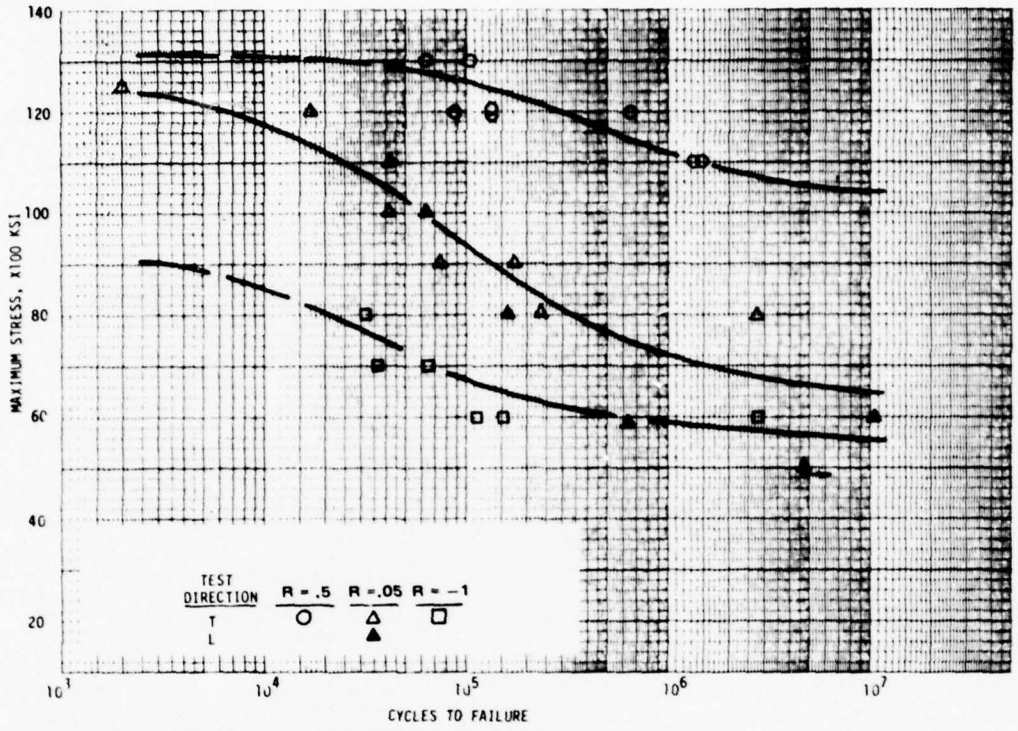

Figure B7.—Fatigue Life of Beta-annealed Ti-6A1-4V Alloy Plate in Air, at Room Temperature, 1800 cpm, $K_t = 1$.

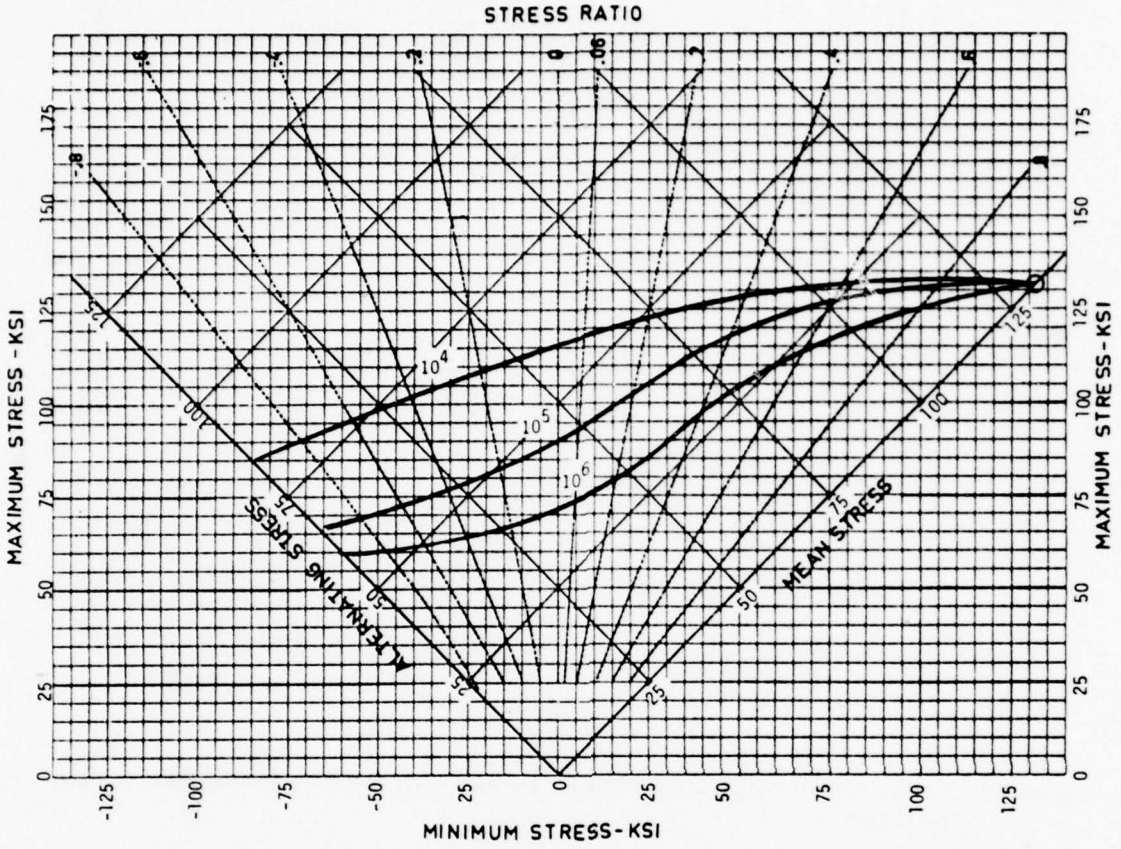

Figure B8.—Constant-life Diagram for Phase III BA Plate Tested at Room Temperature, K_t = 1, f = 1800 cpm.

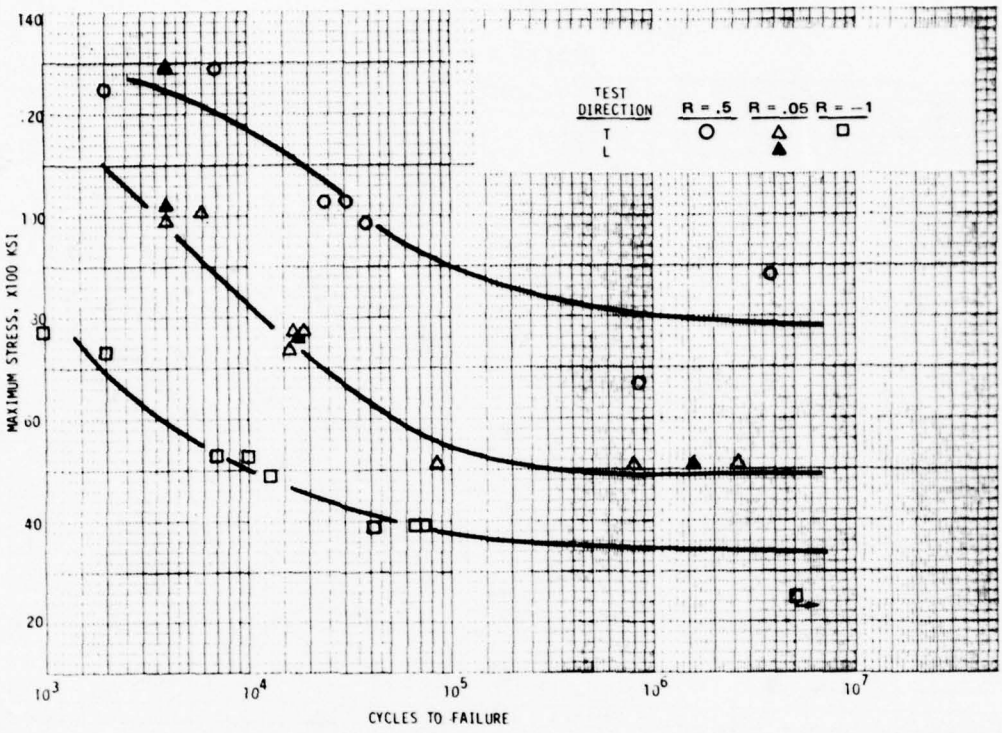

Figure B9.—Fatigue Life of Beta-annealed Ti-6A1-4V Alloy Plate in Air, at Room Temperature, 1800 cpm, K_t = 2.53.

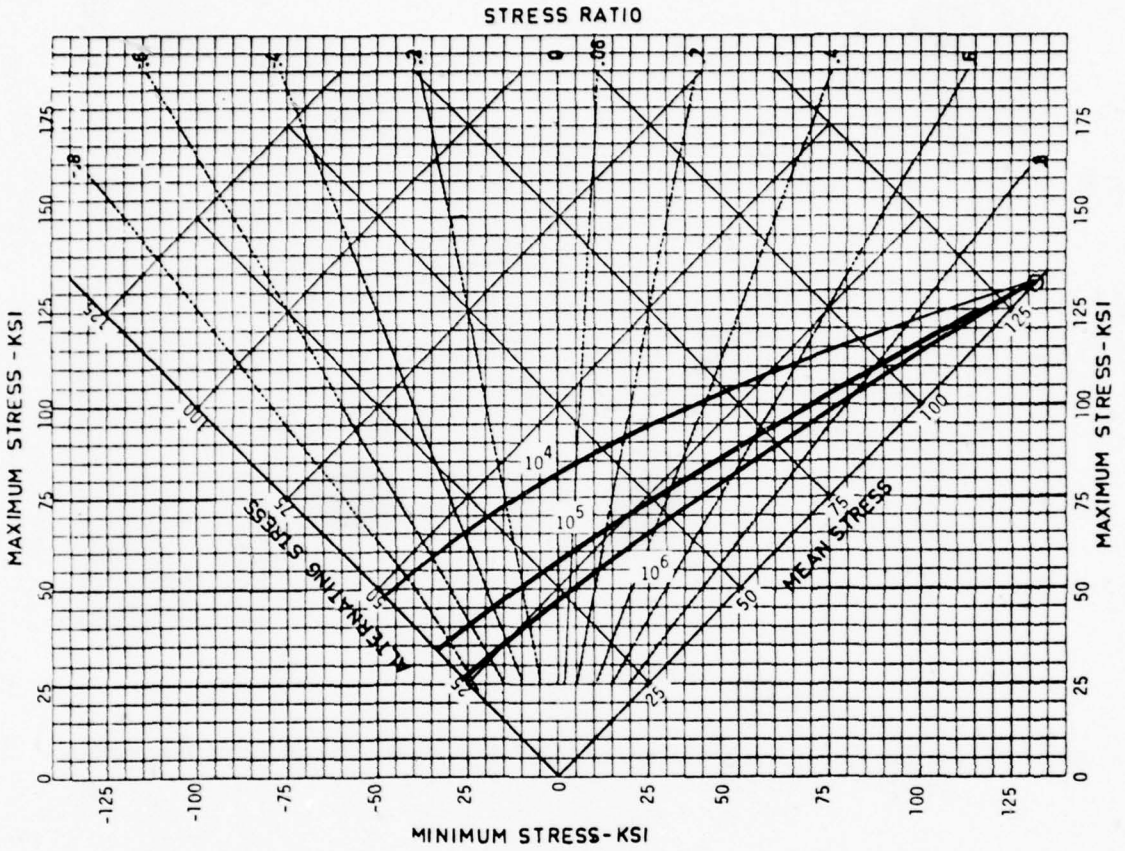

Figure B10.—Constant-life Diagram for Phase III BA Plate Tested at Room Temperature, K_t = 2.53, f = 1800 cpm.

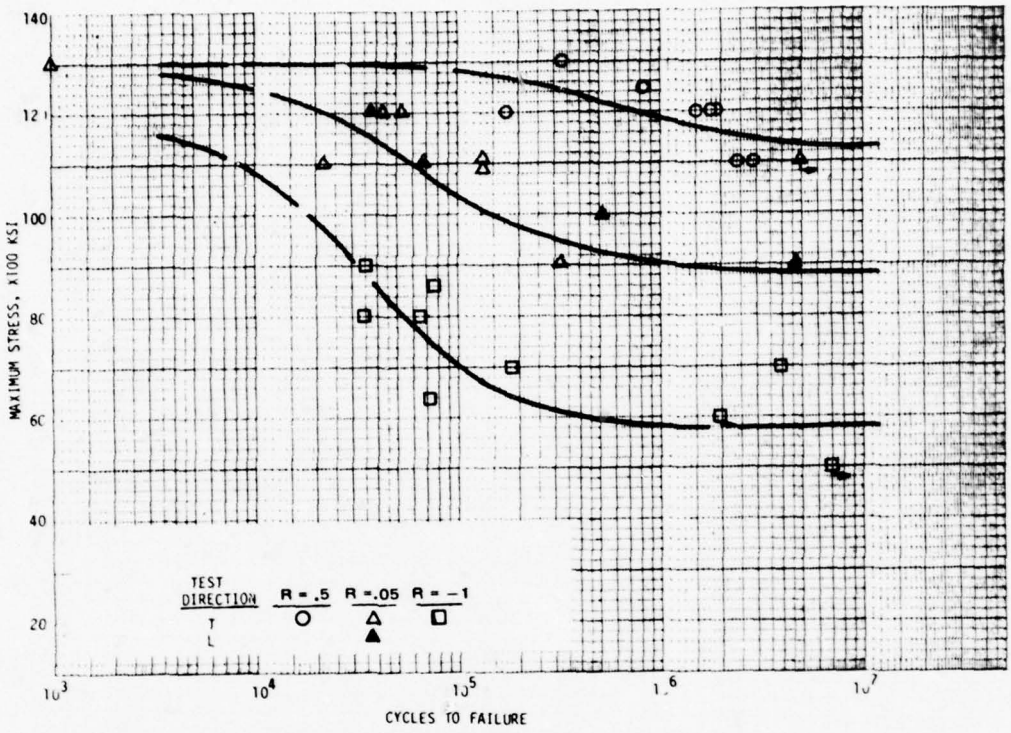

Figure B11.—Fatigue Life of Duplex Annealed Ti-6A1-4V Alloy Sheet in Air, at Room Temperature, 1800 CPM, $K_t = 1$

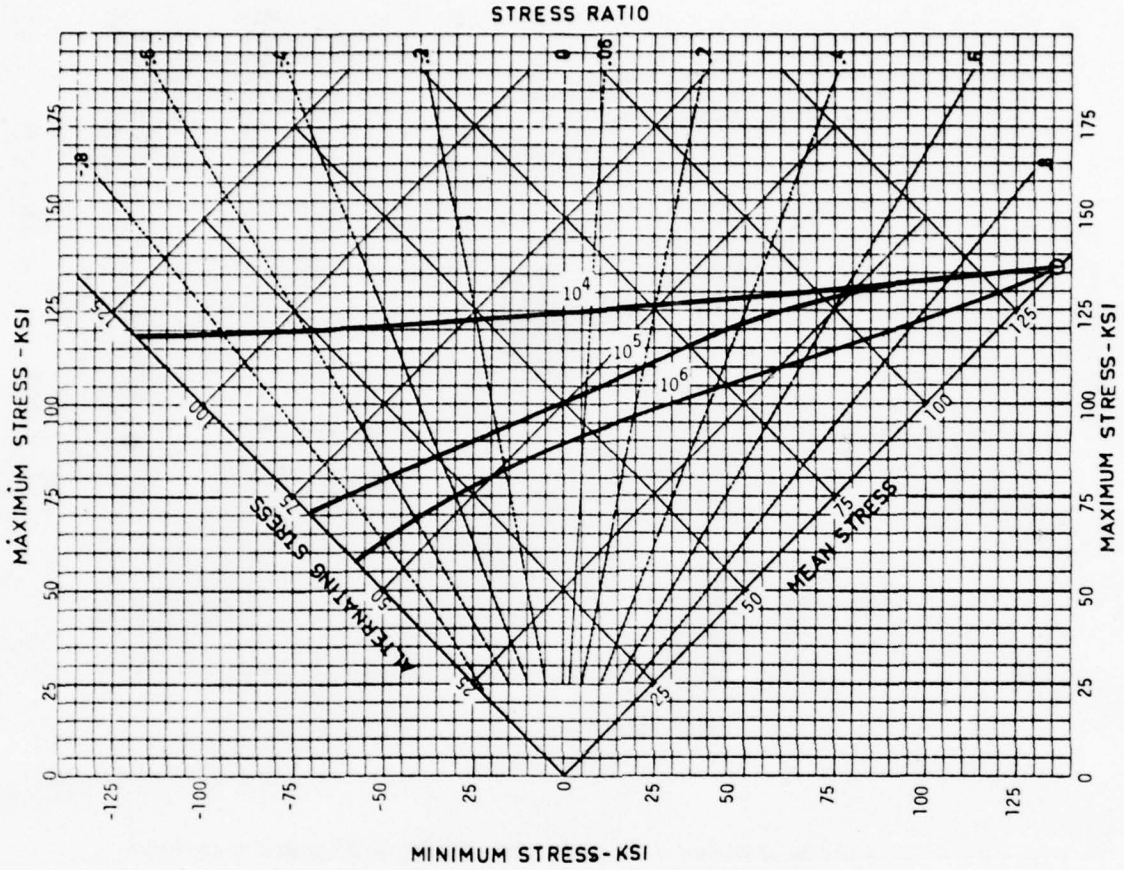

Figure B12.—Constant-life Diagram for Phase III DA Sheet Tested at Room Temperature, K_t = 1, f = 1800 cpm.

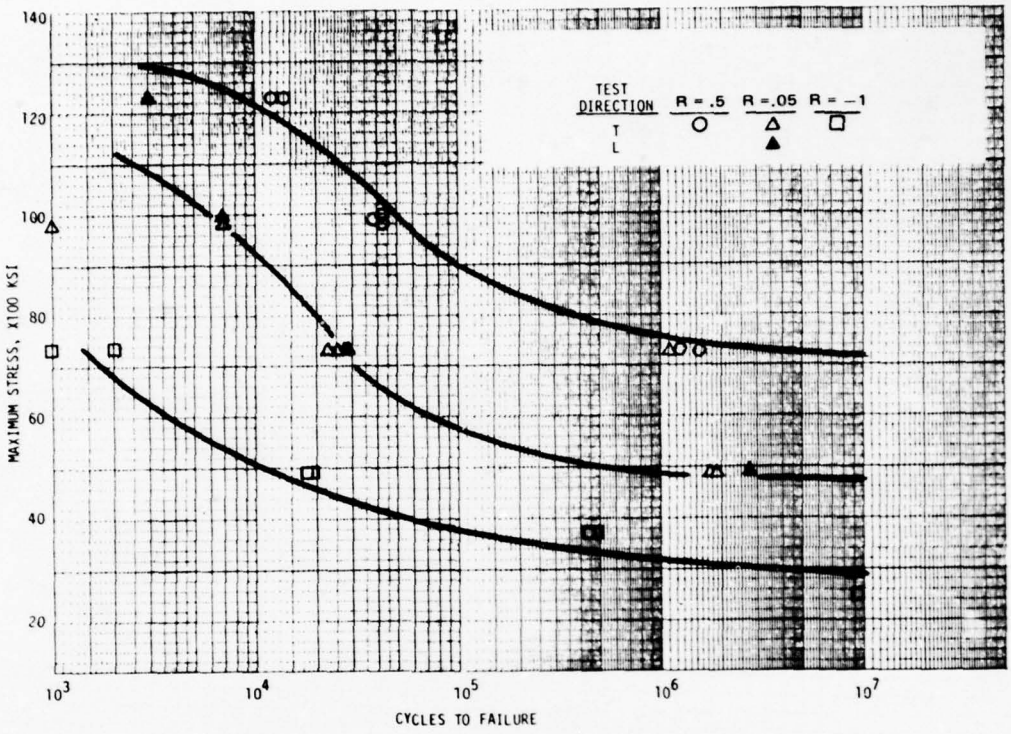

Figure B13.—Fatigue Life of Duplex Annealed Ti-6A1-4V Alloy Sheet in Air, at Room Temperature, 1800 cpm, K_t = 2.53

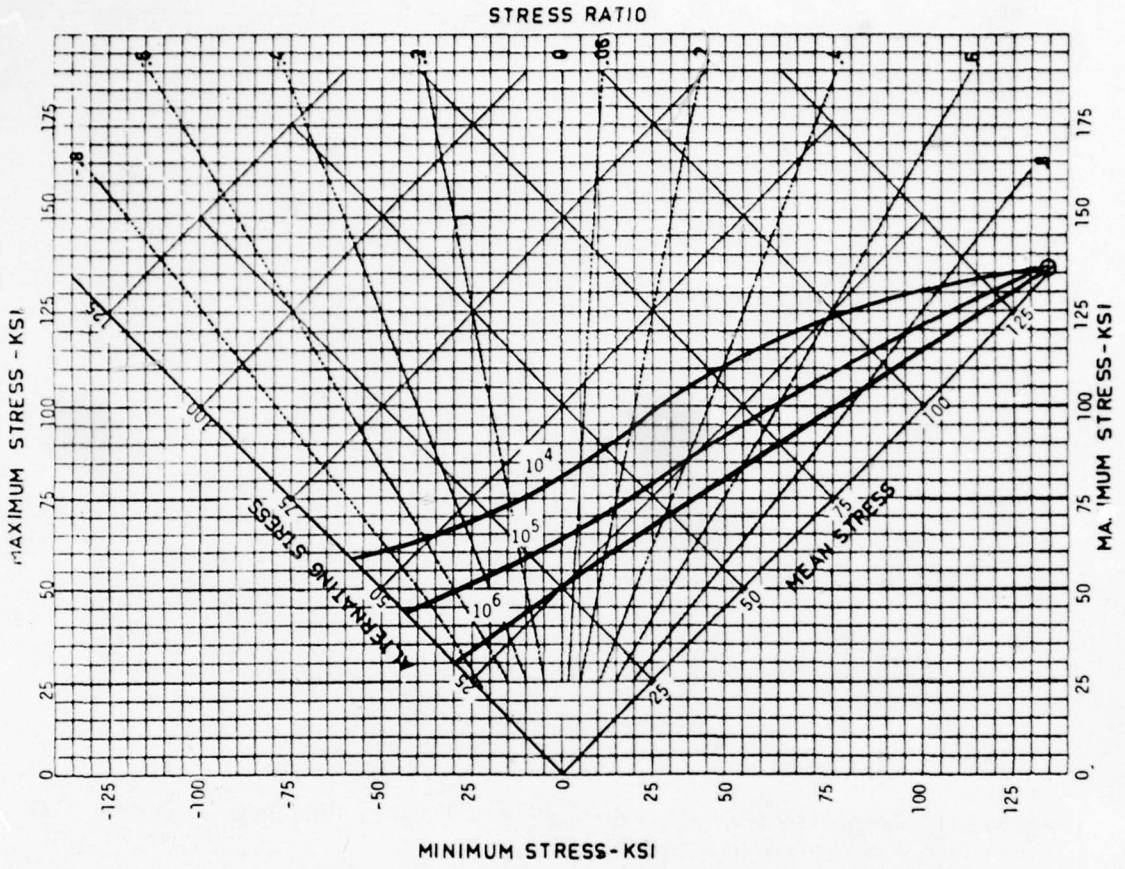

Figure B14.—Constant-life Diagram for Phase III DA Sheet Tested at Room Temperature, K_t = 2.53, f = 1800 cpm.

APPENDIX C

PROPOSED MATERIAL SPECIFICATIONS FOR TITANIUM ALLOY 6Al-4V

DAMAGE-TOLERANT GRADE PLATE AND SHEET

PROPOSED

MILITARY/AIR FORCE MATERIAL SPECIFICATION

TITANIUM ALLOY 6Al-4V DAMAGE-TOLERANT GRADE PLATE

1.0 SCOPE

1.1 Scope - This specification covers beta-annealed titanium alloy Ti-6Al-4V plate for damage-tolerant structure applications.

1.2 Classification - Material shall be furnished in the beta-annealed condition.

2.0 APPLICABLE DOCUMENTS

Except where a specific issue is indicated, the issue of the following documents in effect on the date of invitation for bid shall form a part of this specification to the extent indicated herein.

a. AMS 2242 - Tolerance, Corrosion and Heat Resistant Steel and Iron Base Sheet, Strip, and Plate

b. AMS 2249 - Chemical Check Analysis Limits, Titanium and Titanium Alloys

c. AMS 2631 - Ultrasonic Inspection of Titanium Alloys

d. ASTM E-8, Tension Testing of Metallic Materials

e. ASTM E-120 - Methods of Chemical Analysis for Titanium and Titanium Alloys

f. ASTM E-385 - Test Method for Oxygen Content Using a 14-MeV Neutron Activation and Direct Counting Technique

g. ASTM E-399-74 - Method of Test for Plane Strain Fracture Toughness of Metallic Materials

h. Federal Standard No. 184 - Identification Markings for Aluminum, Titanium and Magnesium

i. MIL-H-81200 - Heat Treatment of Titanium and Titanium Alloys

j. MIL-STD-105 - Sampling Procedures and Tables for Inspection by Attributes

3.0 REQUIREMENTS

3.1 Material

3.1.1 Melting - The material shall be produced by multiple melting under vacuum or inert gas atmosphere. If inert atmosphere is used, pressure shall not exceed 250 mm of mercury. Melting processes shall include, either singly or in combination, consumable electrode arc, electron beam, or other vacuum melting processes suitable for the production of materials meeting the requirements of this specification. Final stage melting shall be in vacuum.

3.1.2 Fabrication - Material shall be cross rolled at a maximum temperature of β_T minus 75°F. The rolling in any one direction shall not exceed 60 percent of the total reduction from starting stock to finished size. Final rolling to finish gage shall be by 50 percent reduction minimum at a maximum temperature of β_T minus 100°F.

3.1.3 Heat Treatment - Material shall be beta annealed at (β_T plus 50°F) $\pm$ 25°F for 30 minutes and cooled at a minimum rate of 50°F per minute to 1200°F. Below 1200°F the cooling rate is optional. The material shall then be annealed at 1350°F $\pm$ 25°F for 2 hours. Cooling rate is optional.

NOTES:

(1) Beta-transus temperature shall be determined in accordance with Section 4.4.6 on the material reduced to 8 inches of thickness or less.

(2) Material shall be held at temperature for sufficient time to assure that the most remote section (e.g., mid-thickness position in the center of plate) is at temperature (β_T plus 50°F) for 30 minutes.

(3) Temperature control and calibration shall be in accordance with MIL-H-81200.

3.1.4 Finish - Plate shall be grit blasted and pickled.

3.2 Chemical Composition - The chemical composition of each lot shall comply with Table I and shall be sampled and analyzed per Section 4.4.1. After all processing has been completed, at least one sample from each lot shall be taken for oxygen and hydrogen analysis.

Table I - Chemical Composition

Element	Composition (Weight Percent) (1)
Titanium (2)	Remainder
Aluminum	5.7-6.2
Vanadium	3.6-4.4
Iron	0.25 max.
Carbon	0.05 max.
Hydrogen	0.0125 max.
Oxygen	0.11 max.
Nitrogen	0.03 max.
Yttrium	0.005 max.
Other Impurities (3)	0.40 max.

NOTES:

(1) Check analysis shall be in accordance with AMS 2249. Check analysis tolerances do not broaden the specified analysis requirements, but cover variations between laboratories in the measurement of chemical content. The producer shall not ship material that is outside the weight percent limits specified in the above table. The purchaser shall not reject for chemical analysis, material within the check analysis tolerance.

(2) Need not be reported.

(3) Need not be reported. Any individual element shall not exceed 0.10 percent. No deliberate additions shall be made.

3.3 Mechanical Properties

3.3.1 Tensile Properties - The tensile properties of the material shall conform to the requirements specified in Table II tested in accordance with Section 4.4.2. One longitudinal (L-T), one transverse (T-L), and for plate over 2.500 inches in thickness one short transverse (S-T) tensile test shall be conducted on specimens cut from each plate until such time as a statistical sampling plan is approved by the purchaser. The specimens shall be cut from the mid-thickness position of the plate. The average results of the tensile tests for each lot shall show a maximum difference between the transverse and longitudinal directions of 4.0 ksi for the ultimate strength and 5.0 ksi for the yield strength.

Table II - Minimum Tensile Properties

Thickness (in.)	Ultimate Strength (ksi)	Yield Strength (0.2% Offset) (ksi)	Elong. % in 2 in. or 4D Long. & Trans.
0.188-0.500	130	117	10.0
0.501-1.000	127	115	10.0
1.001-2.000	125	112	8.0
2.001-4.000	122	110	8.0

3.4 Fracture Properties

3.4.1 Fracture Toughness - Material 0.5 inch and thicker shall meet a K_{IC} or K_Q of 85 ksi$\sqrt{in.}$ minimum when tested in accordance with Section 4.4.3. Two tests shall be made in the transverse direction (T-L) for each lot of material. Both tests shall meet the minimum K_{IC} or K_Q requirements.

3.4.2 Stress Corrosion - Material shall meet a K_{SL} of 60 ksi$\sqrt{in.}$ when tested in accordance with Section 4.4.4. One test shall be conducted in the transverse (T-L) direction per lot until such time as a statistical test plan is agreed upon between purchaser and supplier.

3.5 Microstructure - Microstructure shall be determined in accordance with Section 4.4.5. The microstructure shall show no surface oxygen contamination as evidenced by a different microstructure morphology (stabilized alpha phase) at the surface. The microstructure shall be uniform and consist of basketweave or Widmanstatten morphology and shall not contain primary or equiaxed alpha phase. Prior beta grains exceeding 0.050 inch in width or 0.100 inch in length shall constitute no more than 10 percent of the microstructure when examined at 10-50X magnification. A prior beta grain is a region of basketweave morphology which has transformed from a single beta grain.

3.6 Dimensional Tolerances

3.6.1 Thickness, Length, Width, and Straightness Tolerances - Thickness, length, width, and straightness tolerances shall conform to AMS 2242.

3.6.2 Flatness Tolerances - Plate flatness tolerances shall be as agreed upon by purchaser and supplier when measured in accordance with Section 4.4.7. Cold or hot (lower than 1250°F) flattening of material may be performed if the material is subsequently stress relieved by holding for 30 minutes at 1250 $\pm$ 25°F.

3.7 Ultrasonic Inspection - Plate 1/2 to 4 inches in thickness shall meet the requirements of Class A1 of AMS 2631 and Section 4.4.8 except discontinuity indications (noise or hash) shall not exceed 40% of the response from 3/64-inch flat bottom hole for 0.5- to 1.0-inch plate and 70% for 1.0- to 4.0-inch plate.

3.8 Identification of Product - Each plate shall be marked in accordance with FED-STD-184. In addition, each plate shall be marked with the heat number, the number of this specification, composition, and heat treatment condition.

3.9 Workmanship - The material shall be uniform in quality and condition, free from harmful alloy segregation and surface contaminations by oxygen, nitrogen, or other contaminants, and foreign material. It shall be clean, sound, smooth, and free from buckles or oil cans in excess of flatness tolerances, cracks, seams, grind marks, and other injurious defects detrimental to the fabrication or performance of parts.

4.0 QUALITY ASSURANCE PROVISIONS

4.1 Responsibility for Inspection - Unless otherwise specified in the contract or purchase order, the supplier is responsible for the performance of all inspection requirements as specified herein. Except as otherwise specified, the supplier may utilize his own facilities or any commercial laboratory acceptable to the procuring activity. The purchaser reserves the right to perform any of the inspections set forth in the specification where such inspections are deemed necessary to ensure that material conforms to prescribed requirements.

4.2 Supplier Quality Control - An internal quality control system which outlines procedures followed to assure compliance with all requirements of this specification is required. The system must include, but is not limited to, the following: (1) a plan for periodic heat treatment and test equipment calibration and certification with record control, (2) an in-process control plan and record system for processes subsequent to the final rolling operation, and (3) an end item inspection and testing plan and record system. Records indicating compliance with this system will be made available for review to a qualified representative of the purchaser.

4.3 Examination of Product - Plates shall be individually inspected. Acceptance criteria shall be in accordance with MIL-STD-105, Inspection Level II, Acceptable Quality Level 1.5 percent. All plates shall be visually examined for conformance with requirements for condition, identification, workmanship, and dimensions.

4.4 Quality Conformance Tests

4.4.1 Chemical Analysis - Chemical composition for all elements except hydrogen and oxygen shall be determined using ASTM E-120. Analysis for hydrogen shall be performed using a process calibrated against the NBS standard for hydrogen in titanium. Analysis for oxygen shall be per ASTM E-385. Any other analysis methods having equivalent or better accuracy and precision than the above methods may be used provided they are approved by the purchaser. Analysis for oxygen content shall be performed by a technique having an accuracy standard deviation of 50 ppm or better. Check analysis shall be according to AMS 2249.

4.4.2 Mechanical Properties Testing - Tensile testing shall be done in accordance with ASTM E-8. The strain rate shall be 0.003-0.007 inch per inch per minute through 0.2 percent offset plastic strain and then increased to 0.075-0.125 inch per inch per minute to failure. If a dispute occurs between the purchaser and supplier, a referee test shall be performed on a machine having a strain rate pacer, using a rate of 0.005 inch per inch per minute through the yield strength.

4.4.3 Fracture Toughness Test - Fracture toughness test shall be performed in accordance with ASTM E-399-74.

4.4.3.1 Test Specimen - The specimen used shall be the compact tension specimen specified in ASTM E-399-74, Figure 5, using the "W" dimension specified in Table III.

Table III - Fracture Toughness Specimen Configurations

Plate Thickness, in. (B, ASTM E-399-74)	W (ASTM E 399-74), in.
0.5 - 1.0	2.0
1.1 - 4.00	3.5

NOTES:

(1) The tolerances of Figure 5 in ASTM E-399-74 apply except in the instance of $W/2 \pm 0.010 = B$.

(2) Material may be machined 0.010 inch maximum from each side.

4.4.3.2 Post-Test Validity Verification for Specimen - In order to establish a measured level of K_Q as a valid K_{IC} value, all of the validity criteria of ASTM E399-74 must be satisfied. Otherwise, the value reported shall be K_Q.

4.4.3.3 Test Data - At the time of testing, the following data shall be recorded on the load-displacement test record:

(1) Date
(2) Specimen identification
(3) Load scale calibration (lb/in. chart)
(4) Displacement scale calibration (in./in. chart)
(5) Loading rate in terms of K_I per ASTM E399-74
(6) P_Q (lb)
(7) P_{MAX} (lb)

(8) Temperature

(9) Relative humidity

(10) Testing laboratory

(11) Test machine

(12) Operator

4.4.3.4 Reduction of Test Data - Test data shall be reduced as specified in ASTM E-399-74 to calculate a K_Q value and to determine if a valid K_{IC} property value has been measured.

4.4.3.4.1 Required Tensile Test Data - Tensile test coupons shall be provided for validity verification wherever fracture toughness coupons are called out. In checking for validity, the yield strength value used shall be the yield strength measured for the same plate as the fracture toughness specimen. A minimum of one transverse (T-L) tensile specimen taken immediately adjacent to the location of the fracture toughness specimen is required.

4.4.3.5 Invalid Test Results - If a value of K_Q is invalid solely on the basis of either of the following criteria, (1) $B < 2.5\ (K_Q/TYS)^2$, or (2) $P_{max}/P_Q > 1.10$, then such value K_Q may be compared to the minimum level specified in Section 3.4.1 for qualification purposes. Otherwise (i.e., in the case of a K_Q value invalid on the basis of other ASTM E-399-74 criteria - e.g., crack front curvature, etc.), a minimum of a single retest shall be required.

4.4.4 Stress Corrosion Testing - This testing procedure covers the determination of fracture toughness for Ti-6Al-4V beta processed plate in an environment of 3.5 percent NaCl and distilled water.

4.4.4.1 List of Terms

K	A stress intensity factor derived from fracture mechanics
K_{SL}	A stress intensity factor sustained at a specified level for 20 minutes in aqueous 3.5 percent NaCl

B Specimen thickness

W Specimen width

a Total crack length (sum of notch and fatigue crack length)

4.4.4.2 Apparatus - Stress corrosion test apparatus shall meet the requirements of ASTM E-399-74 for compact tension specimens with the addition of a salt water reservoir.

4.4.4.3 Test Specimen - Compact tension specimens shall be prepared in accordance with Section 4.4.3.1. The specimens shall be precracked in accordance with ASTM E-399-74. Post-test examination shall be made to ensure that the crack front (as precracked) meets the criteria of ASTM E399-74.

4.4.4.4 Test Procedures

a. Calculate the load required to develop K_{SL} = 55 ksi$\sqrt{in.}$ using the calculations for compact tension specimens of ASTM E-399-74.

b. Assemble a saltwater reservoir enclosing the precracked area. Fill the reservoir with saltwater making sure that the crack tip is completely immersed.

c. Load the specimen to K_{SL} = 55 ksi$\sqrt{in.}$ at a load rate in terms of K_I per ASTM E-399-74. Hold the load at K_{SL} for 20 minutes. If the specimen has not failed after 20 minutes at K_{SL}, raise the load at the same rate as used initially until fracture.

d. Calculate K at fracture per ASTM E-399-74.

4.4.5 Determination of Microstructure - One microstructural determination shall be made for each lot. The specimen surface shall be parallel to the rolling direction and perpendicular to the plate surface (transverse section). Examination shall be made by traversing the entire thickness of the plate at a magnification of 500X. Etching shall be by immersion in Kroll's etch (2 percent HF, 10 percent HNO_3, 88 percent H_2O) for approximately 15 seconds with a water rinse followed by immersion in 0.5 percent HF solution for 5-10 seconds. A photograph of the typical microstructure at the center and both surfaces of the plate shall be taken at 200X magnification and one photograph at 10-50X magnification showing representative microstructure.

4.4.6 Beta Transus Determination - The beta transus shall be determined by any suitable methods, subject to approval by the purchaser Quality Control. Thermal controls and readouts shall be calibrated to an accuracy of $\pm$ 5°F. The beta transus determinations from the same lot shall be repeatable within $\pm$ 15°F.

4.4.7 Determination of Flatness Variation - The amount of variation from flat shall be determined by measuring the distance from a straight edge laid in any direction upon the material, to the material surface at the point of greatest deviation. Both sides of each plate shall be inspected for flatness.

4.4.8 Ultrasonic Test - Ultrasonic inspection shall be performed in accordance with AMS 2631. Instruments shall be adjusted to produce a difference in the height of indications from 2/64- and 3/64-inch-diameter holes in reference standards.

5.0 PREPARATION FOR DELIVERY

5.1 Identification - Each plate shall be marked in accordance with Federal Standard No. 184. In addition, each plate shall be marked with Ti-6Al-4V, beta-annealed, heat number, lot, and the number of this specification, including the applicable revision letter.

5.2 Packaging and Marking

a. Packaging shall be such as to assure safe delivery.

b. Each container shall be durably and legibly marked with the following information:

Material specification number including the applicable revision letter, the supplier's name, Ti-6Al-4V, lot number, purchase order number, and quantity.

6.0 NOTES

6.1 Intended Use - The materials procurable under this specification are intended for structural applications in airborne vehicles and equipment where high fracture toughness is required. The materials are weldable by electron beam, plasma arc, friction, and diffusion welding processes.

6.2 Ordering Data - Procurement document should state the following:

a. Title, number, and date of this specification
b. Size and thickness

6.3 Definitions

Plate - A flat rolled product of 3/16 (0.1875) inch and over in thickness and over 12 inches in width with the width at least 10 times the thickness.

Lot - Any plate or group of plates from the same ingot that were processed together through all rolling, thermal, and chemical processing operations. Only plates that are either cut from a large plate after the final rolling operation or are rolled as a stack are considered rolled together.

Beta Transus Temperature (β_T) - The lowest temperature at which 100 percent of the material is converted to the beta phase during a heat treatment of one hour time at temperature as evidenced by microstructural examination.

Test Specimen Orientation - The test specimen orientations referred to in this specification shall be in accordance with ASTM E-399-74: longitudinal, L-T; transverse, T-L; and short transverse, S-T.

6.4 Reporting of Data - The supplier shall furnish the purchaser three copies of actual test data showing conformance to chemical composition, mechanical and fracture properties, and microstructure requirements with each lot of material. In the case of subsequent machining and/or heat treating by a second outside source, these reports will travel from supplier to machining/heat-treat processor, then to the purchaser. The report shall include:

a. Purchase Order Number
b. Material Specification Number and Revision
c. Lot Number
d. Heat Number
e. Billet Number and Billet Conversion Source
f. Quantity and Size
g. Mechanical and Fracture Properties
h. Chemical Analysis
i. Microstructure (200X and 50X Magnification)
j. Beta Transus Temperature
k. Specific Heat Treat Cycle Used
m. Results of Ultrasonic Inspection

Nonproprietary processing information shall be made available to purchaser upon request, and data shall be retained for a period of time determined by purchaser Quality Control and then purged only with the prior concurrence of the purchaser.

PROPOSED

MILITARY/AIR FORCE MATERIAL SPECIFICATION
TITANIUM ALLOY 6Al-4V DAMAGE-TOLERANT GRADE SHEET AND STRIP

1.0 SCOPE

1.1 Scope - This specification covers duplex-annealed Ti-6Al-4V titanium alloy sheet and strip for damage-tolerant structure applications.

1.2 Classification - Material shall be furnished in the duplex-annealed condition.

2.0 APPLICABLE DOCUMENTS

Except where a specific issue is indicated, the issue of the following documents in effect on the date of invitation for bid shall form a part of this specification to the extent indicated herein.

a. AMS 2242 - Tolerance, Corrosion and Heat Resistant Steel Sheet and Iron Base Sheet, Strip, and Plate

b. AMS 2249 - Chemical Check Analysis Limits, Titanium and Titanium Alloys

c. ASTM E-4 - Verification of Testing Machines

d. ASTM E-8 - Tension Testing of Metallic Materials

e. ASTM E-120 - Methods of Chemical Analysis for Titanium and Titanium Alloys

f. ASTM E-290 - Semi-Guided Bend Test for Ductility of Metallic Materials

g. ASTM E-385 - Test Method for Oxygen Content Using 14-MeV Neutron Activation and Direct Counting Technique

h. ASTM E-561-76T - Tentative Recommended Practice for R-Curve Determination

i. Federal Test Method Standard No. 151 - Metals; Test Methods

j. Federal Test Method Standard No. 184 - Identification Markings for Aluminum, Titanium, and Magnesium

k. MIL-H-81200 - Heat Treatment of Titanium and Titanium Alloys

m. MIL-STD-105 - Sampling Procedure and Tables for Inspection by Attributes

3.0 REQUIREMENTS

3.1 Material

3.1.1 Melting - The material shall be produced by multiple melting under vacuum or inert gas atmosphere. If inert atmosphere is used, pressure shall not exceed 250 mm of mercury. Melting processes shall include, either singly or in combination, consumable electrode arc, electron beam, or other vacuum melting processes suitable for the production of materials meeting the requirements of this specification. Final stage melting shall be in vacuum.

3.1.2 Fabrication - Material shall be cross rolled at a maximum temperature of β_T minus 75°F. The rolling in any one direction shall not exceed 60 percent of the total reduction from starting stock to finished size. Final rolling to finish gage shall be by 50 percent reduction minimum at a temperature of β_T minus 100°F maximum.

3.1.3 Heat Treatment - Material shall be annealed at (β_T minus 50°F) $\pm$ 25°F for 10 minutes at temperature and cooled at a minimum rate of 50°F per minute to 1200°F. Below 1200°F the cooling rate is optional. The material shall then be annealed at 1350 $\pm$ 25°F for 2 hours. Cooling rate is optional.

NOTES:

(1) Beta-transus temperature shall be determined in accordance with Section 4.4.7 on the material reduced to 8 inches of thickness or less.

(2) Material shall be held at temperature for sufficient time to assure that the most remote section of the sheet is at temperature (β_T minus 50°F) for 10 minutes.

(3) Temperature control and calibration shall be in accordance with MIL-H-81200.

3.1.4 Finish - Material shall have a surface appearance equivalent to a 2D finish for commercial corrosion resistant steel and shall have a 32 RHR or better surface roughness. All material shall have been sanded and subsequently pickled with a minimum of 0.0015 inch removed by pickling per surface.

3.2 Chemical Composition - The chemical composition of each lot shall comply with Table I and shall be sampled and analyzed per Section 4.4.1. After all processing has been completed, at least one sample from each lot shall be taken for oxygen and hydrogen analysis.

Table I - Chemical Composition

Element	Composition (Weight Percent) (1)
Titanium (2)	Remainder
Aluminum	5.7-6.2
Vanadium	3.6-4.4
Iron	0.25 max.
Carbon	0.05 max.
Hydrogen	0.0125 max.
Oxygen	0.11 max.
Nitrogen	0.03 max.
Yttrium	0.005 max.
Other Impurities, Total (3)	0.40 max.

NOTES:

(1) Check analysis shall be in accordance with AMS 2249. Check analysis tolerances do not broaden the specified analysis requirements, but cover variations between laboratories in the measurement of chemical content. The producer shall not ship material which is outside the weight percent limits specified in the above table. The purchaser shall not reject for chemical analysis, material within the check analysis tolerance.

(2) Need not be reported.

(3) Need not be reported. Any individual element shall not exceed 0.10 percent. No deliberate additions shall be made.

3.3 Mechanical Properties

3.3.1 Tensile Properties - The tensile properties of the material shall conform to the requirements specified in Table II tested in accordance with Section 4.4.2. One longitudinal (L-T) and one transverse (T-L) tensile test shall be conducted on specimens cut from each lot until such time as a statistical sampling plan is approved by the purchaser. The specimens shall be cut from the mid-width position of the sheet. The average results of the tensile tests for each lot shall show a maximum difference between the transverse and longitudinal directions of 4.0 ksi for the ultimate strength and 5.0 ksi for the yield strength.

Table II - Minimum Tensile Properties

Thickness (in.)	Ultimate Strength (ksi)	Yield Strength (0.2% Offset) (ksi)	Elong. % in 2 in. or 4D Long. & Trans.
Under 0.017	130	120	6.0
0.017-0.032	130	120	8.0
0.033-0.187	130	120	10.0

3.3.2 Bend Properties - Material shall meet the bend requirements in Table III at room temperature without showing a separation or cracking of the outer fibers as observed at 20X magnification when tested in accordance with Section 4.4.3. At least three transverse and three longitudinal specimens shall be tested from each sheet until such time as a statistical sampling plan is approved by the purchaser.

TABLE III - Bend Properties

Nominal Thickness (in.)	Ratio of Bend Radius to Thickness
under 0.070	4.0
0.070-0.187	4.5

3.4 Fracture Properties

3.4.1 Fracture Toughness - Material shall meet a K_C of 140 ksi$\sqrt{in.}$ minimum when tested in accordance with Section 4.4.4. One test shall be made in the transverse (T) direction for each lot of material.

3.4.2 Stress Corrosion - Material shall meet a minimum K_{SL} of 120 ksi$\sqrt{in.}$ when tested in accordance with Section 4.4.5. One test shall be conducted in the transverse (T) direction per lot until such time as a statistical test plan is agreed upon between purchaser and supplier.

3.5 Microstructure - Microstructure shall be determined in accordance with Section 4.4.6. The microstructure shall show no surface oxygen contamination as evidenced by a different microstructure morphology (stabilized alpha phase) at the surface. The microstructure shall consist of primary alpha grains and regions of transformed beta. The regions of transformed beta shall constitute at least 40 percent of the microstructure by area, but no more than 80 percent.

3.6 Dimensional Tolerances

3.6.1 Thickness, Length, Width, and Straightness Tolerances - Thickness, length, width, and straightness tolerances shall conform to AMS 2242, except the length tolerance for sheet over 20 feet long shall be plus 3/4 inch minus 0.

3.6.2 Flatness Tolerances - All material shall meet the following requirements when measured in accordance with Section 4.4.8:

Gage (in.)	Width (in.)	Flatness (%)
under 0.025	36 and under	5
0.025-0.187	36 and under	3

3.7 Identification of Product - Each sheet shall be marked in accordance with FED-STD-184. In addition, each sheet shall be marked with the heat number, the number of this specification, composition, and heat treatment condition.

3.8 Workmanship - The material shall be uniform in microstructure, quality, strength, and condition. It shall be clean, sound, and free from oil cans and ripples of depth in excess of the flatness tolerance, harmful alloy segregation, foreign materials, internal and external imperfections, and characteristics detrimental to the fabrication and/or performance of parts. Evidence of contamination and surface imperfections such as folds, laminations, inclusions, sanded finish, rolled-in scale, pits, cracks, cuts, seams, blisters, dents, and grind marks shall be cause for rejection.

4.0 QUALITY ASSURANCE PROVISIONS

4.1 Responsibility for Inspection - Unless otherwise specified in the contract or purchase order, the supplier is responsible for the performance of all inspection requirements as specified herein. Except as otherwise specified, the supplier may utilize his own facilities or any commercial laboratory acceptable to the procuring activity. The purchaser reserves the right to perform any of the inspections set forth in the specification where such inspections are deemed necessary to ensure that material conforms to prescribed requirements.

4.2 Supplier Quality Control - An internal quality control system which outlines procedures followed to assure compliance with all requirements of this specification is required. The system must include, but is not limited to, the following: (1) a plan for periodic heat treatment and test equipment calibration and certification with record control, (2) an in-process control plan and record system for processes subsequent to the final rolling operation, and (3) an end item inspection and testing plan and record system. Records indicating compliance with this system will be made available for review to a qualified representative of the purchaser.

4.3 Sampling - Except as otherwise specified, sampling plans and procedures in the determination of the acceptability of products submitted by a supplier shall be in accordance with the provisions set forth in MIL-STD-105.

4.3.1 Examination of Product - Sheet and strip shall be individually inspected. Acceptance criteria shall be in accordance with MIL-STD-105, Inspection Level II, Acceptable Quality Level 1.5 percent. All sheet and strip shall be visually examined for conformance with requirements for condition, identification, workmanship, and dimensions.

4.4 Quality Conformance Tests

4.4.1 Chemical Analysis - Chemical composition for all elements except hydrogen and oxygen shall be determined using ASTM E-120. Analysis for hydrogen shall be performed using the hot extraction method described in ASTM E-146. Oxygen shall be determined by neutron activation in accordance with ASTM E-385. Check analysis shall be according to AMS 2249. Any other analysis methods having equivalent or better accuracy and precision than the above methods may be used provided they are approved by the purchaser.

4.4.2 Tensile Test - Tensile testing shall be done in accordance with ASTM E-8. The strain rate shall be 0.003-0.007 inch per inch per minute through 0.2 percent offset plastic strain and then increased to 0.075-0.125 inch per inch per minute to failure. If a dispute occurs between the purchaser and supplier, a referee test shall be performed on a machine having a strain rate pacer, using a rate of 0.005 inch per inch per minute through the yield strength.

4.4.3 Bend Test - Specimens shall be selected and tested by bending in accordance with ASTM E-290 so that each side of the material is stressed in tension in the longitudinal and transverse directions. Specimens from material up to 0.075 inch thickness shall be not less than 0.750 inch wide. Specimens from material 0.075 inch thickness and over shall have width equal to at least ten times the thickness. Specimen length shall be at least 2 inches and shall be parallel and perpendicular to the rolling direction, respectively. The specimens shall be bent to a final unrestrained included angle of 75 degrees maximum at room temperature using an open lower die. The nominal thickness of the sheet shall be used for calculation of R/t and tool clearance values. The radius of the punch shall be used for calculation of R/t and tool clearance values. The radius of the punch shall be equal to the bend radius.

4.4.4 Fracture Toughness Test - The determination of resistance to fracturing of Ti-6Al-4V sheet and strip in air at room temperature shall be made using center-cracked tension (CCT) panel specimens and test procedures in accordance with ASTM E561-76T. The minimum width of the test specimen shall be 12 inches.

4.4.5 Stress Corrosion Test - This testing procedure covers the determination of fracture toughness for Ti-6Al-4V duplex-annealed sheet in a solution of 3.5 percent NaCl and distilled water.

4.4.5.1 List of Terms

K	A stress intensity factor derived from fracture mechanics
K_{SL}	A stress intensity factor sustained at a specified level for 20 minutes in aqueous 3.5 percent NaCl
B	Specimen thickness
W	Specimen width
a	Total crack length (sum of notch and fatigue crack length)

4.4.5.2 Apparatus - The K_{SL} test shall be conducted on any tensile machine capable of developing 30,000 pounds load, and conforming in other respects to ASTM E4, Verification of Testing Machines. The machine shall also be capable of sustaining load at a specified level within $\pm$ 2 percent for a period of 20 minutes. Test fixtures shall be capable of maintaining alignment in the transfer of load from the machine to the specimen. It is required that the precracked area of the specimen be completely immersed throughout the test in 3.5 percent solution of sodium chloride and distilled water.

4.4.5.3 Test Specimen - Single-edge-crack tension specimens (3 inches wide) shall be prepared in accordance with Figure 1. The specimen thickness shall be that of the product. The notch may be prepared by mill cutting. It is mandatory that the root radius be no larger than 0.015 inch.

The specimens shall be precracked by fatigue loading until the crack extends a minimum of 0.050 inch and a maximum of 0.200 inch on each side of the specimen. The crack may be started at higher K values, but during the final 0.050 inch of extension, the maximum K should not exceed 2/3 of K_{SL}.

4.4.5.4 Test Procedure

a. Measure the specimen's thickness at two points, one on each side of the notch. Average the measurements.

b. Measure the specimen's width from edge to edge on each side surface along the crack plane. Average the measurements.

c. Measure the crack length from the edge to the crack tip on each surface of the specimen. Average the measurements.

d. Calculate the load required to develop K_{SL} using the equation of step h.

e. Assemble a saltwater reservoir enclosing the precracked area.

f. Fill the reservoir with saltwater making sure that the crack tip is completely immersed.

g. Load the specimen to K_{SL} = 140 ksi in. at a crosshead separation rate of approximately 0.05 inch per minute. Hold the load at K_{SL} for 20 minutes. If the specimen has not failed after 20 minutes at K_{SL}, raise the load at the same rate until failure.

h. Calculate K_{SL} at fracture as follows:

$$K_{SL} \text{ or } K = \frac{Pa}{BW} \left[1.99 - 0.41\,(a/W) + 18.70\,(a/W)^2 - 38.48\,(a/W)^3 + 53.85\,(a/W)^4\right]$$

where:

P is the load required to develop a desired K level

a is the crack length

B is specimen thickness

W is specimen width

4.4.6 Determination of Microstructure - One microstructural determination shall be made for each lot. The specimen surface shall be parallel to the rolling direction and perpendicular to the sheet surface (transverse section). Examination shall be made by traversing the entire thickness of the sheet at a magnification of 500X. Etching shall be by immersion in Kroll's etch (2 percent HF, 10 percent HNO_3, 88 percent H_2O) for approximately 15 seconds with a water rinse followed by immersion in 0.5 percent HF solution for 5-10 seconds. A photograph of the typical microstructure at the center and both surfaces of the sheet shall be taken at 500X magnification and one photograph at 10-50X magnification showing representative microstructure.

4.4.7 Beta Transus Determination - The beta transus shall be determined by any suitable methods, subject to approval by the purchaser Quality Control. Thermal controls and readouts shall be calibrated to an accuracy of $\pm$ 5°F. The beta transus determinations from the same lot shall be repeatable within $\pm$ 15°F.

4.4.8 Determination of Flatness Variation - Flatness shall be determined from the expression 100H/L where "L" is the distance between contact points of a straight edge laid in any direction on the sheet and "H" is the distance from the straight edge to the sheet at the point of the greatest separati

5.0 PREPARATION FOR DELIVERY

5.1 Identification - Each sheet shall be marked in accordance with Federal Standard No. 184. In addition, each sheet shall be marked with Ti-6Al-4V, annealed, heat number, lot, and the number of this specification, including the applicable revision letter.

5.2 Packaging and Marking

a. Packaging shall be such as to assure safe delivery.

b. Each container shall be durably and legibly marked with the following information:

Material specification number including the applicable revision letter, the supplier's name, Ti-6Al-4V, lot number, purchase order number, and quantity.

6.0 NOTES

6.1 Intended Use - The materials procurable under this specification are intended for structural applications in airborne vehicles and equipment where high fracture toughness is required. The materials are weldable by electron beam, plasma arc, friction, and diffusion welding processes.

6.2 Ordering Data - Procurement document should state the following:

a. Title, number, and date of this specification
b. Finish
c. Size and thickness

6.3 Definitions

Sheet - A flat rolled product up to and including 0.1875 inch in thickness and 24 inches and over in width.

Strip - A flat rolled product up to and including 0.1875 inch in thickness and generally furnished with slit, sheared, or slit and edge rolled in widths up to 24 inches inclusive; or with finished drawn or rolled edges in widths over 1-1/4 inches to 12 inches inclusive.

Lot - Any sheet or group of sheets from the same ingot that were processed together through all rolling, thermal, and chemical processing operations. Only sheets that are either cut from a large sheet after the final rolling operation or are rolled together as a stack are considered rolled together.

Beta Transus Temperature (β_T) - The lowest temperature at which 100 percent of the material is converted to the beta phase during a heat treatment of 1 hour at temperature as evidenced by microstructural examination.

Test Specimen Orientation - The test specimen orientations referred to in this specification shall be as follows: longitudinal (L) - the length of the specimen parallel to the rolling direction; transverse (T) - the length of the specimen normal to the rolling direction.

6.4 Reporting of Data - The supplier shall furnish the purchaser three copies of actual test data showing conformance to chemical composition, mechanical and fracture properties, and microstructure requirements with each lot of material. In the case of subsequent heat treating by a second outside source, these reports will travel from supplier to heat-treat processor, then to the purchaser. The report shall include:

a. Purchase Order Number
b. Material Specification Number and Revision
c. Lot Number
d. Heat Number
e. Billet Number and Billet Conversion Source
f. Quantity and Size
g. Mechanical and Fracture Properties
h. Chemical Analysis
i. Microstructure (500X Magnification)
j. Beta Transus Temperature
k. Specific Heat Treat Cycle Used

Nonproprietary processing information shall be made available to purchaser upon request, and data shall be retained for a period of time determined by purchaser Quality Control and then purged only with the prior concurrence of the purchaser.

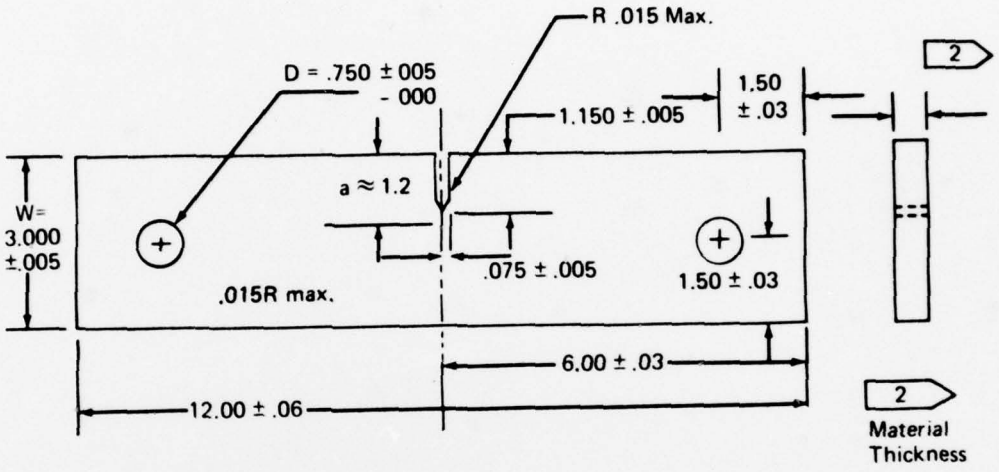

Figure C1.–K_{SL} Test Specimen